Assessing Flight Performance of a Supersonic Airliner with Swing Wing Capabilities using Energy Maneuverability Theory

by

Bhargav Chaudhari

A Thesis Presented in Partial Fulfillment
Of the Requirements for the Degree
Master of Science

Approved April 2021 by the
Graduate Supervisory Committee:

Timothy Takahashi, Chair
Werner Dahm
Jeonglae Kim

ARIZONA STATE UNIVERSITY

May 2021

ABSTRACT

The objective of this study is to estimate the variation of flight performance of a variable sweep wing geometry on the reverse engineered Boeing 2707-100 SST, when compared against the traditional delta wing approach used on supersonic airliner. The reason for this lies beneath the fact that supersonic orientations of wings doesn't seem to work well for subsonic conditions, and subsonic wings are inefficient for supersonic flight. This would likely mean that flying long haul subsonic with supersonic wing geometry is inefficient compared to regular aircraft, but more importantly requires high takeoff/landing speeds and even long runways to bring the aircraft to hold. One might be able to get around this problem - partially - by adding thrust either by using afterburners, or by using variable geometry wings. To assess the flight performance, the research work done in this report focuses on implementing the latter solution to the abovementioned problem by using the aerodynamic performance parameters such as Coefficient of Lift, Coefficient of Drag along with its components specific to every test Mach number and altitude, along with the propulsion performance parameters such as thrust and thrust specific fuel consumption at different iterations of power settings of engine, flight Mach number and altitude in a propulsion database file to estimate flight performance using flight missions and energy-maneuverability theory approach. The flight performance was studied at several sweep angles of the aircraft to estimate the best possible sweep orientation based on the requirement of mission and an optimal flight mission was developed for an aircraft with swing wing capabilities.

ACKNOWLEDGEMENTS

I am grateful to all of those with whom I have had the pleasure to work during this and other related projects. Each of my thesis committee members, Prof. Takahashi, Prof. Dahm, and Prof. Kim have provided me extensive personal and professional guidance and taught me a great deal about both scientific research and life in general. I would especially like to thank Dr. Timothy Takahashi, the chair of my committee. As my teacher and mentor, he has taught me more than I could ever give him credit for here. His has been always helpful whenever I ran into a trouble spot or had a question about my research or writing. He consistently allowed this research to be my own work but steered me in the right the direction whenever he thought I needed it.

Nobody has been more important to me in the pursuit of this project than my friends and family. I would like to thank my parents; for providing me with unfailing support and continuous encouragement throughout my years of study and through the process of researching and writing this thesis. This accomplishment would not have been possible without them.

Thank you.

TABLE OF CONTENTS

Page

Page

Page

Page

Page

LIST OF FIGURES

Figure Page

Figure Page

Figure Page

Figure Page

Figure Page

Figure Page

Figure Page

Figure Page

Figure Page

Figure Page

Figure Page

Figure Page

LIST OF TABLES

Table Page

Table Page

1. INTRODUCTION

A return of an era of commercial supersonic flight might be just around the corner, but there are a few challenges to overcome when it comes to flying faster than the speed of sound.

Concorde, the aeronautical marvel that made its last flight in October 2003, only conquered the engineering aspect of supersonic aviation. The world's most slender civilian aircraft could make a round trip across the Atlantic in less time than other commercial airliners could make a one-way trip, but the enormous impacts on the environment and noise from flying such an aircraft were neglected.

In the race for commercial supersonic travel in the 60's and 70's, Concorde, as it turned out, wasn't the only frontrunner. On the other side of the Iron Curtain, the Russian design bureau Tupolev were also creating a supersonic transport and airliner, the Tupolev Tu-144. To be beaten in the supersonic airliner arena by the British and the French was one thing, but to be shown a clean pair of heels by the Russians was another to take for Americans, who until that point of time prided themselves on the advances made in the field of aeronautics.

The quest for a supersonic airliner became almost as important to the USA as the race to the Moon. The United States government's carrot to likely contenders was that the government would pick up approximately $3/4^{th}$ of the cost of the program if they could produce a design that could rival Concorde and Tupolev [1]. Until that time, both Lockheed Martin and Boeing, two aerospace sector giants, were heavily involved with supersonic

research. Most of these studies involved around a traditional approach of wing design, a delta-winged aircraft.

As jet aircraft started flying at transonic speeds, the standard design that had served propeller-driven aircraft for decades was no longer desirable; straight, plank-like wings create too much drag at high speeds. The triangular shape of delta wings reduced high speed drag and could withstand the stresses of supersonic flight. Moreover, aircraft like the French Mirage III fighter and the Russian MiG-21 had already proven the delta shape could easily go twice the speed of sound and beyond.

Using this basis, Lockheed chose a traditional delta wing planform for their design, intended to fly at Mach 2.6 while carrying 270 passengers. Meanwhile, Boeing proposed a design to fly at Mach 2.7, carry more than 270 passengers, and be able to fly more than 4,200 miles (~ 6,700 kilometers). Boeing opted for a rather unorthodox design feature what's known as 'variable geometry' – or swing wings, as they became known – in their initial design. The wings would be unswept at low speeds, improving the aircraft's handling at take-off and landing, and then swing back closer to the aircraft's body as it picked up speed. The U.S. government chose Boeing's concept as the winner on 1st January 1967. But the Boeing B2707's progress was anything but smooth. It was intended to be much larger and faster than preceding SST designs such as Concorde.

During development the required weight and size of this mechanism continued to grow, forcing the team to start over using a conventional delta wing. Eventually the rising costs and the lack of a clear market led to its cancellation in 1971 before two prototypes had been completed. The Boeing 2707 SST became known as "*the airplane that almost ate*

Seattle". Boeing was a major economic force in the region, and was stretched so thin that a Sea Tac billboard was erected that read, "*Will the last person leaving Seattle - turn out the lights?*"

What could have been if the Boeing SST program was not cancelled?

This is an interesting issue. Had the original swing-wing aircraft (the B2707-100) met the design specifications presented to the FAA in late 1966, it might have done relatively well. On paper, its Cost per Available Seat Mile (CASM) was relatively less than its predecessor, the 707-320B's and much lower than Concorde's (the Boeing 707 was economically viable to fly through the early 1980s). This was because its swing wing was significantly more aerodynamically efficient across the speed range compared to either Concorde's ogival wing or the later B2707-300 double-delta. Higher *(L/D)*s are critical as they require a smaller fuel load, smaller engines, lighter airframe, etc. which would have been on offer from Boeing's B2707 airliner.

If the program had proceeded on schedule and on spec, Congress could not have killed it in 1971, as the prototype would have been flying and commercial pre-production would have been underway. Since 1970's were economically depressing, the aircraft might have survived the decade with low production rates and then achieved more success in the 1980's as the economy recovered and fuel prices dropped. However, sales in the 1980's almost certainly would have required a much cleaner and quieter engine than the GE4, probably something with a low-bypass turbofan would have an upper hand on the one proposed in the early stages of design.

While the B2707-300 - where they discarded the swing wing in favor of more traditional double delta wings - may have been technically feasible, it was economically a shockingly inferior aircraft compared to its predecessors. Takeoff weight soared, flight range plummeted, payload (both weight and pax counts) fell significantly, and engine size increased apace. CASM data somehow managed to disappear from published specs papers around this point of design.

Moreover, the delta wings are inherently inefficient at low speed, and to cope with runway and noise constraints, Boeing noticeably oversized and underswept the -300's primary delta wing for better takeoff and landing performance. Unfortunately, this resulted in lower subsonic and much lower supersonic *(L/D)*s, with knock-on effects on CASM and range. By cancellation in 1971, projected takeoff weight was above 800,000 lbs. with a standard range of 3,500 miles with 273 pax, compared with the -100's 675,000 lb. Maximum Takeoff Weight (MTOW) and range of 4,400 miles with 280 pax. All in all, it was a downgrade to the original version of intended Supersonic Transport Aircraft.

The following research presents a detailed analysis of the approach that could have been used to optimize the swing wing capabilities of the aircraft, had one been developed. It also compares the data obtained from swing wing aircraft against the traditional delta wing and fixed sweep aircrafts to estimate the variation in the aerodynamic flight performance associated with each geometrical change made on aircraft.

2. DESIGN AND OPERATING CONDITIONS

The Boeing B2707 aircraft studied in this thesis seeks to determine if it would have been an economic disaster. To explain in brief, the two major problems associated with large SST's are listed below:

1) The Wave drag (aerodynamic drag generated by supersonic flow) increases with the size and decreases with the fineness ratio. This leads to an optimum length to diameter ratio which is quite high. This makes the SST's difficult because the need for a standup cabin implies a fuselage more than 100 ft long.

2) Reducing costs is great, but does it get cheap enough to attract enough passengers? That's one of the problems of the A380, it had the lowest cost per seat of any long haul aircraft (except the 777X) but selling enough tickets requires even lower prices.

Another problem of SST's is that supersonic orientations of wings doesn't seem to work well for subsonic conditions, and subsonic wings are inefficient for supersonic flight. This would likely mean that flying long haul subsonic with supersonic wing geometry is inefficient compared to regular aircraft, but more importantly requires high takeoff/landing speeds and even long runways to bring the aircraft to hold. One might be able to get around this problem - partially - by adding thrust either by using afterburners, or by using variable geometry wings. This thesis will show why a subsonic fixed wing SST does not match the fuel economy of a regular subsonic aircraft.

Boeing B2707-100 SST concept was a land based, four-engine airliner for commercial transport of passengers and cargo. Boeing designed to cruise at about Mach 2.7. The aircraft was supposed to have a maximum taxi weight of about 675,000 lbs. and allowable payload of 75,000 lbs. with a range of around 4,440 miles [2]. The fuselage body had a total passenger cabin volume of 18,000 ft^3. During the wing forward orientation, the leading edge sweep of the wing would be 20^o and it would rotate to around 72^o during the wing aft position to become a "delta wing". The wingspan of the aircraft would be ~180 ft at 20^o wing sweep angle and reduce to just ~105 ft at full sweep aft condition during its intended supersonic cruise condition [2].

As discussed in the introduction section, Boeing B2707-100 aircraft was designed to use the swing wing mechanism. This would have reduced the sweep angles at lower speeds especially subsonic and then as the speed would increase and go through the transonic and into supersonic regimes, it would make the wings more aft by increasing the sweep angles from the point of pivot that was used to rotate the wings. This pivot point was located at around ~29 % of the chord length from the leading edge of the aircraft, due to it being the most feasible and pragmatic option considering the stability, weight, aerodynamic efficiency, and other interrelated configurations of aircraft [3].

The entire dimensions of the B2707-100 geometry, along with the location of swing wing pivots have been displayed following this in Figure 1.

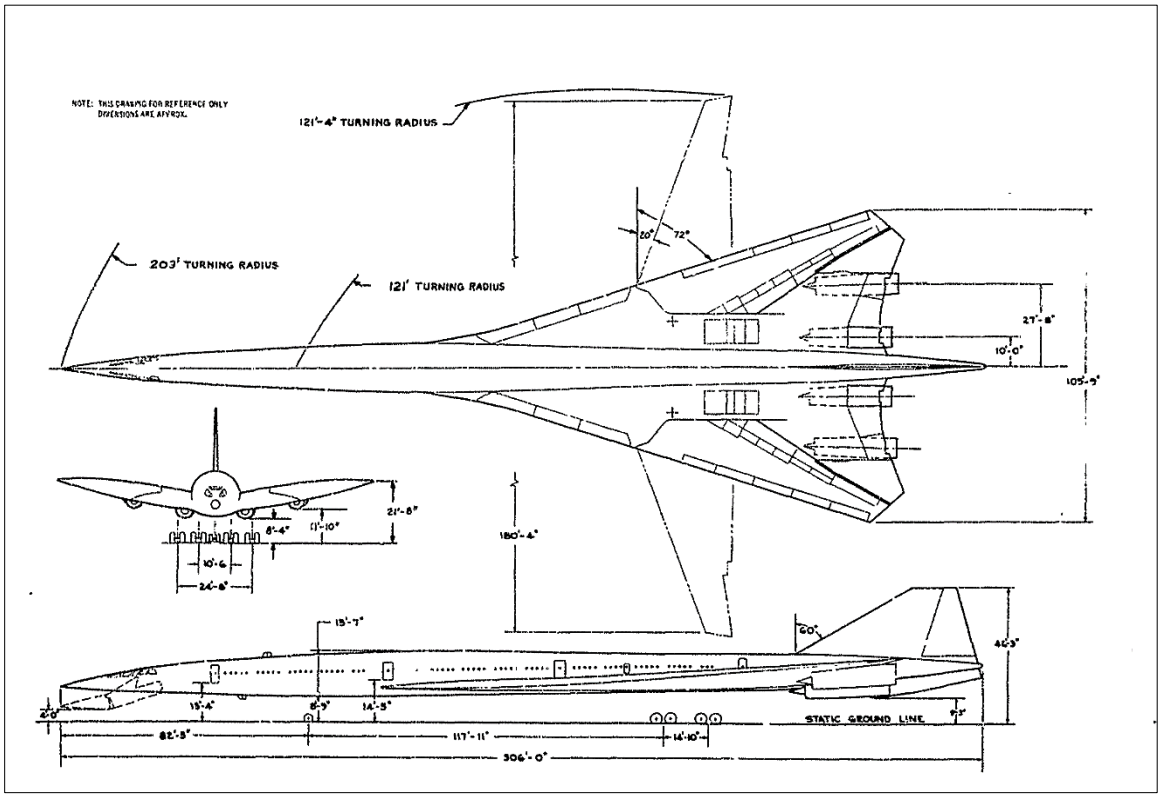

Figure 1 Geometric Dimensional Representation of Boeing B2707-100 SST

The location of pivot point was of great importance especially in the case of Boeing. If an inboard location of pivot at the side of the body was chosen, then it would have resulted in maximum wingspan, but at the same time that it would have also produced a large shift in aerodynamic center with wing sweep. Moreover, such an orientation would also have resulted in highest possible weights of the wing and pivot weights since the bending moment would also have been highest. Alternatively, if the location of pivot was chosen at outward position, then in that case it would have lowest possible wingspan, and an overbalance or rearward shift in aerodynamic center at low sweeps.

Boeing had shortlisted two companies for powering the aircraft – General Electric and Pratt and Whitney. The allowable structural weight requirement for both company's turbojet engine meant that it could have no more than 635,000 lbs. of design taxi weight, and 627,000 lbs. of maximum flight weight with flaps up configuration. The maximum design landing weight was 425,000 lbs. Whereas the only weight requirement that both engine differed were in maximum zero fuel weight, where General Electric's GE4/J5P turbojet engine would offer a 2,000 lbs. more structural design margin over the Pratt and Whitney's JTF17A-21B engine, which was rated at 357,200 lbs.

The thesis aims at using the data at a very wide range of altitudes ranging from sea level to 75,000 ft and from static to supersonic Mach numbers. The cruise altitude range of the Boeing 2707-100 airliner was supposed to be from 36,089 ft at subsonic speeds to nearly 75,000 ft at cruise conditions. This also coincides with the General Electric turbojet and turbofan engines that were proposed during the development of the aircraft. The most important engines that were supposed to be used were GE4/J4C turbojet engine and GE4/F6A turbofan engine which were both capable of reaching Mach 3 capabilities at its utmost maximum. More on this engine performances will be discussed in the propulsion database generation section later in the report.

The thesis report contains the aerodynamic database of flat plate model of airplane geometry at sweep of 20°, 25°, 30°, 35°, 40°, 45°, 50°, 55°, 60°, 65°, and the maximum aft sweep configuration of 72°. This process helps to understand and compare the performance differences observed at different sweep angle during the flight. The different configurations of wing are displayed in images below along with design orientation (72° sweep).

VORLAX interpreted model for 20° wing sweepback angle (red part is swing wing) along with on-design wing orientation (72°) have been displayed following this in Figure 2 and Figure 3.

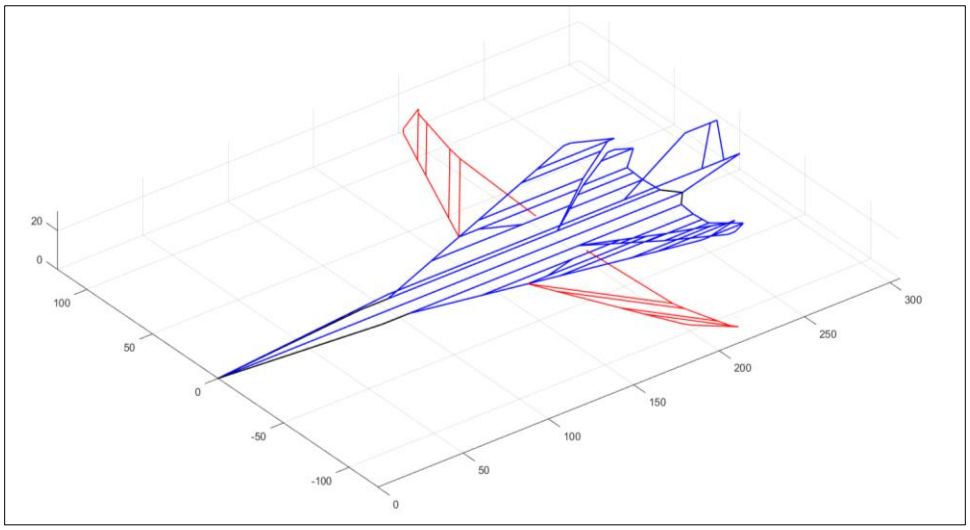

Figure 2 MATLAB Isometric View of Boeing B2707-100 with Sweep Angle of 20º

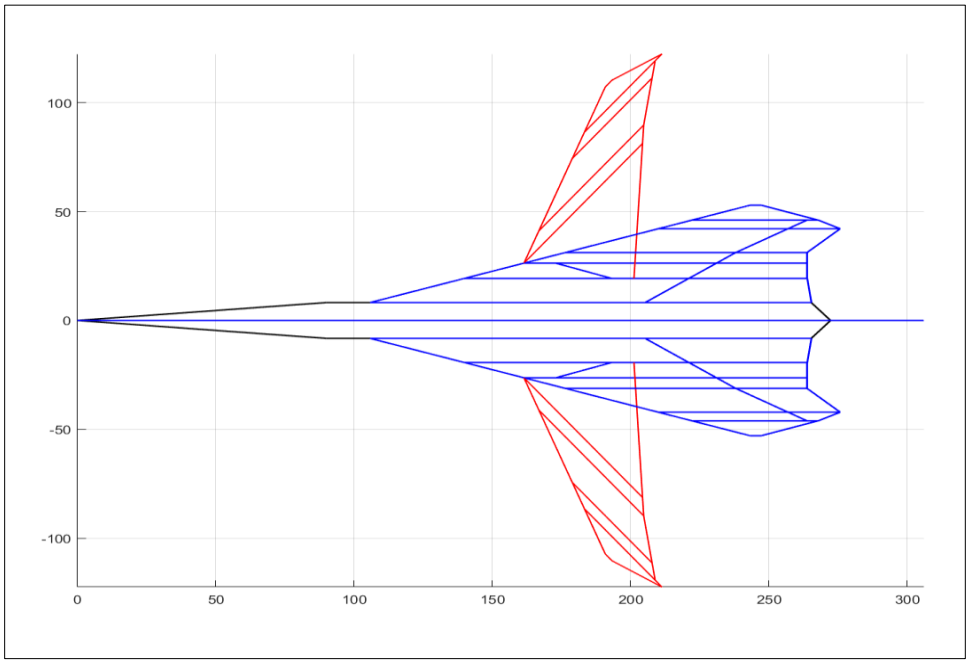

Figure 3 MATLAB Top View of Boeing B2707-100 with Sweep Angle of 20º

VORLAX interpreted model for 25° wing sweepback angle (red part is swing wing) along with on-design wing orientation (72°) have been displayed following this in Figure 4 and Figure 5.

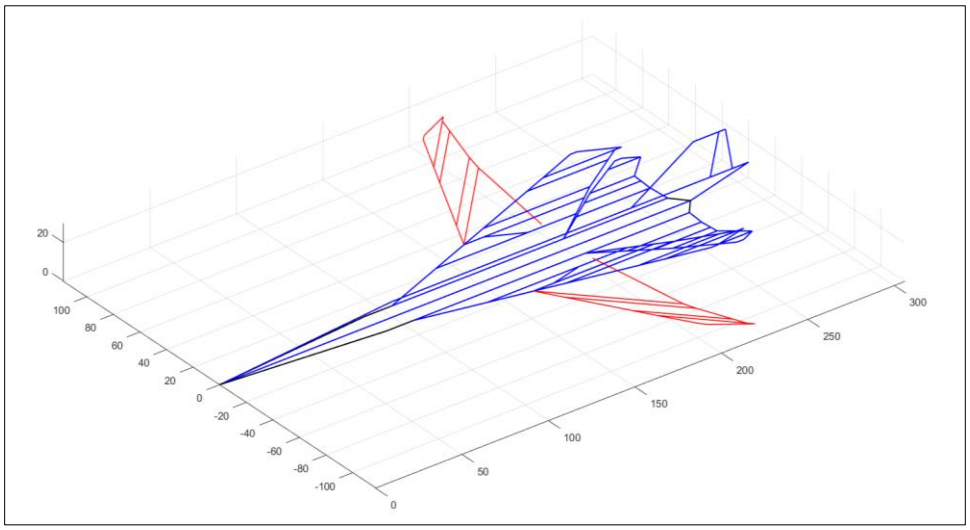

Figure 4 MATLAB Isometric View of Boeing B2707-100 with Sweep Angle of 25º

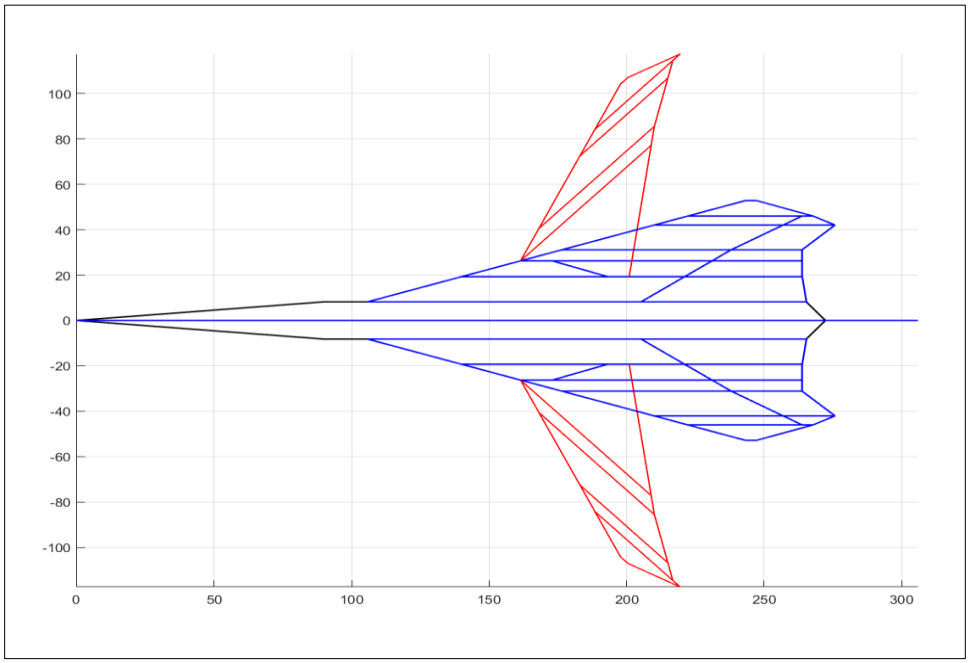

Figure 5 MATLAB Top View of Boeing B2707-100 with Sweep Angle of 25º

VORLAX interpreted model for 30° wing sweepback angle (red part is swing wing) along with on-design wing orientation (72°) have been displayed following this in Figure 6 and Figure 7.

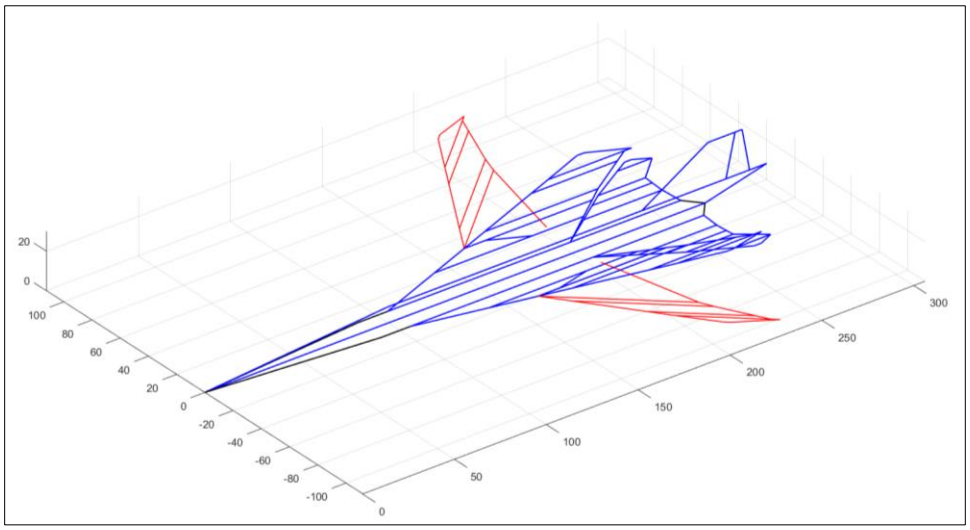

Figure 6 MATLAB Isometric View of Boeing B2707-100 with Sweep Angle of 30º

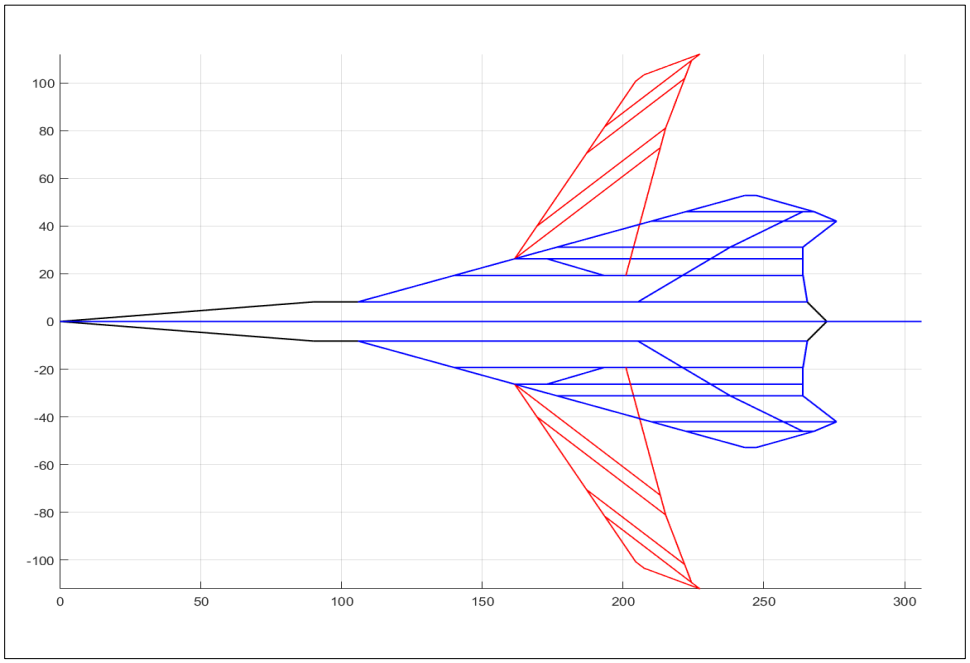

Figure 7 MATLAB Top View of Boeing B2707-100 with Sweep Angle of 30º

VORLAX interpreted model for 35° wing sweepback angle (red part is swing wing) along with on-design wing orientation (72°) have been displayed following this in Figure 8 and Figure 9.

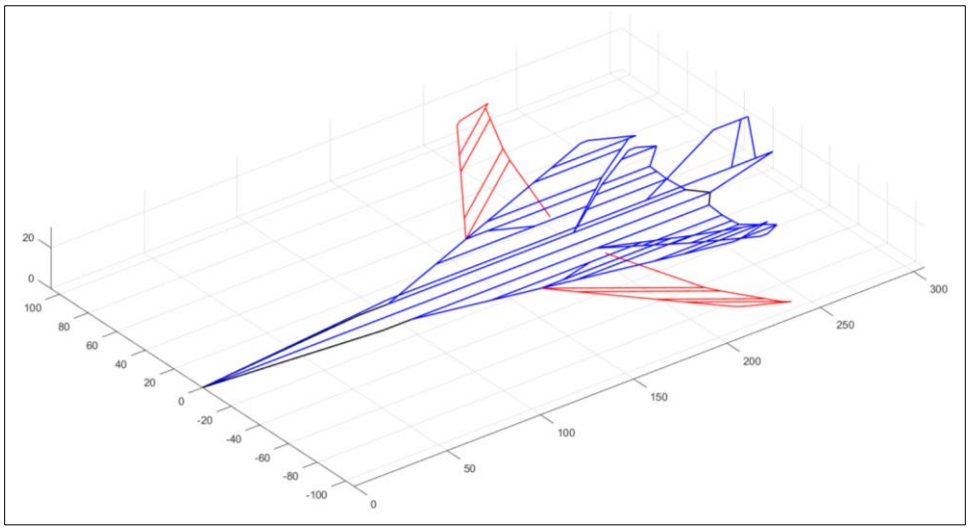

Figure 8 MATLAB Isometric View of Boeing B2707-100 with Sweep Angle of 35º

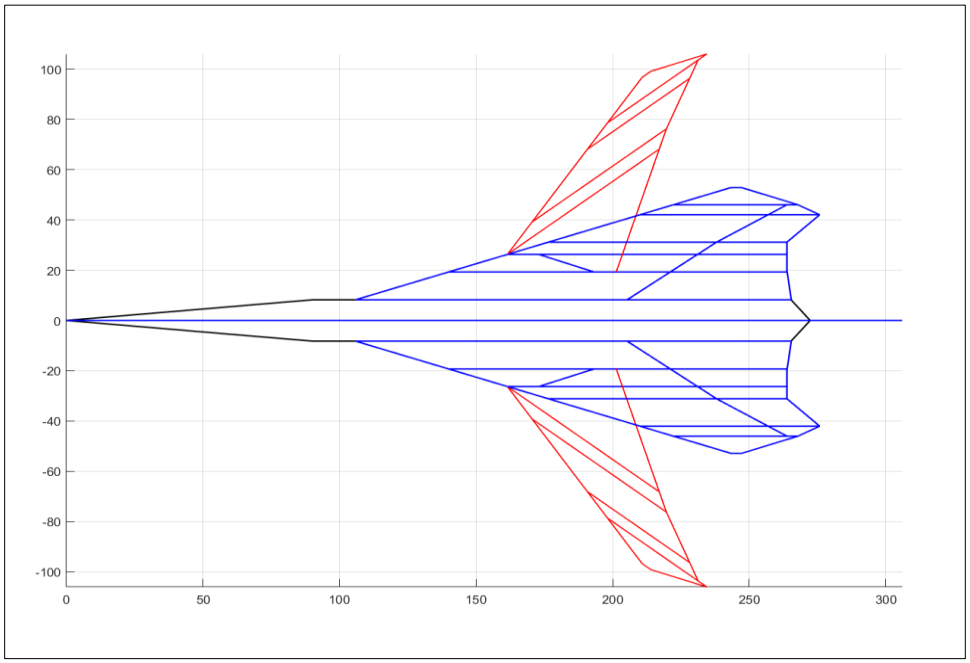

Figure 9 MATLAB Top View of Boeing B2707-100 with Sweep Angle of 35º

VORLAX interpreted model for 40° wing sweepback angle (red part is swing wing) along with on-design wing orientation (72°) have been displayed following this in Figure 10 and Figure 11.

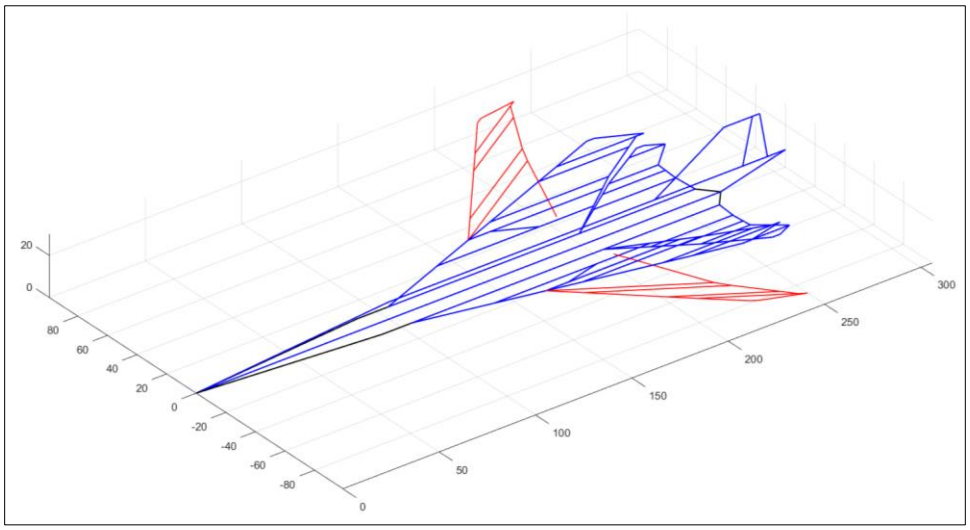

Figure 10 MATLAB Isometric View of Boeing B2707-100 with Sweep Angle of 40º

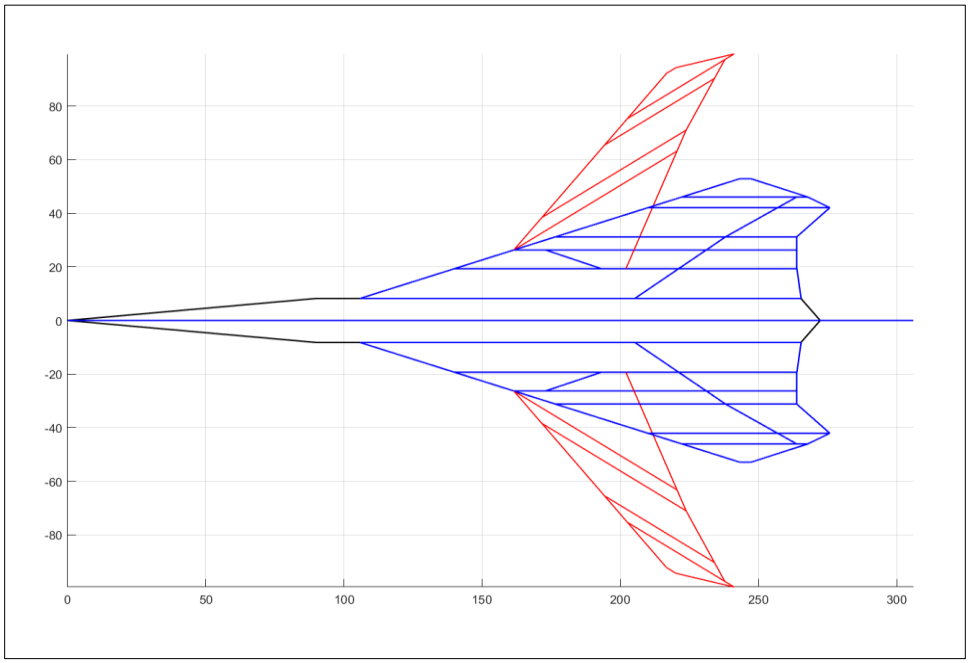

Figure 11 MATLAB Top View of Boeing B2707-100 with Sweep Angle of 40º

VORLAX interpreted model for 45° wing sweepback angle (red part is swing wing) along with on-design wing orientation (72°) have been displayed following this in Figure 12 and Figure 13.

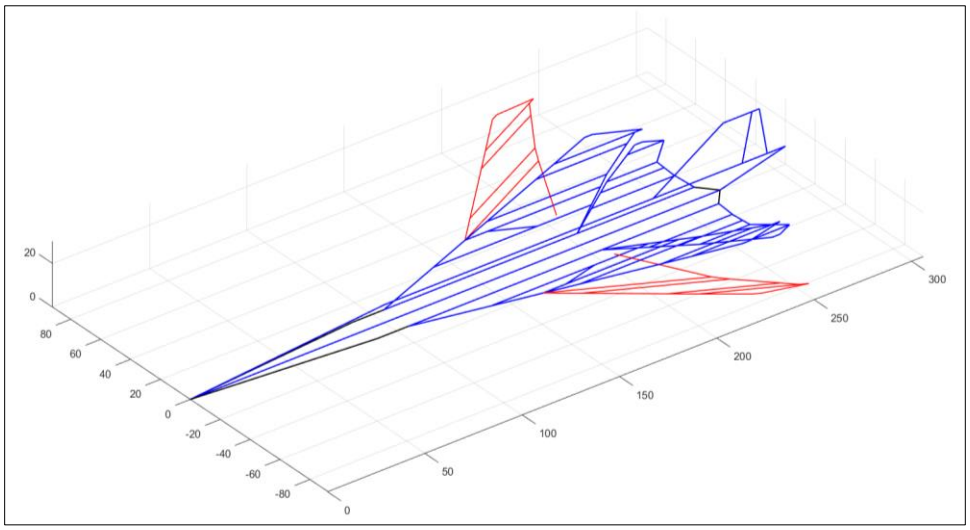

Figure 12 MATLAB Isometric View of Boeing B2707-100 with Sweep Angle of 45º

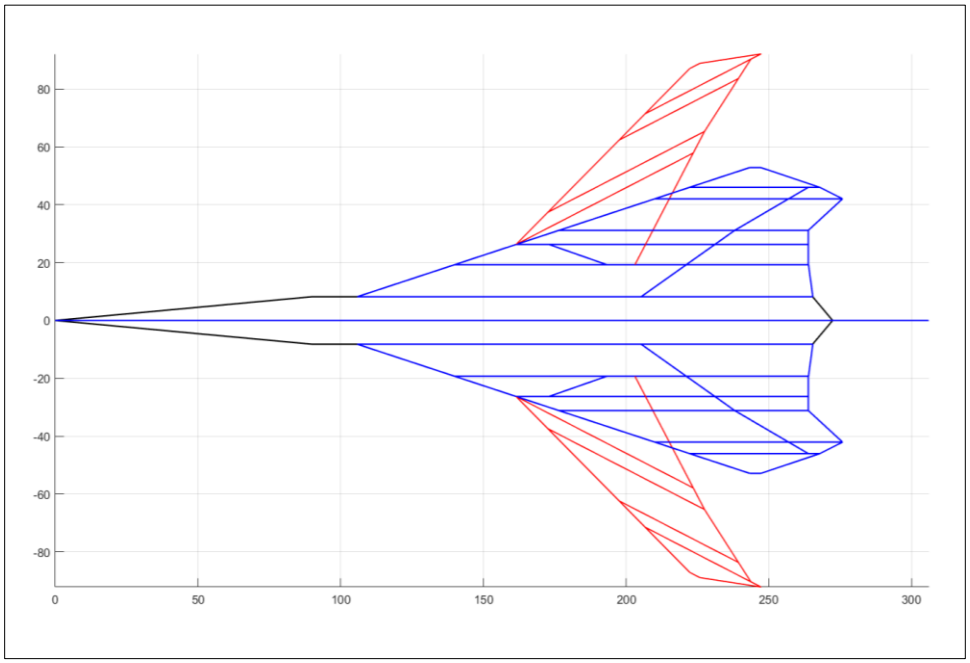

Figure 13 MATLAB Top View of Boeing B2707-100 with Sweep Angle of 45º

VORLAX interpreted model for 50° wing sweepback angle (red part is swing wing) along with on-design wing orientation (72°) have been displayed following this in Figure 14 and Figure 15.

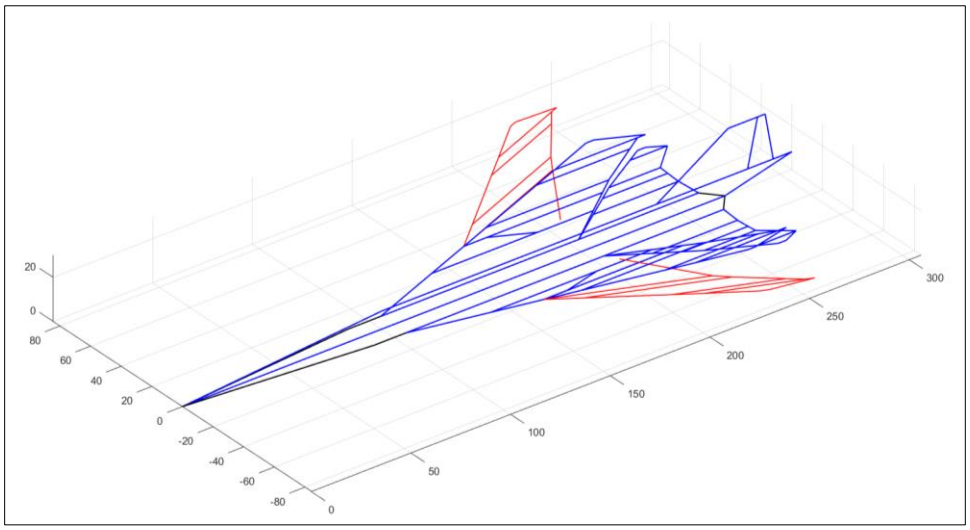

Figure 14 MATLAB Isometric View of Boeing B2707-100 with Sweep Angle of 50º

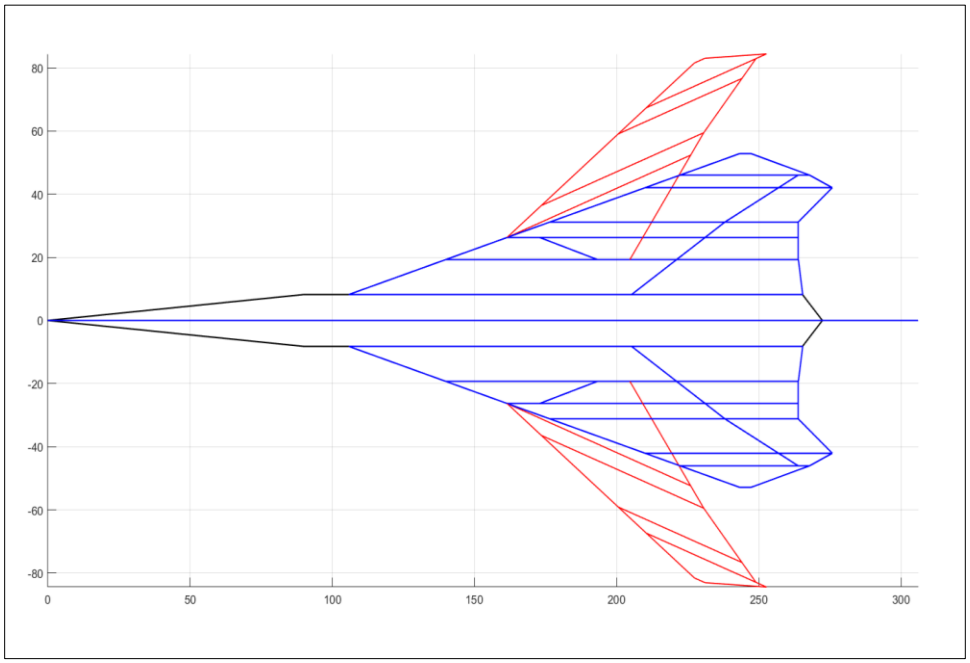

Figure 15 MATLAB Top View of Boeing B2707-100 with Sweep Angle of 50º

VORLAX interpreted model for 55° wing sweepback angle (red part is swing wing) along with on-design wing orientation (72°) have been displayed following this in Figure 16 and Figure 17.

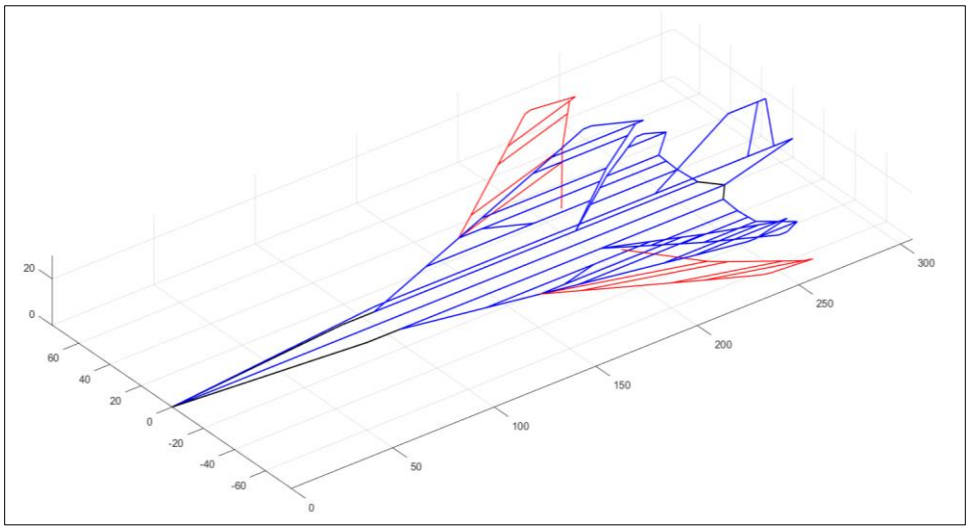

Figure 16 MATLAB Isometric View of Boeing B2707-100 with Sweep Angle of 55º

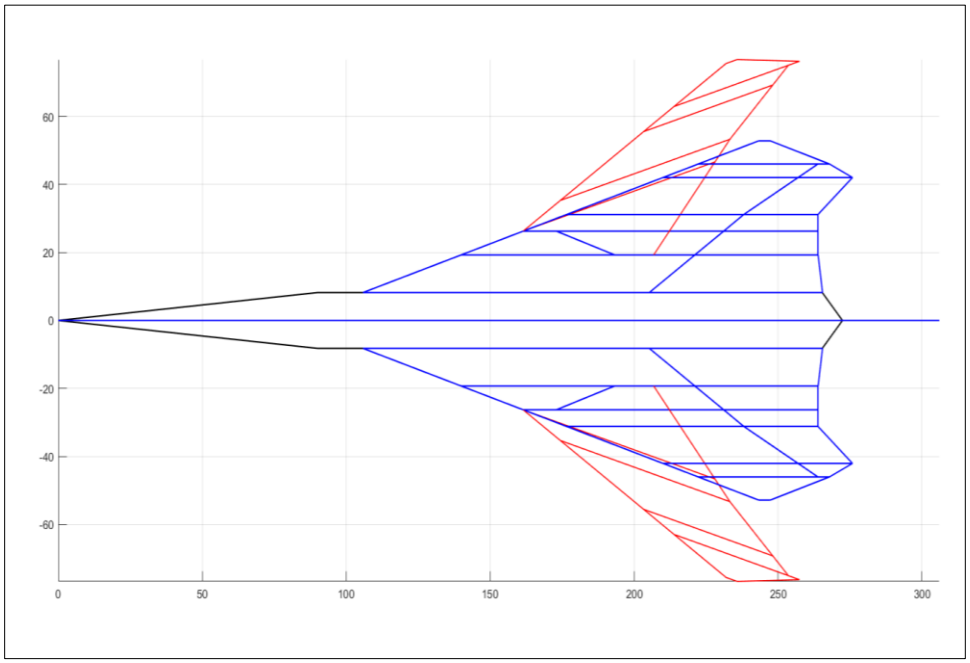

Figure 17 MATLAB Top View of Boeing B2707-100 with Sweep Angle of 55º

VORLAX interpreted model for 60° wing sweepback angle (red part is swing wing) along with on-design wing orientation (72°) have been displayed following this in Figure 18 and Figure 19.

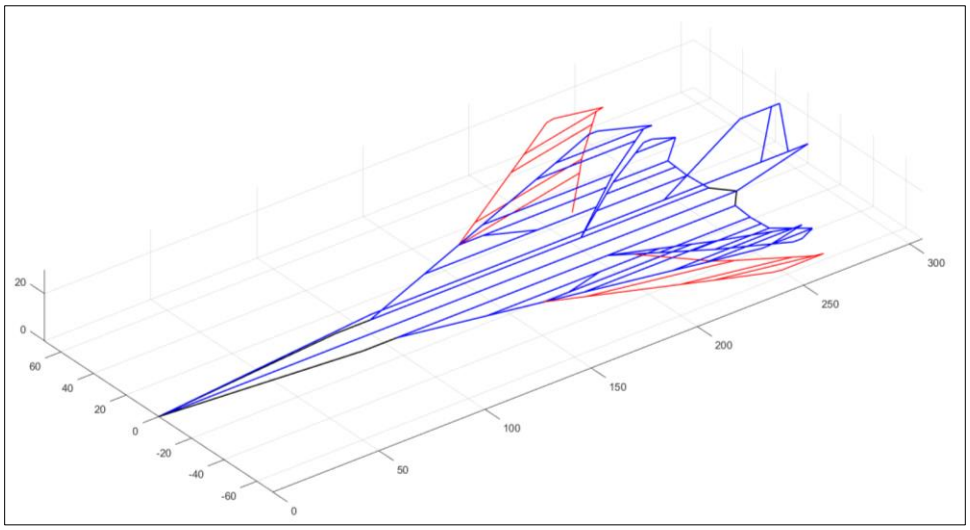

Figure 18 MATLAB Isometric View of Boeing B2707-100 with Sweep Angle of 60º

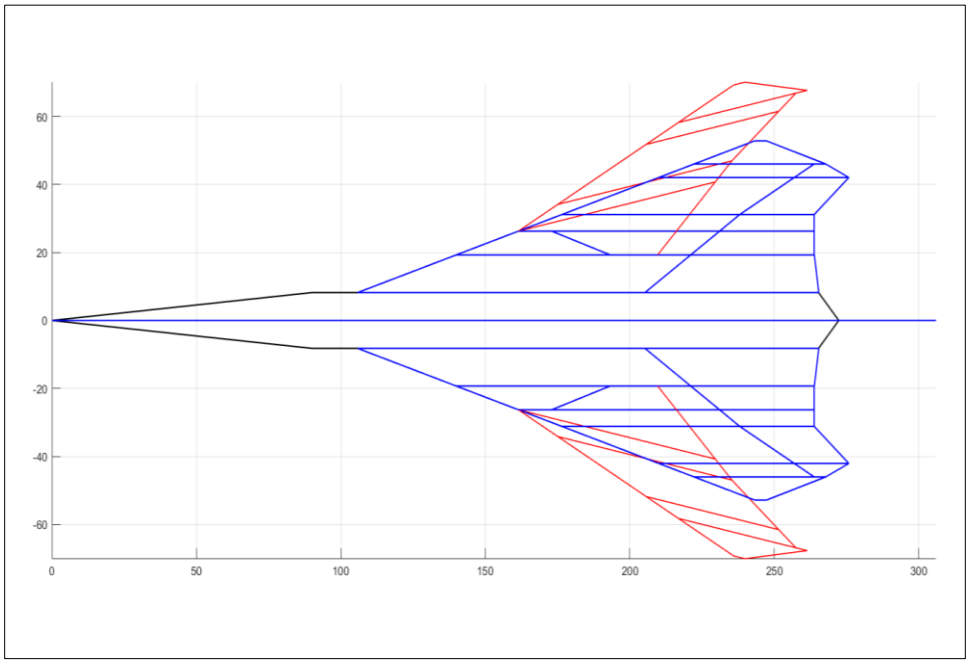

Figure 19 MATLAB Top View of Boeing B2707-100 with Sweep Angle of 60º

VORLAX interpreted model for 65° wing sweepback angle (red part is swing wing) along with on-design wing orientation (72°) have been displayed following this in Figure 20 and Figure 21.

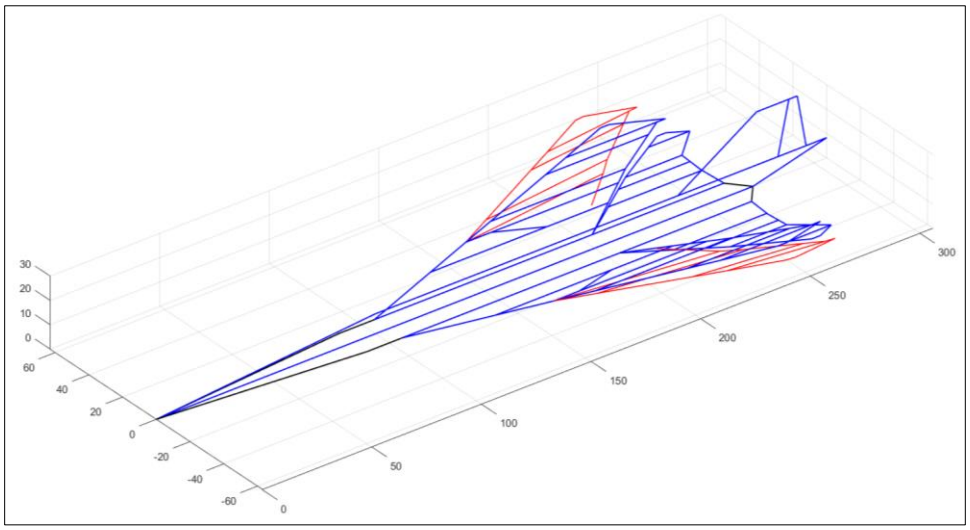

Figure 20 MATLAB Isometric View of Boeing B2707-100 with Sweep Angle of 65º

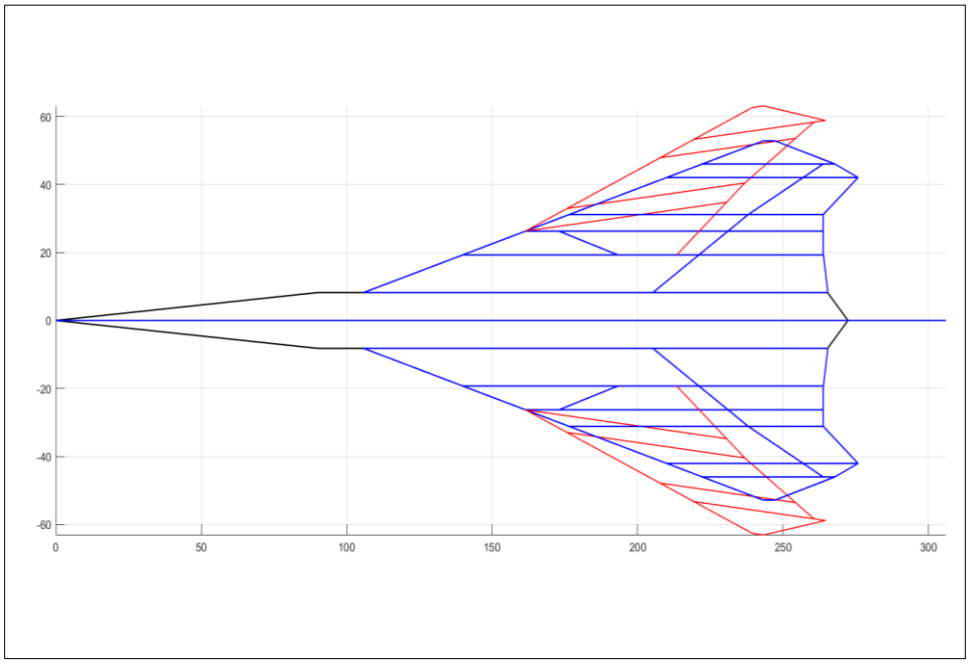

Figure 21 MATLAB Top View of Boeing B2707-100 with Sweep Angle of 65º

VORLAX interpreted model for 72° wing sweepback angle (red part is swing wing) which makes the wing planform look like delta wing upon aligning with the horizontal tail have been displayed following this in Figure 22 and Figure 23.

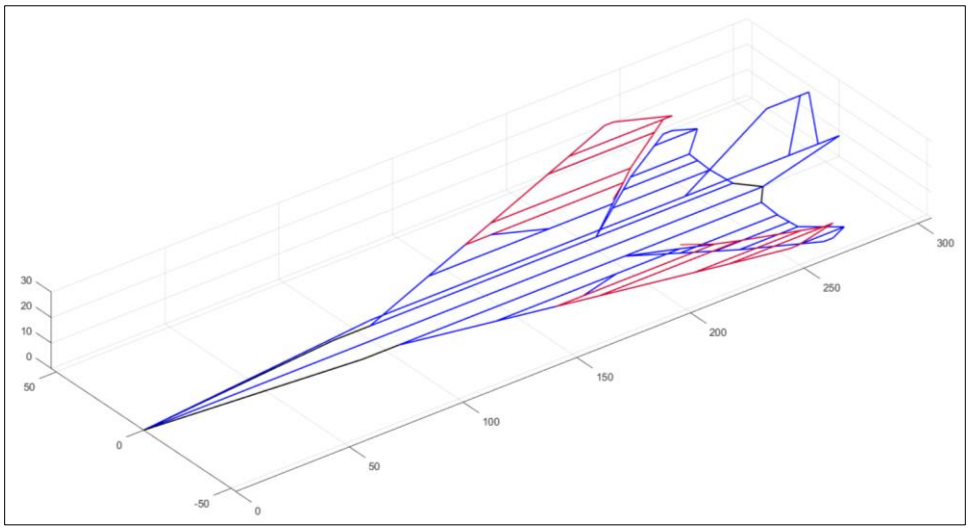

Figure 22 MATLAB Isometric View of Boeing B2707-100 with Sweep Angle of 72º

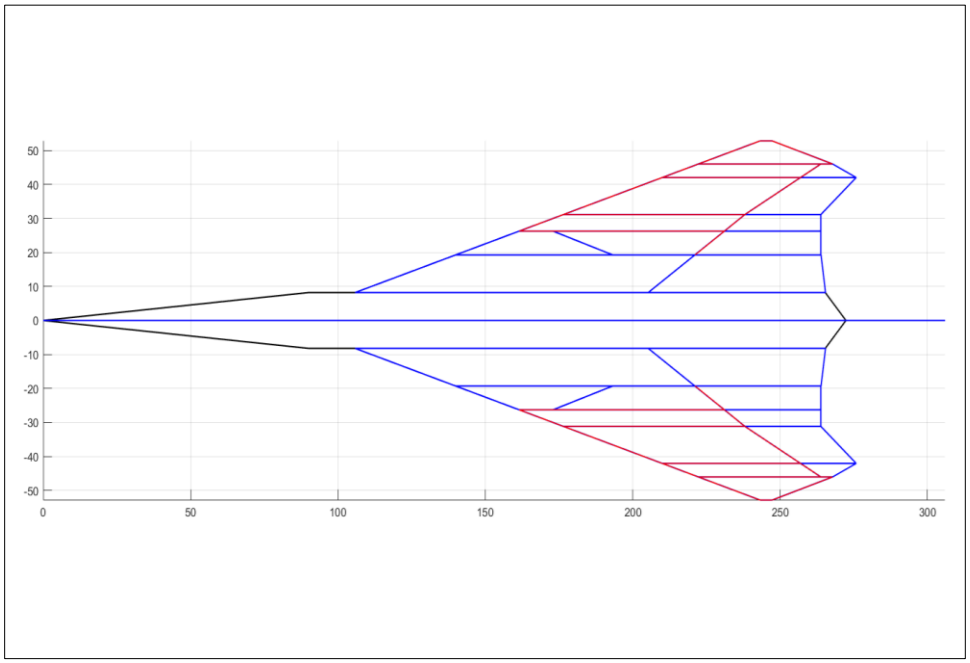

Figure 23 MATLAB Top View of Boeing B2707-100 with Sweep Angle of 72º

Since, the main aim of this research lies underneath understanding the feasibility of such a swing wing aircraft, the wing thickness used for research remains unchanged from what was supposed to be used in the Boeing B2707-100 SST. The maximum wing thickness is 4% of the chord length at around 30% of chord length at design condition configuration of wing. However, this location of maximum thickness varies based on the sweep angle changes. The explanation for this lies in the fact that since the wing is designed for the cruise condition, hence for any off-design orientation of wing the maximum thickness starts to shift away from the mean line of on design condition based on the direction of sweep. If the sweep increases, the maximum thickness point moves towards the intended location and vice versa.

The values mentioned in Table 1 are of utmost importance throughout the estimation of flight performance and hence will be used throughout the span of this thesis especially for estimation of coefficient of drag due to shockwave generation. They will be used along with the Mach number performance at each combination of altitudes and power setting to generate aerodynamics and propulsion database packages which will be used in together to simulate performance of the so formed aircraft to study its performance in detail.

The following table provides information on the average position of the maximum thickness point on the wing with respect to the sweep angle.

Sweep Angle of Wing	*Average Maximum Thickness Position in terms of % Chord Length from Leading Edge*	*Thickness in terms of % Chord length at 30% of Chord Length*
72 ^{o} (Design Condition)	30 %	4 %
65 ^{o}	27.53 %	3.97 %
60 ^{o}	26.20 %	3.95 %
55 ^{o}	25.62 %	3.92 %
50 ^{o}	24.72 %	3.89 %
45 ^{o}	24.24 %	3.87 %
40 ^{o}	23.74 %	3.84 %
35 ^{o}	23.35 %	3.83 %
30 ^{o}	22.68 %	3.81 %
25 ^{o}	22.33 %	3.78 %
20 ^{o}	22.15 %	3.72 %

Table 1 Thickness Variation Due to Change in Sweep of Wing on B2707 SST

3. TOOLS AND PROCESSES

3.1. VORLAX Overview

VORLAX is a linear panel method computational fluid dynamic (CFD) code, sponsored by NASA [4]. Its goal is to estimate aerodynamics performance parameters such as force and moment coefficients. It was released in December of 1977 for NASA under Contract NAS1-12972 by the then Lockheed-California Company. VORLAX was originally coded in FORTRAN 66.

VORLAX uses perturbation velocity components to compute the pressure coefficients. Force and moment coefficients are estimated by numerically integrating the pressure coefficient distribution while considering the effects of the edge forces on it. Based on the spacing of lattices, different approaches are used to calculate leading edge suction in VORLAX software. The cosine chordwise lattice spacing carries out the computation of leading edge suction using Lan's procedure [5]. On the flip side, for the equal chordwise lattice spacing, the contribution of the leading edge suction singularity to forces and moments is calculated using the method illustrated in Hancock's paper [6].

This computer program is specifically designed for the aerodynamic analysis and design of arbitrary aircraft configurations in subsonic and supersonic flow. The program can analyze configurations defined as a series of three dimensional non-planar quadrilateral elements with the nose tip being considered as the origin of the system. The program has by default been assigned the air flow in positive *x*-direction, which also is the axial direction for the fuselage, whereas the lateral components are usually used to define the wing

planform and canards of the aircraft. The thickness effects for non-flat plate models can be simulated using biplanar “sandwich” arrangements.

By feeding the input values of the aircraft at correct spacing as mentioned in the NASA published instruction manual for VORLAX coding support, VORLAX will estimate the flight whether it be design or off-design condition and produce an output file of various aerodynamic performance parameters of the given airplane geometry that will help enhance understanding of the dynamics and characteristics of the inputted airplane. Lockheed produced a manual that fully explains the working process of the VORLAX program. A detailed analysis and clarification of the equations and calculations that VORLAX uses to estimate output data is mentioned in this document. An output file of the VORLAX program usually generate a database of six particular parameters namely: Lift coefficient (*CL*), Drag coefficient (*CD*), Lateral force coefficient (*CY*), Pitching moment coefficient (*CPM*), Rolling moment coefficient (*CRM*), and Yawing moment coefficient (*CYM*), along with this it also gives out the simulated Mach numbers and its iteration with different angles of attack (α). Other important aircraft configuration parameters displayed in this database are mean aerodynamic chord length (*CBAR*), total wing span (*WSPAN*), reference area (*SREF*), and coordinates of moment reference point (*XBAR & ZBAR*) The file also displays other input database such as sideslip angle (*PSI*) in degrees, pitch rate (*PITCHR*), roll rate (*ROLLR*) and yaw rate (*YAWR*) in degree/seconds.

Along with this a log file could also be generated by the user which has a rather more detailed database of the entire simulation. This files are particularly useful when estimating the lengthwise i.e. either chordwise or spanwise distribution of pressure or lift.

A part of the VORLAX input file used for the aerodynamic analysis at 30º wing sweep angle of the Boeing B2707 SST has been displayed following this in Figure 24.

```
B2707-100 VORLAX File - No Twist / No Camber Version - with rudder - 30 DEG SWEEP
*
*ISOLV       LAX       LAY    REXPAR       HAG    FLOATX    FLOATY    ITRMAX
   0          1         1      0.20        0.00    0.00      0.00       299
*
*NMACH      MACH
  1         3.000000
*NALPHA    ALPHA
  1         9.144000
*
*LATRL       PSI    PITCHQ     ROLLQ      YAWQ      VINF
   0    0.00        0.00     0.00     0.00     1.00
*
*
*NPAN       SREF      CBAR      XBAR      ZBAR     WSPAN
   18.00     12419     55.36      153.00      0.00    224.30
*
*123456789!123456789!123456789!123456789!----------------
*    X1        Y1        Z1      CORD1   COMMENT: BODY-H
      0.00      0.00     0.00    272.350
     90.00      8.21     0.00    175.350
*     NVOR      RNCV       SPC       PDL
     5.00     50.00      1.00      0.00
*    AINC1     AINC2       ITS       NAP    IQUANT     ISYNT       NPP
    0.0000       0.0000     0     0         2       0         0
*
*    X1        Y1        Z1      CORD1   COMMENT: BODY-V
      0.00      0.00     0.00    272.350
    100.00      0.00     8.21    206.000
*     NVOR      RNCV       SPC       PDL
     5.00     50.00      1.00      0.00
*    AINC1     AINC2       ITS       NAP    IQUANT     ISYNT       NPP
    0.0000    0.0000       0      0       1         0         0
*
*    X1        Y1        Z1      CORD1   COMMENT: WING1 - 72 DEG SWEEP
    105.83      8.21     0.00    99.441
    139.93     19.29     2.44    81.170
*     NVOR      RNCV       SPC       PDL
    7.00     10.00      1.00      0.00
*    AINC1     AINC2       ITS       NAP    IQUANT     ISYNT       NPP
    0.0000    0.0000       0      0       2         0         0
*
*    X1        Y1        Z1      CORD1   COMMENT: WING2
    139.93     19.29     2.44    53.290
    161.47     26.29     3.01    11.510
*     NVOR      RNCV       SPC       PDL
    6.00     10.00      1.00      0.00
*    AINC1     AINC2       ITS       NAP    IQUANT     ISYNT       NPP
    0.0000    0.0000       0      0       2         0         0
*
*    X1        Y1        Z1      CORD1   COMMENT: WING3_VARIABLE
    193.22     19.29     2.44    7.769
    172.98     26.29     3.01    29.607
*     NVOR      RNCV       SPC       PDL
    6.00     10.00      1.00      0.00
*    AINC1     AINC2       ITS       NAP    IQUANT     ISYNT       NPP
    0.0000    0.0000       0      0       2         0         0
*
*    X1        Y1        Z1      CORD1   COMMENT: WING4_VARIABLE
    161.47     26.29     3.01    41.117
    164.28     31.16     3.41    39.418
*     NVOR      RNCV       SPC       PDL
    4.00     10.00      1.00      0.00
*    AINC1     AINC2       ITS       NAP    IQUANT     ISYNT       NPP
    0.0000    0.0000       0      0       2         0         0
*
```

Figure 24 Sample VORLAX Input File for B2707 at 30º Sweep Orientation

3.2. EDET Overview

EDET is short form for Empirical Drag Estimation Technique. It is a program written by Richard Feagin and William Morrison at Lockheed-California Company under the contract for NASA Ames Contract NAS2-8612 during the during the late 1970's [7]. It is another FORTRAN code.

Based on this technique, EDET can estimate the total configuration drag polar near the cruise lift coefficient and a wide spectrum of speed ranging from low speeds of Mach 0.1 to high supersonic speeds of Mach 3. EDET is based on the study and experiments performed on 19 subsonic and supersonic military aircrafts and 15 advanced or supercritical airfoils implementing the concepts of empirical drag correlations.

Moreover, EDET is capable of predicting Buffet Onset to a very high accuracy. To define in short, Mach buffet is a function of the speed of the airflow over the wing—not necessarily the speed of the aircraft. Any time that too great a lift demand is made on the wing, whether from too fast an airspeed or from too high an angle of attack near the Maximum Operating Speed, the "high-speed" buffet occurs. On the flip side, when an aircraft flown at a speed too slow for its weight and altitude necessitating a high angle of attack is the most likely situation to cause a low-speed Mach buffet. Buffet is a one of the very important characteristics to study when approaching the aerodynamic conceptual design of the aircraft, since it is always undesirable to fly the aircraft above the buffet onset Mach number and coefficient of lift.

The input file for EDET doesn't deal with the exact orientations of the wing planform like thickness of each individual sections of the wing. Instead, it deals with the

rather simpler yet to the point approach which uses first principle buildups from wetted area, planform area and mean thickness of the wing to be analyzed. It reads wetted areas for wing, fuselage, and interferences such as nacelles, horizontal tails, vertical tails, etc. The other primary configuration data that the program requires before being executed are aspect ratio, taper ratio, mean camber percentage, tech factor to classify between Whitcomb and Peaky airfoil design, fuselage dimensions, and crud factor. Along with this, the input file should also provide reference altitude and Mach number along with enough evidence of existence of any extra interference objects by defining its length, area, fineness ratio and if any increment to zero lift drag coefficient by each component.

The output file generated by the EDET program consists of inputs that were parsed to the program to establish the geometry and system. Along with this, the database for the total drag of the aircraft is also available along with breakdown for each components including interference objects. Following this are the databases of important terms that might come handy while estimating aerodynamic performance of the aircrafts. Firstly, there is a very large database of iterations of Mach number and altitudes ranging from sea level to 85,000 ft along with its corresponding value for any change in drag coefficients from cruise condition. Following this is a drag polar database for combinations of Mach numbers and angle of attack at reference altitude. Next comes the database of buffet coefficient of lift with coefficient of drag values due to skin friction and compressibility at different Mach numbers. The database is summed up by tables of coefficient of lift with induced drag coefficients and pressure drag coefficients.

The complete EDET input file used for the aerodynamic analysis at 30^{o} wing sweep angle of the Boeing 2707 SST has been displayed following this in Figure 25.

```
* EDET INPUT FILE - B2707-100 at 30DEG SWEEP
*
*        1         2         3         4         5         6         7         8
*2345678901234567890123456789012345678901234567890123456789012345678901234567890
*
*SREF (FT^2) AR        TC       SW25      TR
13262.      4.05       0.040      32.25    0.025
*
* SWET_WING  %CAMBER  AITEK     TRU       TRL
*234567!234567!234567!234567!234567!234567!234567!234567!234567!234567
 8532.       0.0      1.0        0.0      0.0
*
* SWET_FUSE  S_LEN    BODY_L/D  SBASE    CP_BASE
*234567!234567!234567!234567!234567!234567!234567!234567!234567!234567
 2621.      306.0     18.64      1.       -9.9
*
* CRUDFACTOR
0.28
*
* REFERENCE CONDITIONS
* REF_ALT   REF_MACH
*234567!234567!234567!234567!234567!234567!234567!234567!234567!234567
35000.        0.8
*
* EXTRA STUFF
* COMPONENT
*  S_WET      LEN      TC/FR   DELTA_CD0
V-TAIL
*234567!234567!234567!234567!234567!234567!234567!234567!234567!234567
 843.        21.84     0.025    0.000000
H-TAIL
*234567!234567!234567!234567!234567!234567!234567!234567!234567!234567
 1266.       46.05     0.025    0.000000
```

Figure 25 Sample EDET Input File for B2707 at 30^{o} Sweep Orientation

3.3. D2500 WAVEDRAG Overview

D2500 Wavedrag program was written by Roy V. Harris Jr. for NASA at Langley Research Center during the early 1964 [8]. It is based on the concepts of Whitcomb's supersonic area rule and was written in FORTRAN language. The program aims at estimating the drag associated with formation of shock waves around the aircraft whilst in transonic and supersonic speeds. The area rule also known as Whitcomb area rule termed after Richard T. Whitcomb for discovering this phenomenon, says that two aircrafts with identical longitudinal cross-sectional area should have the same wave drag, irrespective of how the area has been distributed laterally over the entire wingspan of aircraft [9].

Additionally, the rule also states that in order to avoid the formation of strong shockwaves, the total area distribution should be as gradual and smooth as possible. For this reason, many of the aircrafts flying in and around the transonic speed range, often have a waisted fuselage when they are integrated with wings. This phenomenon of narrowing the area of fuselage near the wings is also called as "coke bottling" area-ruling. This phenomenon is also used near the canopy of military aircrafts and horizontal and vertical stabilizers at the rear end of the aircraft. To make it useful for even higher Mach numbers, a few more efforts were put in that culminated in development of the supersonic area rule, which also uses the equivalent body area distribution but harder to implement than transonic area rule.

The input file for D2500 wave drag analysis program is in column sensitive format. The key contributors to the inputs to this program are defined by filling up the control records in the first line of the file with values defining various configuration elements. The next control card specifies the reference area of the aircraft. The cards following this define the profiles of wings, fuselage, pod/nacelle, fins (vertical orientation only), canards (horizontal orientation only), in the same order as mentioned here. Wavedrag considers the longitudinal *x*-coordinates value for wing, fin, and canard as non-dimensional whereas those for fuselage and pod are considered dimensional. Following this, the user specifies the different cases of simulation at which the program is expected to run such as Mach number entries, total number of angle of attack, etc.

The main output file contains the final results of wavedrag coefficient, *D/Q* associated with it and volume of the aircraft along with the test case Mach numbers. D2500 also produces a detailed output log with an enriched set of data actually used for calculation of fuselage area distribution along the length of the fuselage, the area distribution along longitudinal direction for *S(B), S(BW), S(BWP), S(BWPF), S(BWPFC)* where each sectional areas of wing, pods, fins, and canards are added to fuselage body as we go towards right in the log file. This database repeats for each Mach number and angle of attack. This database file also contains the *D/Q* associated with each theta angle for every case of Mach number. Upon completion of each case, an optimum cross-sectional area of equivalent body is displayed in the similar additive area format as mentioned above. And additional section of coefficient of zero-lift wavedrag is also mentioned which displays the optimal wavedrag coefficient, average equivalent body wavedrag coefficient, and any potential change in wavedrag if needed due to transfer in area.

The complete D2500 input file used for the aerodynamic analysis at 30º wing sweep angle of the Boeing 2707 SST has been displayed following this in Figure 26.

```
BHARGAV'S B2707-100 AIRLINER 30 deg SWEEP
*J0 J1 J2 J3 J4 J5 J6#AF#ORFUS#R1#F1#R2#F2#R3#F3#R4#F4POD#POFIN#FOCAN#CO
*23123123123123123123123123123123123123123123123123123123123123123123123123123
  1 -1 -1  0  1  1 -1 10 10  1 12 20  0  0  0  0  0  0  0  0  1 10 2 10 CONTROL
*234567
12419.0                                                                 REFA
*2341234123412341234123412341234123412341234123412341234123412341234123412341234
  0.000 05.000 10.000 20.000 30.000 40.000 50.000 60.000 80.000100.000  XAF 1
*234567!234567!234567!234567!
105.83   8.21   0.00  99.441                                           WAFORG  1
139.93  19.29   2.44  81.170                                           WAFORG  2
139.93  19.29   2.44  61.059                                           WAFORG  3
161.47  26.29   3.01  41.117                                           WAFORG  4
164.28  31.16   3.41  39.418                                           WAFORG  5
170.58  42.07   4.29  35.610                                           WAFORG  6
172.88  46.05   4.62  34.221                                           WAFORG  7
193.14  81.14   7.48  20.997                                           WAFORG  8
209.50 109.47   9.78  14.169                                           WAFORG  9
225.30 112.15  10.00   2.500                                           WAFORG 10
*234567!234567!234567!234567!234567!234567!234567!234567!234567!234567
 0.0000 1.100  1.561  1.913  2.001  1.934  1.765  1.521  0.874  0.0000  WAFORD  1-1
 0.0000 1.100  1.561  1.913  2.001  1.934  1.765  1.521  0.874  0.0000  WAFORD  2-1
 0.0000 1.100  1.561  1.913  2.001  1.934  1.765  1.521  0.874  0.0000  WAFORD  3-1
 0.0000 1.100  1.561  1.913  2.001  1.934  1.765  1.521  0.874  0.0000  WAFORD  4-1
 0.0000 1.250  1.750  2.001  1.955  1.845  1.680  1.430  0.800  0.0000  WAFORD  5-1
 0.0000 1.250  1.750  2.001  1.955  1.845  1.680  1.430  0.800  0.0000  WAFORD  6-1
 0.0000 1.250  1.750  2.001  1.955  1.845  1.680  1.430  0.800  0.0000  WAFORD  7-1
 0.0000 1.250  1.750  2.001  1.955  1.845  1.680  1.430  0.800  0.0000  WAFORD  8-1
 0.0000 1.250  1.750  2.001  1.955  1.845  1.680  1.430  0.800  0.0000  WAFORD  9-1
 0.0000 1.250  1.750  2.001  1.955  1.845  1.680  1.430  0.800  0.0000  WAFORD 10-1
*234567!234567!234567!234567!234567!234567!234567!234567!234567!234567
  0.00  16.11  32.21   48.32  64.42  80.53  90.00 112.74 128.84 144.95  XFUS 1-1
161.05 177.16 193.26  209.37 225.47 241.58 257.68 272.35 289.89 306.00  XFUS 1-2
*234567!234567!234567!234567!234567!234567!234567!234567!234567!234567
  0.00   6.79  27.15  61.10 108.62 169.72  211.76 211.76 211.76 211.76  FUSARD 1-1
211.76 211.76 211.76 211.76 211.76 211.76  211.76 211.76  48.54   0.00  FUSARD 1-2
* XLE ! YLE ! ZLE ! CHORD! XLE2 ! YLE2 ! ZLE2 ! CHORD!
*23456!23456!23456!123456!123456!123456!123456!123456!
238.05  0.0   8.21  58.56  274.0   0.0   30.05  18.58                   FINORG
*23456!23456!23456!123456!123456!123456!123456!123456!123456!123456! %chord
0.0    10.0   20.0   30.0   40.0   50.0   60.0   70.0   80.0   100.0    XFIN
*23456!23456!23456!123456!123456!123456!123456!123456!123456!123456! ordinates
0.0    .45    .80    1.05   1.20   1.25   1.20   1.05   .80    0.0      FINORD
* XLE ! YLE ! ZLE ! CHORD! XLE2 ! YLE2 ! ZLE2 ! CHORD!
*23456!23456!23456!123456!123456!123456!123456!123456!
205.27  8.21  0.00  60.16 238.05  31.16   2.91  25.78                   CANORG 1
*23456!23456!23456!123456!123456!123456!123456!123456!123456!123456! %chord
0.0    10.0   20.0   30.0   40.0   50.0   60.0   70.0   80.0   100.0    XCAN   1
*23456!23456!23456!123456!123456!123456!123456!123456!123456!123456! ordinates
0.0    .45    .80    1.05   1.20   1.25   1.20   1.05   .80    0.0      CANORD 1
* XLE ! YLE ! ZLE ! CHORD! XLE2 ! YLE2 ! ZLE2 ! CHORD!
*23456!23456!23456!123456!123456!123456!123456!123456!
238.05 31.16  2.91  25.78 263.84  46.05   3.50  13.07                   CANORG 2
*23456!23456!23456!123456!123456!123456!123456!123456!123456!123456! %chord
0.0    10.0   20.0   30.0   40.0   50.0   60.0   70.0   80.0   100.0    XCAN   2
*23456!23456!23456!123456!123456!123456!123456!123456!123456!123456! ordinates
0.0    .45    .80    1.05   1.20   1.25   1.20   1.05   .80    0.0      CANORD 2
*2341234123412341234123412341234123412341234123412341234123412341234123412341234
M1051050  60  20                  1                                     CASE 1
M1101100  60  20                  1                                     CASE 2
M1151150  60  20                  1                                     CASE 3
M1201200  60  20                  1                                     CASE 4
M1301300  60  20                  1                                     CASE 5
M1401400  60  20                  1                                     CASE 6
M1501500  60  20                  1                                     CASE 7
M1601600  60  20                  1                                     CASE 8
M1701700  60  20                  1                                     CASE 9
M1801850  60  20                  1                                     CASE10
M2002000  60  20                  1                                     CASE11
M3003000  60  20                  1                                     CASE12
```

Figure 26 Sample D2500 Wavedrag Input File for B2707 at 30º Sweep Orientation

3.4. Energy Maneuverability Plots Overview - Skymaps

To better understand the aircraft performance, we may plot contours of steady-state cruise conditions of the aircraft as well as climb rates at fixed power setting conditions such as maximum augmented, partial augmented, and military thrust. These contours are plotted as a function of speed of travel (Mach number of the aircraft) and altitude of the flight, this format is known as an “energy maneuverability” plot. They are an essential to study the flight performance pattern of an aircraft at steady conditions.

The energy maneuverability plots used in this report are prepared using an Excel/VBA code written by Prof. Takahashi as mentioned in his publication on Aircraft concept design performance visualization [10]. The end user can easily navigate between the hard coded formula used for estimating values at every point (consistent with the reference values used in aerodynamic and propulsion database) within the range of the contours and the plots.

A few important performance parameters that will be used to discuss the efficacy of a certain orientation during the flight at any certain Mach number and altitude level are Aerodynamic Efficiency *(L/D)*, Performance Efficiency (*M(L/D)*), Specific Range of the analyzed aircraft. A detailed understanding of each parameter along with the significance of each parameter on flight of the aircraft is mentioned following this.

3.5. Significance of Performance Parameters

3.5.1. Aerodynamic Efficiency *(L/D)*

The basic forces often related with the aircraft when flying are lift, weight, thrust and drag. Since, weight of the aircraft is estimated by its dimension, materials used and the payload it carries and the thrust is determined using the forward force generated by the propulsion system associated with the aircraft, hence they are not the key factor in influencing the aerodynamic prospect of the aircraft efficacy during flight. However, the other two important forces acting on the aircraft, the lift and drag forces influence the aerodynamic efficiency since they depend on the shape and size of the aircraft, condition of atmosphere and the flight speed.

The ratio of lift over the drag forces or coefficients is often referred to as the "Aerodynamic Efficiency" of the aircraft. It is very important during design process because an aircraft with high *(L/D)* ratio will either produce a relatively larger amount of lift or smaller magnitude of drag. Under the designed conditions, the lift of the aircraft is equal to weight. A high lift aircraft can carry a large payload. Likewise, at the same cruise condition, the thrust is equal to drag. A low drag aircraft requires low thrust. Thrust is achieved by exhausting fuel and a low thrust aircraft requires small amounts of fuel be burned. Hence if the *(L/D)* ratio is higher, low fuel usage allows an aircraft to stay aloft for a long time, and that means the aircraft can fly long range missions. So, an aircraft with higher *(L/D)* ratio can carry a large payload, for a long time, over a long distance compared to its counterpart with lower *(L/D)* ratio.

3.5.2. Aerodynamics Performance Efficiency (*M(L/D)*)

"Aerodynamic Performance Efficiency" is a scalar quantity derived from the above mentioned parameter used to indicate the significance and worthiness of the aerodynamic efficiency *(L/D)* at the expense of speed of the flight. It is the product of the Mach number associated with the steady-state flight and the corresponding lift over drag ratio which is obtained by dividing the coefficients of lift and drag at the same condition.

This parameter is of at least equal importance if not more to the aerodynamic efficiency. As discussed by G Gabrielli and Th von Karman, to find measure for the "price of speed", they considered the work needed to be done and concluded that for every aircraft, there is a certain limiting speed beyond which the transportation through that vehicle becomes uneconomical [11]. This term will be important to understand the rather complex nature of sweep angle economics associated with flight. In terms of economics of flying, sweep is primarily a means for reducing the flying time for a given range, by increasing the speed at no additional cost. Finally, it might not come as a surprise to hear that the *(L/D)* ratio and *M(L/D)* contours have different speed and altitude for best operating condition.

3.5.3. Specific Range *(SR)*

"Specific Range" is the horizontal distance an aircraft travels per unit of fuel consumed. Typically, this is expressed in nautical mile per pound of fuel. It can be evaluated by using the weight of the aircraft, aerodynamic and propulsion database values.

To plot the contours, the dimensional value of the specific range of aircraft is the ratio of true airspeed of flow as a function of Mach and Altitude at specific flight condition to the product of thrust specific fuel consumption (TSFC) and thrust generated by the propulsion system. Larger values for Specific Range indicate a more efficient aerostructure and vice versa.

The working interface of all the aerodynamic performance parameters using the flight envelope approach used by the solver have been displayed in Figure 27 below.

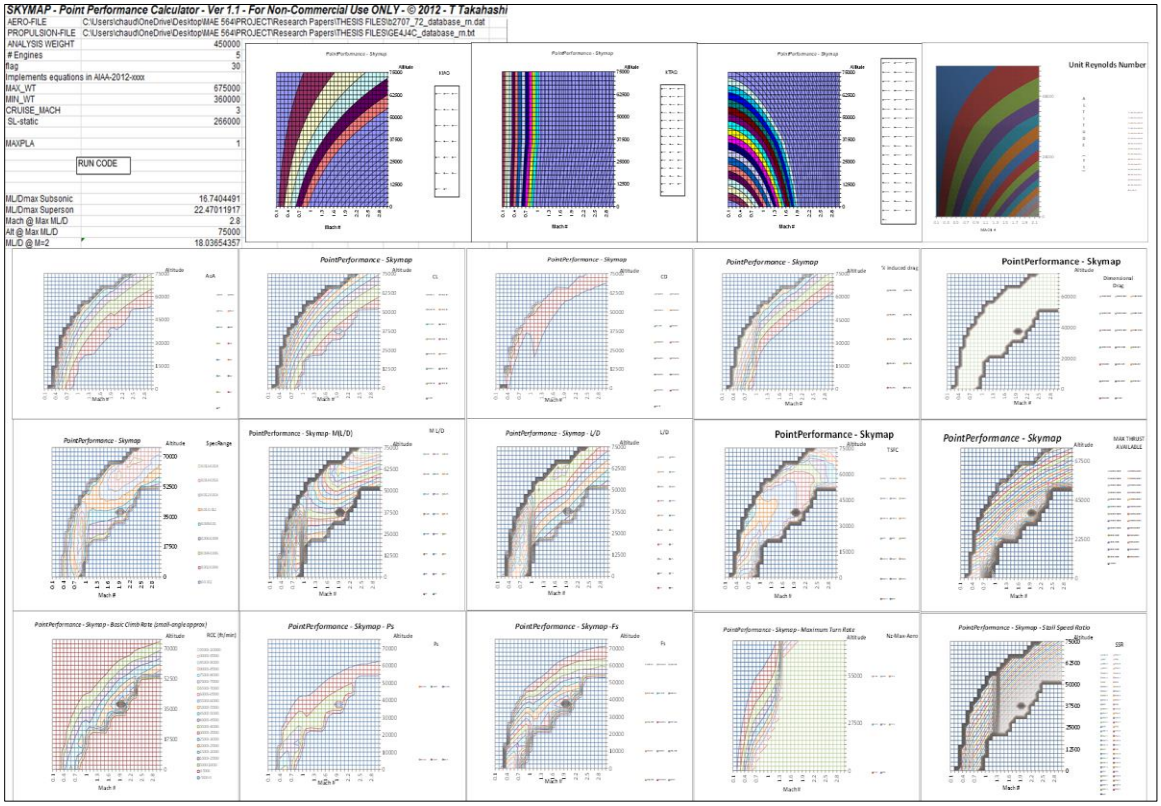

Figure 27 Sample Energy Maneuverability Plot Interface Showing Contours of Various Aerodynamics Performance Parameters

4. DATABASE GENERATION

4.1. Aerodynamic Database Generation

Aerodynamic database is a collection of important aerodynamics performance quantities that are crucial is conceptual design and analysis of an aircraft. It is important to understand what data were fed to the solvers in order to get the above mentioned results. Following are the values that defined geometry along with its surrounding and fed to different solvers in order to calculate desired parameters.

4.1.1. VORLAX

The number of panels used for designing the geometry at any instance of sweep varied between 16 to 18 based on the complexity to design orientation.

The stationary frame of the wing geometry defined in the input file for VORLAX contained fuselage (horizontal and vertical), stationary 72^{o} swept wing which would make the first part of the ogival delta planform at aft sweep condition (wing runs from fuselage i.e. wing root to the pivot of the wing for swing wing), rudder, vertical tail, and horizontal tail.

The moving part of the geometry was defined by calculating the coordinates at different rotation angles of the pivot through homogeneous transformation methods for accurately calculating 3D coordinates without neglecting rotations or twist associated with the pivots. It contained the variable wing geometry. No additional twist was provided to any panels described above in order to get desired solution.

The test was carried out for 30 iteration of Mach numbers and 15 different degrees of angle of attack to correctly capture and replicate the performance of the aircraft in under different situations.

The overview section of the underwritten solver gives details on the different outputs obtained upon solving the vortex lattice method for the given object.

4.1.2. EDET

While the EDET input file does not need the entire detailed version of the input files through panel modelling, it however works on the area, and aspect ratio followed by taper ratio and thickness of the profile to interpret the design and find the data accordingly. Hence for this purpose, reference area consistent with what was used in the VORLAX input file was used, followed by calculating the aspect ratio of the aircraft orientation at any instance of sweep being worked on by using the reference area and wing-span, the sweep angle of the 25% chord line along the wingspan direction which is always smaller than the actual leading edge sweep for this case, since the chord length varied throughout the wingspan length (decreasing from root towards tip). The highest reference area used for EDET estimation was 13584 ft^2 at 20^o sweep and the lowest was at 72^o circa 11566 ft^2. The Mach number and angle of attack runs done on VORLAX solver were extracted from the runs that EDET had performed in order to get consistent results.

4.1.3. D2500 – WAVEDRAG

WAVEDRAG input file is similar to the VORLAX input file. The similarity arises due to the details associated with the panels being designed. Since, VORLAX was a flat plate model design, it wasn't enough to accurately estimate the drag associated with shockwaves formation due to the profile of the wing in chordwise direction (i.e. thickness distribution).

Wavedrag input file contains the same data used in the VORLAX input file but in different format to any observed above in order to make it compatible for D2500 Wavedrag solver to calculate the drag associated with the aircraft at different conditions. In all the Wavedrag calculations were done above Mach 1 for obvious reason and carried out 12 test for each case of sweep. The Mach numbers here again were same as that in any other file mentioned above to get consistent results but with the exception of being above the sonic speed for D2500-Wavedrag to run accurately.

The quantities that were used for the generation of the aerodynamic database file are listed below in the Table 2 along with the source of each quantity.

Quantity	***Output Source***
Mach Number (M)	VORLAX
Angle of Attack (AoA)	VORLAX
Coefficient of Lift (C_L)	VORLAX
Coefficient of Drag (C_D)	VORLAX
Altitude (Alt)	EDET
Change in Drag Coefficient (ΔC_D)	EDET
Coefficient of Lift – Buffet ($C_{L\text{-}Buffet}$)	EDET
Coefficient of Drag – Skin Friction (C_{DF})	EDET
Coefficient of Drag – Compressibility Effect (C_{DC})	EDET
Coefficient of Drag – Wavedrag (C_{DW})	D2500 – WaveDrag

Table 2 Aerodynamic Data Extraction Sources for Aerodynamic Database File Generation

4.1.4. Aerodynamic Database Buildup

4.1.4.1. Drag Polar Values Data

The drag polar table is made by combining the results obtained from all three solvers. The drag polar table consists of data in the column sequence of Mach number, Angle of Attack, Coefficient of Lift, and Coefficient of Drag.

The first two values are easily available from the VORLAX runs that were made to be consistent with the results obtained from the EDET output file. Coefficient of Lift is directly taken from the VORLAX output file where it is obtained as a result of Mach and Angle of attack variation.

The Coefficient of Drag is relatively a harder one to build. The C_D value from VORLAX output file, which is a function of Mach and Angle of Attack is added up with the skin friction value i.e. C_{DF} to get a new skin friction influenced value. Now this new generated value is then weighed by the Mach number associated with it and then based on the it, the selection of the final coefficient of drag term is done between compressibility drag C_{DC} and wavedrag C_{DW}. If the Mach number is less than sonic speed i.e. unity, then in that case the compressibility drag is added, whereas if the Mach number is above the speed of sound, the wavedrag coefficient is added to the already calculated value.

Mathematically,

$$C_{D-Total}\,(\text{Mach}, \text{AoA}) = C_{D-VORLAX}\,(\text{Mach}, \text{AoA}) + C_{DF-EDET}\,(\text{Mach}) + \begin{cases} C_{DC-EDET}\,(Mach), & Mach < 1 \\ C_{DW-D2500}\,(Mach), & Mach \geq 1 \end{cases} \qquad \textit{Eq. 1}$$

Even though the EDET program offers the drag polar values at the above configurations of Mach and Angle of attack, one can perform a higher fidelity replacement of the table by using the above mentioned approach.

The syntax of the drag polar table implemented in the aerodynamic database file is displayed in Figure 28.

```
*****************************************
* B2707-100                              *
*****************************************
*
* SREF
 13584
* NALPHA
 15
* NMACH
 30
* NALT
 18
*
* MACH ALFA CL CD
DATA
 0.10     0.0000         0.00         0.0039
 0.10     0.6531         0.04         0.0041
 0.10     1.3063         0.07         0.0046
 0.10     1.9594         0.11         0.0054
 0.10     2.6126         0.14         0.0067
 0.10     3.2657         0.18         0.0083
 0.10     3.9189         0.21         0.0101
 0.10     4.5720         0.25         0.0124
 0.10     5.2252         0.28         0.0151
 0.10     5.8783         0.32         0.0180
 0.10     6.5315         0.35         0.0213
 0.10     7.1846         0.39         0.0249
 0.10     7.8378         0.42         0.0290
 0.10     8.4909         0.46         0.0335
 0.10     9.1440         0.49         0.0382
 0.20     0.0000         0.00         0.0036
 0.20     0.6531         0.04         0.0038
 0.20     1.3063         0.07         0.0043
 0.20     1.9594         0.11         0.0052
 0.20     2.6126         0.14         0.0063
 0.20     3.2657         0.18         0.0080
 0.20     3.9189         0.22         0.0098
 0.20     4.5720         0.25         0.0121
 0.20     5.2252         0.29         0.0148
 0.20     5.8783         0.32         0.0177
 0.20     6.5315         0.36         0.0211
 0.20     7.1846         0.39         0.0248
```

Figure 28 Drag Polar Table as Written in Aerodatabase File for 20^{o} Sweep of B2707 SST

4.1.4.2. Change in Drag coefficient from cruise altitude due to Reynolds number effect

The data for this section of database is directly extracted from the EDET file without any change. EDET returns the results of ΔC_D with respect to its corresponding Mach number and altitude.

The syntax of the change in drag coefficient iterations with altitude as implemented in the aerodynamic database file is displayed in Figure 29 below.

```
* CHANGE IN DRAG COEFFICIENT FROM CRUISE ALTITUDE
* ALTITUDE  MACH_#  DELTA_CD
      0.     0.100     -0.00061
      0.     0.200     -0.00052
      0.     0.300     -0.00047
      0.     0.400     -0.00044
      0.     0.500     -0.00042
      0.     0.600     -0.00040
      0.     0.700     -0.00039
      0.     0.750     -0.00038
      0.     0.780     -0.00037
      0.     0.800     -0.00037
      0.     0.820     -0.00037
      0.     0.840     -0.00037
      0.     0.860     -0.00036
      0.     0.880     -0.00036
      0.     0.900     -0.00036
      0.     0.920     -0.00036
      0.     0.940     -0.00036
      0.     0.960     -0.00035
      0.     1.050     -0.00034
      0.     1.100     -0.00034
      0.     1.150     -0.00033
      0.     1.200     -0.00033
      0.     1.300     -0.00032
      0.     1.400     -0.00031
      0.     1.500     -0.00030
      0.     1.600     -0.00029
      0.     1.700     -0.00028
      0.     1.800     -0.00028
      0.     2.000     -0.00026
      0.     3.000     -0.00020
   5000.     0.100     -0.00056
   5000.     0.200     -0.00047
   5000.     0.300     -0.00043
   5000.     0.400     -0.00040
   5000.     0.500     -0.00038
   5000.     0.600     -0.00037
   5000.     0.700     -0.00035
   5000.     0.750     -0.00035
   5000.     0.780     -0.00034
   5000.     0.800     -0.00034
```

Figure 29 Change in Drag Coefficient Table as Written in Aerodatabase File for 20^o Sweep of B2707 SST

4.1.4.3. Buffet Onset Data

The Buffet onset value of coefficient of lift is available in the EDET output file along with the values of skin fiction drag coefficient and compressibility drag coefficient which were used in previous steps. Coefficient of lift at buffet onset is only displayed for certain Mach numbers after which one has to manually update the values that depict that the occurrence is over by feeding in the value 1 at missing spaces. The missing spaces will continue from the buffet onset Mach number till the very last test Mach number.

The image labelled Figure 30 succeeding this illustrates the format of buffet onset values fed to the aerodynamic database file for solver to process.

```
* BUFFET ONSET
*NMACH
 30
* MACH  CL_BUFFET
 0.1           0.784
 0.2           0.779
 0.3           0.764
 0.4           0.726
 0.5           0.682
 0.6           0.634
 0.7           0.603
 0.75          0.589
 0.78          0.587
 0.8           0.593
 0.82          0.598
 0.84          0.604
 0.86          0.609
 0.88          0.626
 0.9           0.653
 0.92          0.680
 0.94          0.727
 0.96          0.775
 1.05          1.000
 1.1           1.000
 1.15          1.000
 1.2           1.000
 1.3           1.000
 1.4           1.000
 1.5           1.000
 1.6           1.000
 1.7           1.000
 1.8           1.000
 2.0           1.000
 3.0           1.000
* END
```

Figure 30 Buffet Onset Table as Written in Aerodatabase File for 20^{o} Sweep of B2707 SST

4.2. Propulsion Database Generation

The propulsion database is a wide collection of net thrust and specific fuel consumption values at different power lever angle (PLA) settings combination of Mach number and altitude. The PLA ratings are the way of sorting and identifying the high priority of power stage from the lower stages by the Skymap solver. Hence, for this purpose, the stage when afterburner is used at full capacity with the full power in normal turbojet engine is rated the highest and stands at 1, whereas on the other side, the partial power generated by engine under no augmentation is assigned the lowest PLA rating. The specifically assigned PLA ratings for this report are illustrated in the table following the specification of the engine used.

The database generated for the research work here is based on the performance of General Electric's GE4/J4C turbojet engine [12]. This is a lightweight, high performance augmented engine especially optimized for the Boeing B2707 SST. The engine has Mach 3 speed capability with a maximum altitude capacity of 80,000 ft. It has an enormous take-off thrust which soars to just under 52,000 lbs static with afterburner engaged. Based on the data available, the compression ratio of Boeing B2707's GE4 was 12.5:1, and it has a 9.5:1 overall pressure ratio at take-off.

The flight performance curves are depicted below in the images showing net thrust, and specific fuel consumption as a function of engine power setting and Mach number of the flight. These performance values were measured at Sea Level, 15,000 ft, 25,000 ft, 36,089 ft, 45,000 ft, 55,000 ft, 65,000 ft, and 75,000 ft altitude range.

This curves are based on U.S. Standard Atmosphere- 1962 [13], with no bleed or power extraction, fuel conforming to G. E. Commercial Jet Fuel. Specification A50T27A and follows MIL-E-5008B [12] standard for ram recovery which states that, ram recovery is 1 up to sonic speed, after which it reduces as a function of Mach number of the flight.

Performance parameters associated with the propulsion database generation were assessed on different power settings. This power settings are mentioned below in Table 3 with the PLA rating sequences used to make it compatible to be utilized by the energy-maneuverability curves.

Power Setting Name	***G.E. Power Setting Number***	***PLA Rating***
Maximum thrust, augmented	1	1
Partial augmentation	2	0.99
Partial augmentation	3	0.98
Minimum thrust, augmented	4	0.97
Mid power thrust	-	0.96
Maximum thrust, non-augmented	5	0.95
95% engine RPM	7	0.90
85% engine RPM	9	0.88
75% engine RPM	11	0.85

Table 3 Power Settings Incorporated in Propulsion Database File for 5 Column Data

The Mid power thrust is an averaged value of non-augmented maximum thrust i.e. military thrust and least thrust generated upon partial augmented stage. This setting is not mentioned in the General Electric report, but it proves to be very important to distinguish two different augmentation stages from each other.

The net thrust and thrust specific fuel consumption (TSFC) values as published in the General Electric's GE4/J4C engine performance report are presented below at all the testing altitudes [12]. The power setting values for TSFC at idle condition are not displayed in the chart due to inconsistent trend observed which can be often related to corresponding negative thrust and its significance on TSFC. Figures 31 through 38 are net thrust and Figures 39 through 46 are TSFC representations from the published report.

4.2.1. Net Thrust Performance Curves

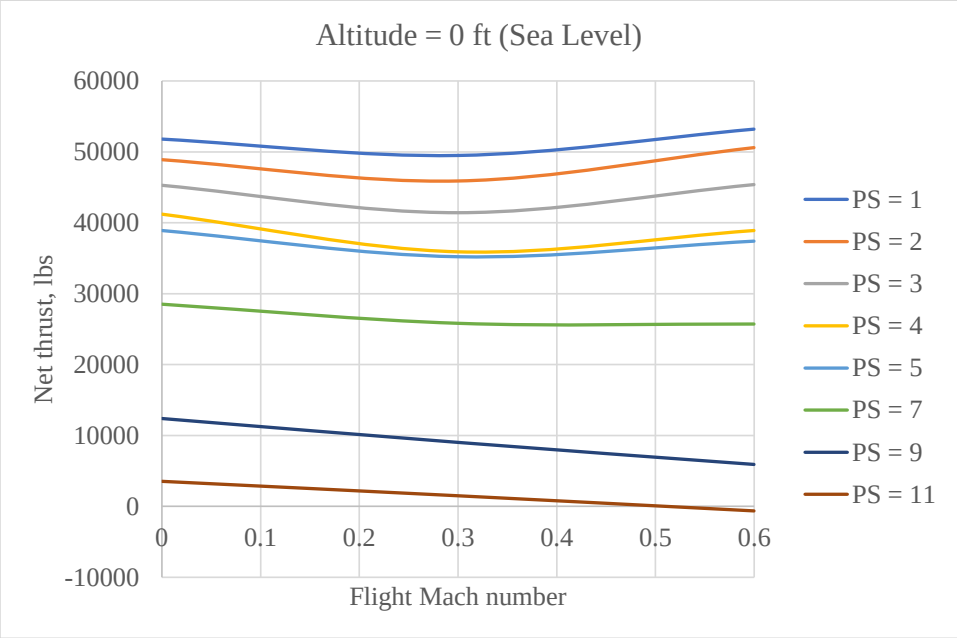

Figure 31 Variation in Net Thrust of GE4/J4C Engine at Sea Level for Different Power Settings

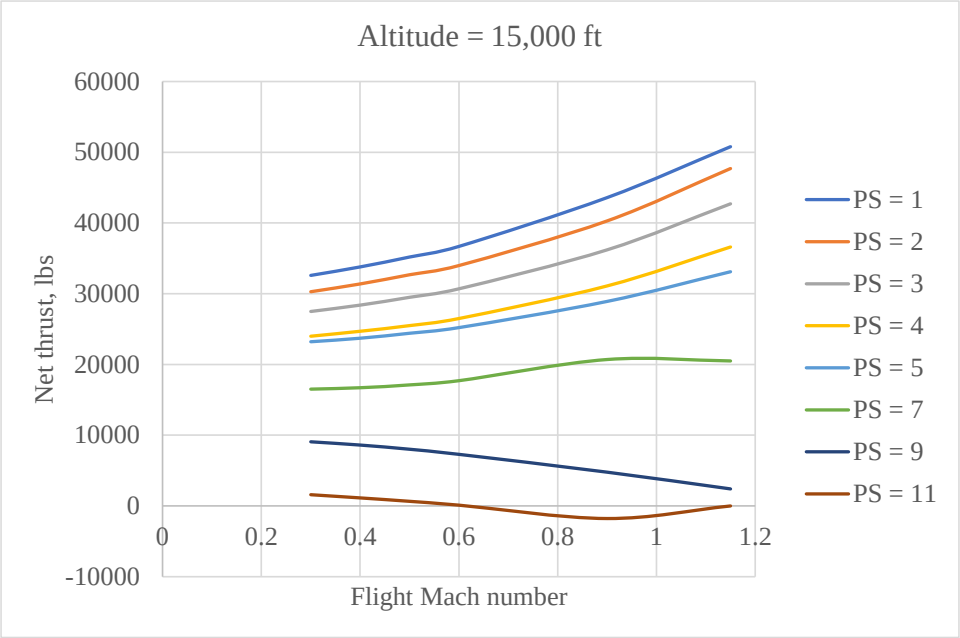

Figure 32 Variation in Net Thrust of GE4/J4C Engine at 15,000 ft for Different Power Settings

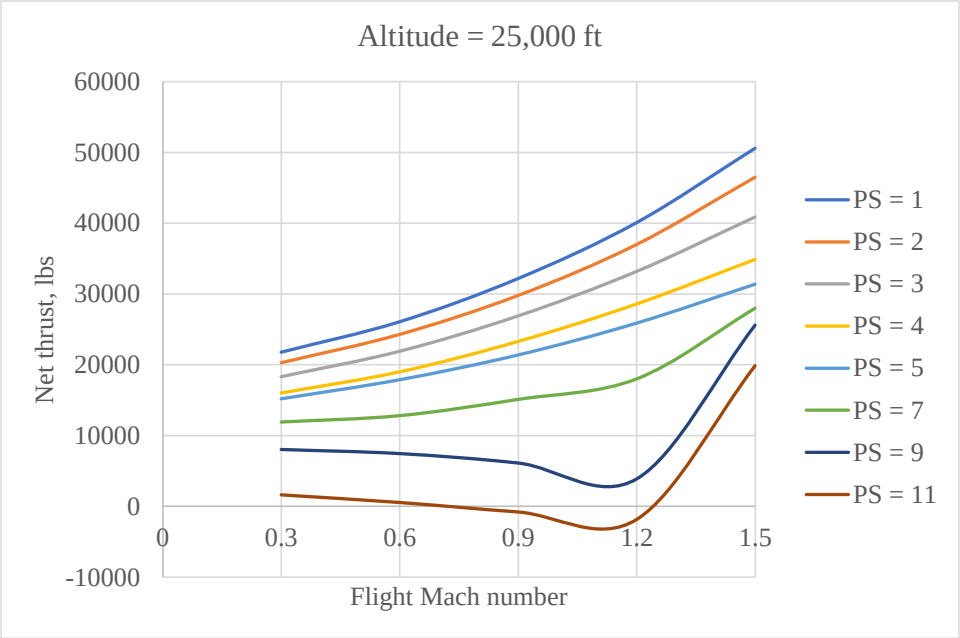

Figure 33 Variation in Net Thrust of GE4/J4C Engine at 25,000 ft for Different Power Settings

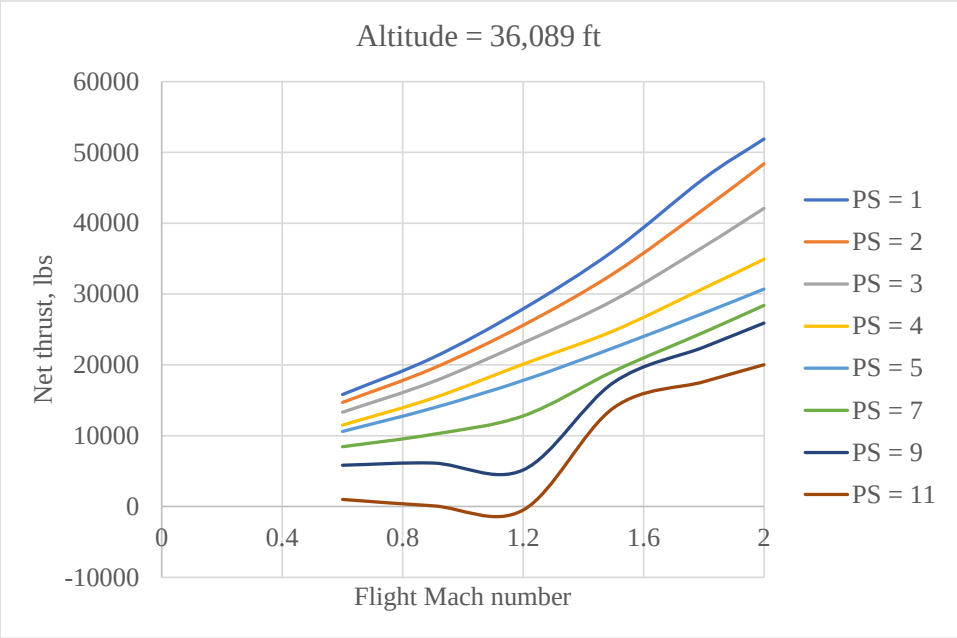

Figure 34 Variation in Net Thrust of GE4/J4C Engine at 36,089 ft for Different Power Settings

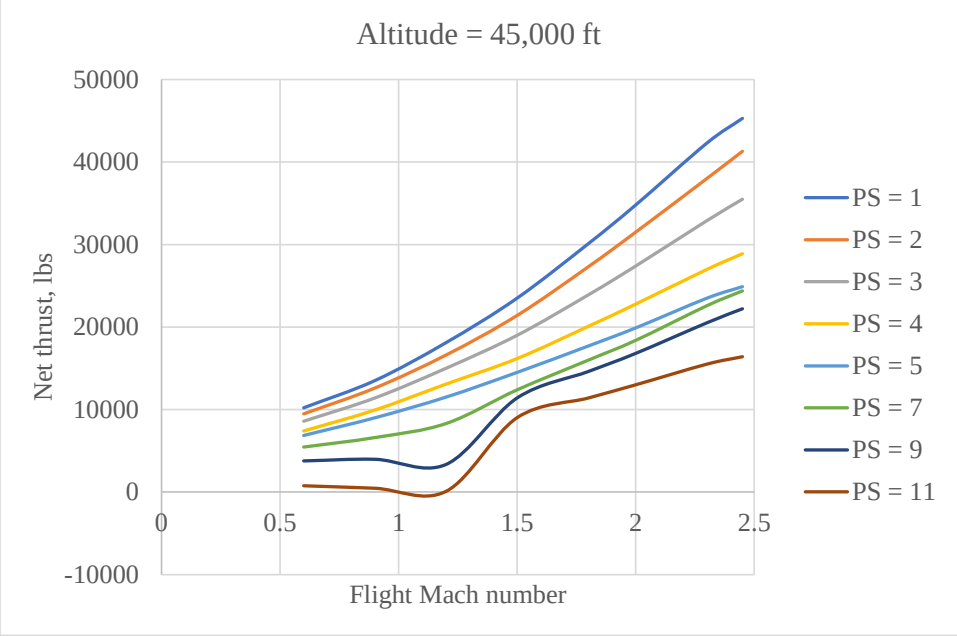

Figure 35 Variation in Net Thrust of GE4/J4C Engine at 45,000 ft for Different Power Settings

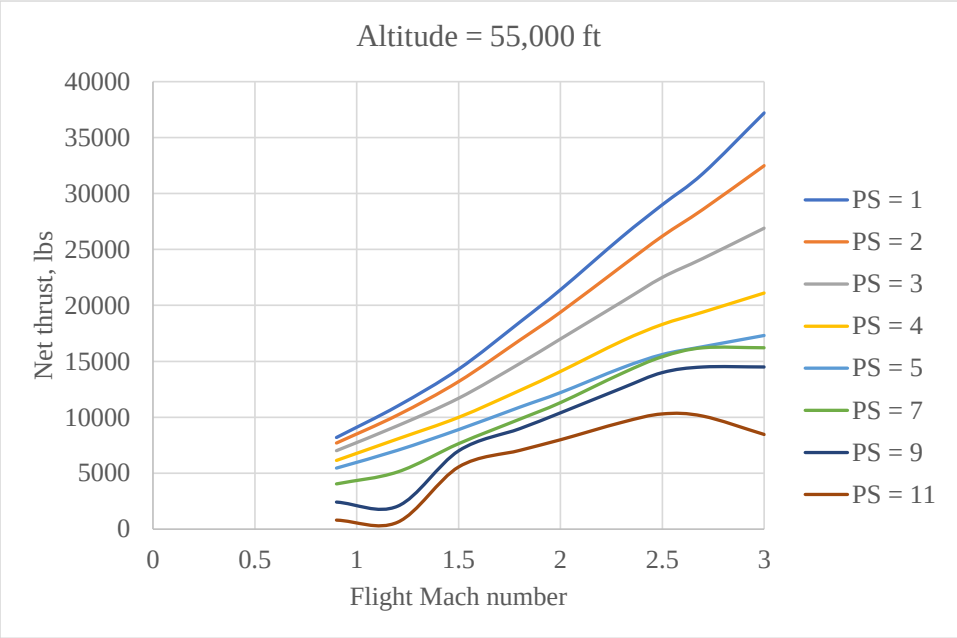

Figure 36 Variation in Net Thrust of GE4/J4C Engine at 55,000 ft for Different Power Settings

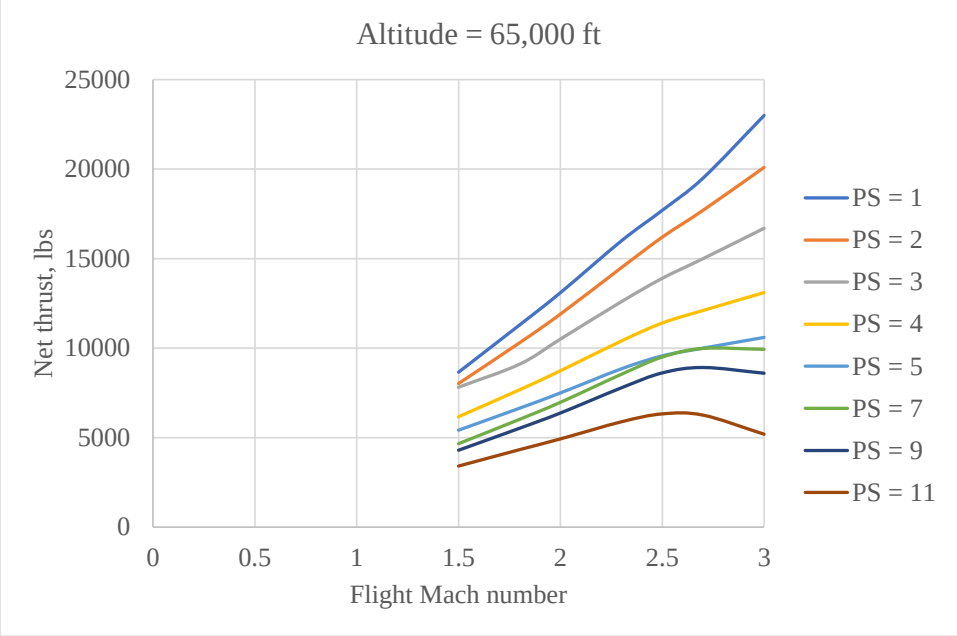

Figure 37 Variation in Net Thrust of GE4/J4C Engine at 65,000 ft for Different Power Settings

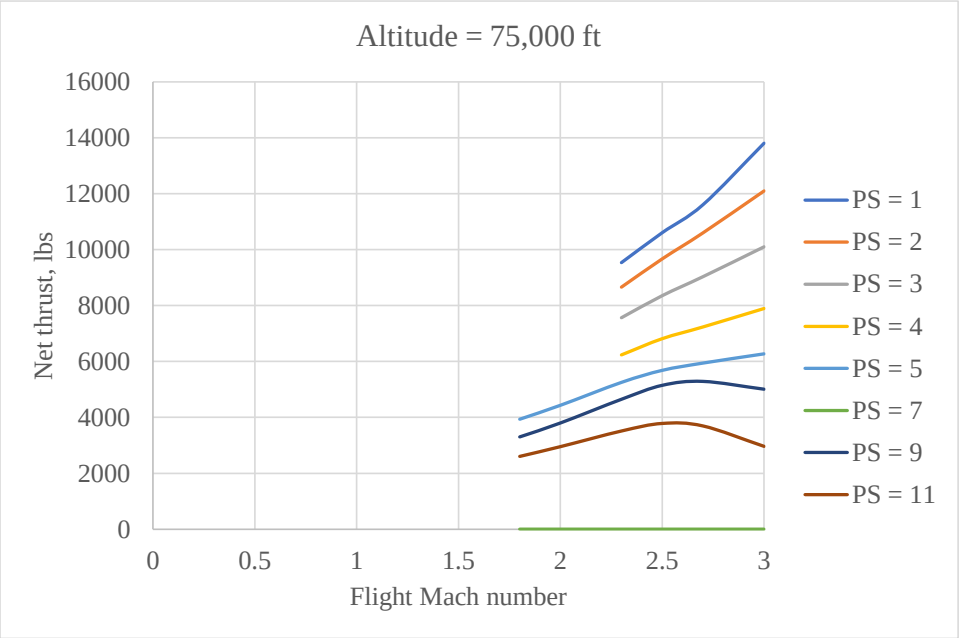

Figure 38 Variation in Net Thrust of GE4/J4C Engine at 75,000 ft for Different Power Settings

4.2.2. Specific Fuel Consumption Performance Curves

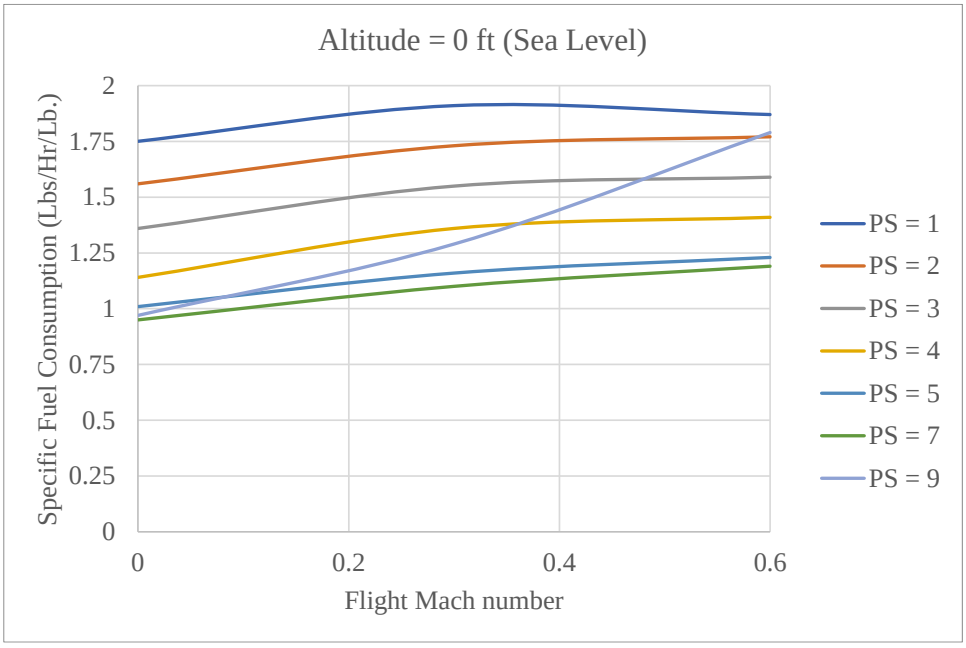

Figure 39 Variation in TSFC of GE4/J4C Engine at Sea Level for Different Power Settings

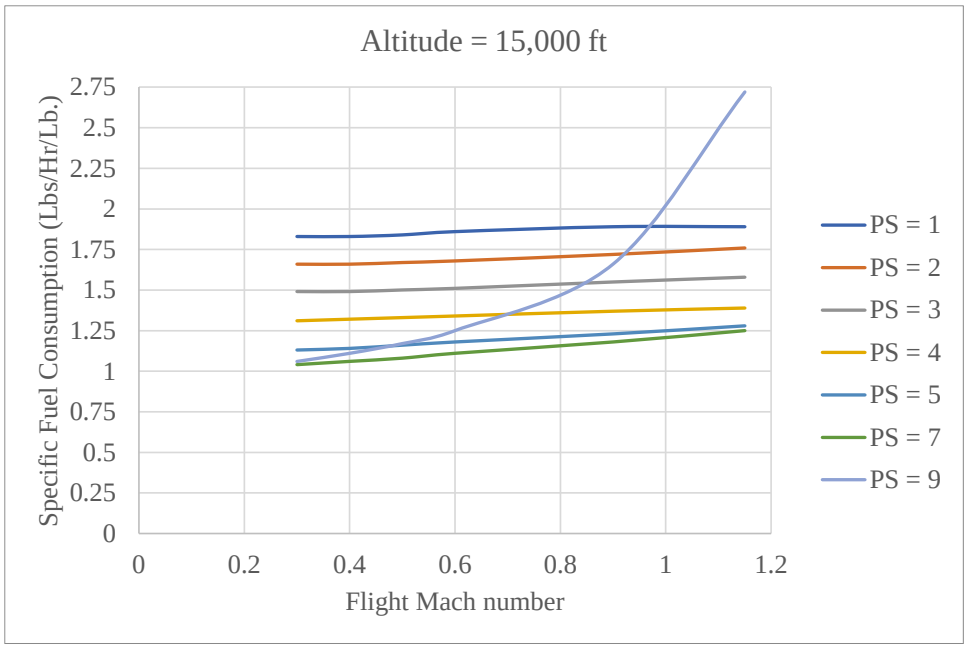

Figure 40 Variation in TSFC of GE4/J4C Engine at 15,000 ft for Different Power Settings

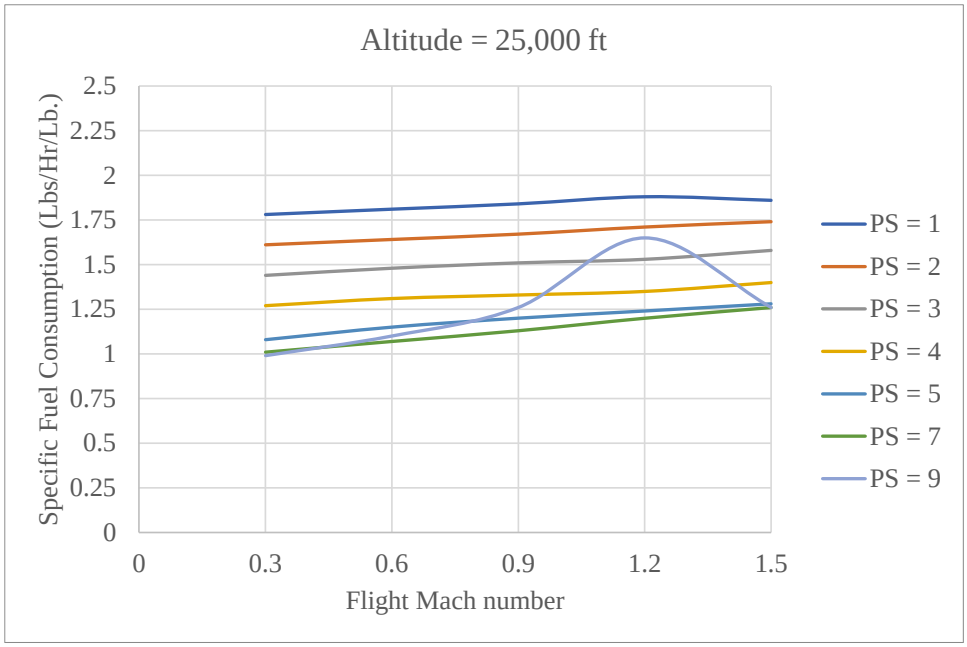

Figure 41 Variation in TSFC of GE4/J4C Engine at 25,000 ft for Different Power Settings

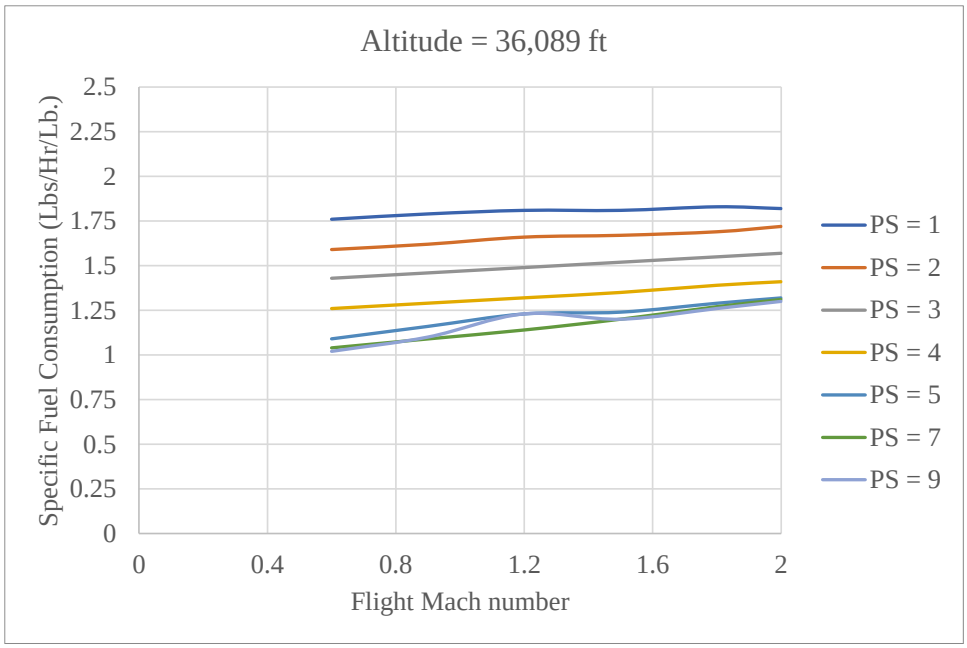

Figure 42 Variation in TSFC of GE4/J4C Engine at 36,089 ft for Different Power Settings

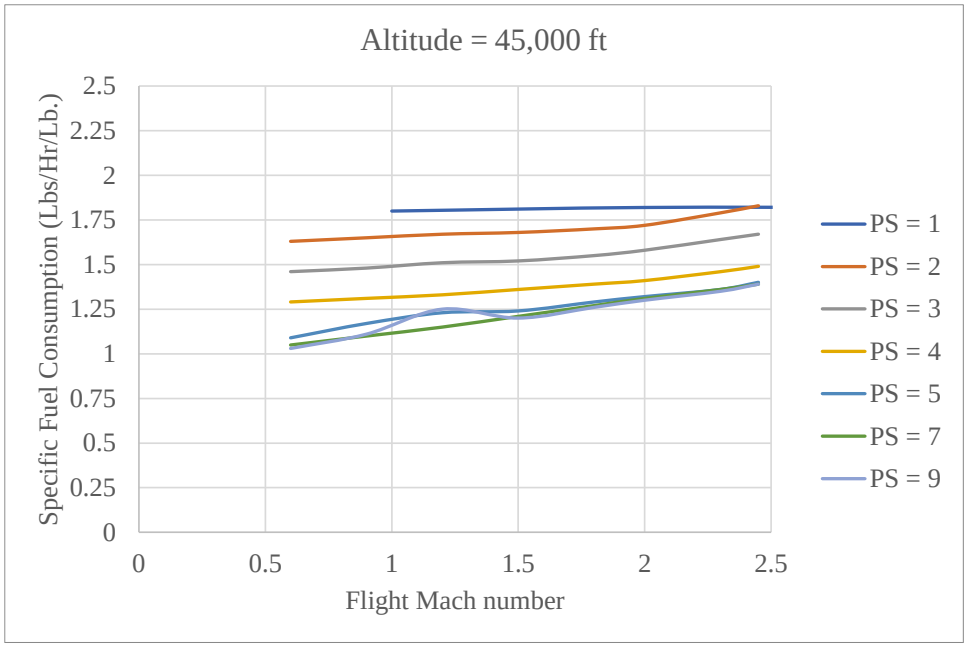

Figure 43 Variation in TSFC of GE4/J4C Engine at 45,000 ft for Different Power Settings

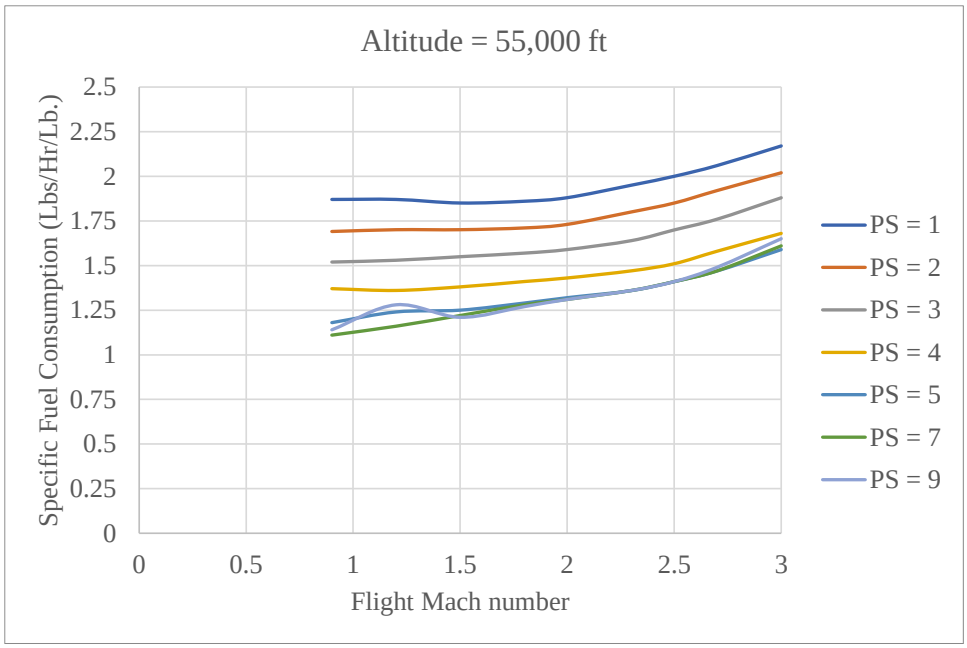

Figure 44 Variation in TSFC of GE4/J4C Engine at 55,000 ft for Different Power Settings

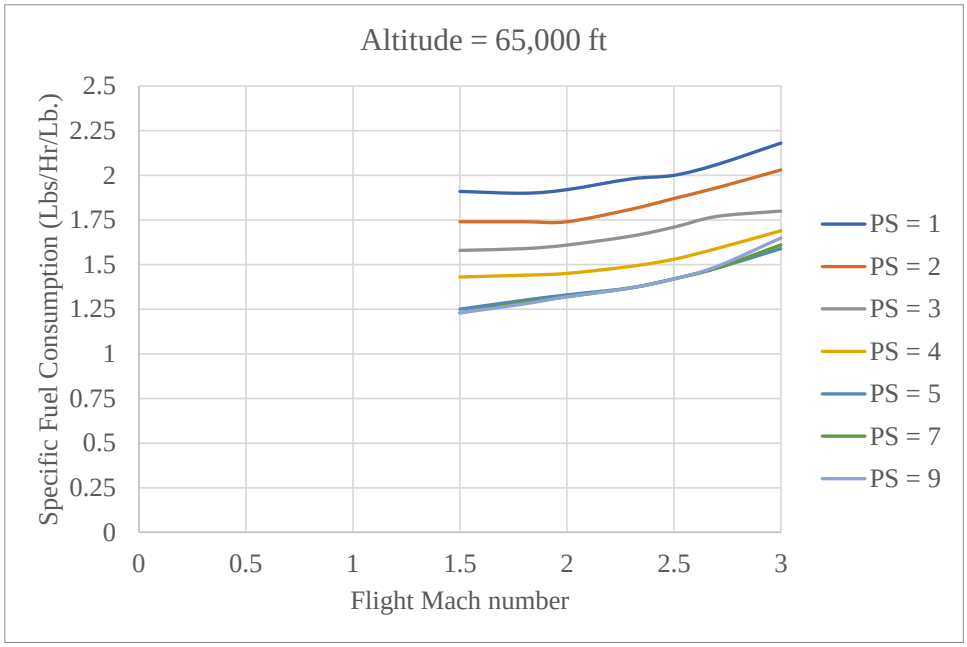

Figure 45 Variation in TSFC of GE4/J4C Engine at 65,000 ft for Different Power Settings

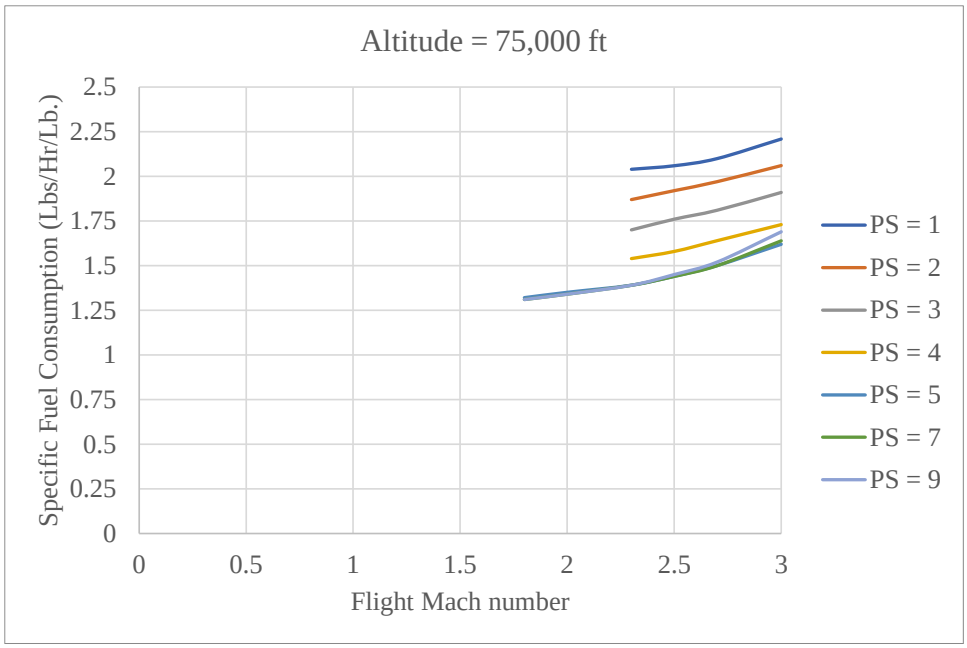

Figure 46 Variation in TSFC of GE4/J4C Engine at 75,000 ft for Different Power Settings

Based on the data illustrated above, the propulsion database can be generated from looking at the values at every test Mach number that are required to carry out analysis. One must never leave a blank space in database, even if the data is unavailable. It can be filled by either using 0 for thrust value or 9.99 for TSFC value. This values allow for consistent reading of the data and at the same time doesn't allow the solver to impact the solution, since this values will create no difference to the solution due to zero thrust.

Along with this the database needs to be fed with number of Mach number cases, number of altitude range and the total number of PLA ratings that will be used for assessing the flight performance of any given aircraft. Moreover, it is imperative that the PLA ratings are always fed in decreasing order for any particular case of flight Mach number and altitude level, if not filled accordingly, the solver won't be able to estimate required

performance parameters and instead return a blank contour without any errors on the screen for end user to troubleshoot.

Figure 47 depicts a sample propulsion database file in terms of five column data.

```
PROP
*GE4-J4C SUPERSONIC ENGINE
NPLA
9
NMACH
12
NALT
8
* MACH  ALT     PLA     THRUST  TSFC
DATA
0       0       0.85    3520    1.64
0       0       0.88    12400   0.97
0       0       0.9     28500   0.95
0       0       0.95    38900   1.01
0       0       0.96    40050   1.08
0       0       0.97    41200   1.14
0       0       0.98    45300   1.36
0       0       0.99    48900   1.56
0       0       1       51800   1.75
0       15000   0.85    0       9.99
0       15000   0.88    0       9.99
0       15000   0.9     0       9.99
0       15000   0.95    0       9.99
0       15000   0.96    0       9.99
0       15000   0.97    0       9.99
0       15000   0.98    0       9.99
0       15000   0.99    0       9.99
0       15000   1       0       9.99
0       25000   0.85    0       9.99
0       25000   0.88    0       9.99
0       25000   0.9     0       9.99
0       25000   0.95    0       9.99
0       25000   0.96    0       9.99
0       25000   0.97    0       9.99
0       25000   0.98    0       9.99
```

Figure 47 Five Column Data Sample for GE4/J4C Turbojet Engine as Used in Propulsion Database File

The above depicted Figure 47 displays the syntax of writing the propulsion database file as mentioned above for the ease of the end user to understand. Along with the PLA rating order, it is also advisable that the flight Mach number and altitude levels be fed in increasing order to avoid any troubles with contours generation.

5. PROPULSION DATA VERIFICATION

5.1. Significance of Verification of Propulsion Data

The performance report papers published during the development of SST used a General Electric engine and performance of the same GE4/J4C engine which has a relatively vague description of its performance basis [12]. The engine never saw installation on the B2707 aircraft since it was never developed. Most of the data is extrapolated from flight on a subsonic B-52 and the supersonic XB-70; a J93 not a GE4/J4C engine.

The XB-70 as mentioned above, used the J93-GE-3 engine, for which some data is available online, including the single-spool design, 11-stage compressor and 2-stage turbine, turbine inlet temperature of 1422 ^{o}K at max thrust, inlet air mass flow rate of 125 kg/s at max thrust, and max thrust of 98 kN without afterburner and 130 kN with afterburner. The key missing piece is the OPR at max thrust, which still remains uncertain at this point. Having the OPR would let you perform a turbojet flow path analysis with assumed values of component efficiencies based on the vintage of the engine. However, there are other engines from which one can draw reasonable then-state-of-the-art component efficiencies.

Although the power hook curves look consistent with other engine performance data available from the time, it still remains very important to relate the values and check for its plausibility.

5.2. Methodology and Platform Preparation

For the above mentioned purpose, a sample turbojet engine analysis has been performed to estimate the thrust and specific fuel consumption data. The engine used for checking the credibility of the GE4 engine uses the same data as could be obtained from the official report, along with different resources available online and some forums. Several other values which still remain confidential to this point has been either reverse engineered or best guessed to serve the same purpose.

The available data for GE-4 engine contains the standard atmosphere data from 1962 since it was the one used in propulsion calculation [12] [13]. This would mean an input data block would be ready for inlet/diffusor condition for analysis. Along with this it was specifically stated that the GE4 engine would have 12.5:1 overall pressure ratio [14]. Hence, this pressure ratio has been split up based on the fact that having equal compression would provide consistent and better result.

The other parts of the engine were mostly the component efficiencies which would be used for turbojet flow-path analysis. The data for this still remains unclear for GE-4 engine. However, one could use the data of other engines from the same era on the internet at different sources. It is not unusual for legacy engines like this GE-4 to have poor characterization in online sources, and much of what is online might actually be wrong. So, it becomes important to do some real sleuthing to get decent numbers. There are many amazing engines from that era that can be used for reference.

Yet, one need to understand and acknowledge the fact that engines use the then-available state-of-the-art values in terms of Turbine Inlet Temperature (TIT), Static Pressure Ratio (SPR), and component efficiencies. Most of the data used for this turbojet analysis is based on several engine references such as YJ93-GE3 and P&W J58 engine. Based on Paul H. Wilkinson as mentioned in his book [14], the diameters of compressor inlet and exhaust nozzle for the GE-4 engine are 60.6 inches and 74.2 inches respectively.

The data for geometry and working of inlet and the conical spike are not available for general public use. As a result, several part of this had to be reverse engineered based on the data available and other engine references. A supersonic axisymmetric spike was developed to understand and develop the inlet performance chart. For this purpose, a reference variable geometry translating axisymmetric spike was studied which was implemented on SR-71 [15]. Figure 48 below depicts the changing inlet capture area at inlet entry for a SR-71's axisymmetric spike which was used as a reference in this case.

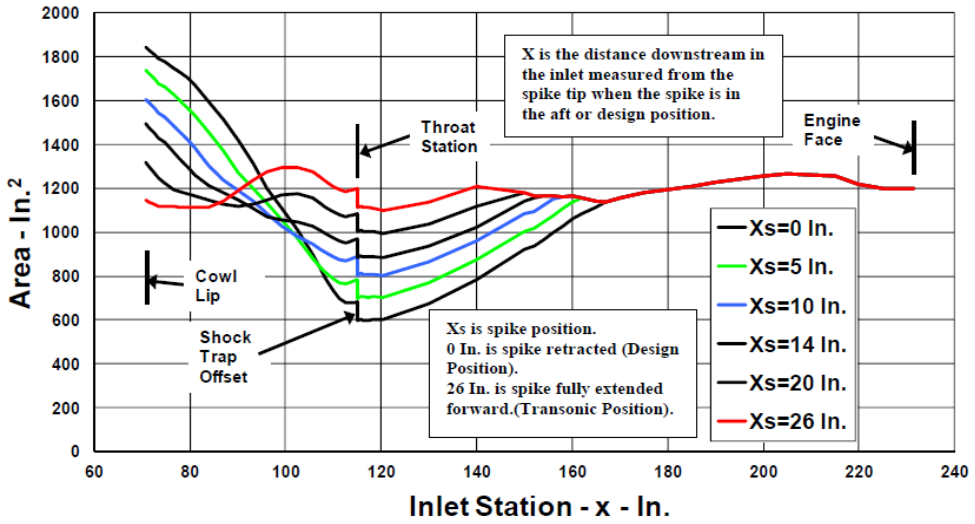

Figure 48 Inlet Area Distribution at Different Position of Cowl as Used on SR-71 [15]

Based on this data available and considering other important aspect which could be reverse engineered such as diffusion ratio from back tracking the design condition Mach number after series of oblique shocks followed by a normal shock, a conical axisymmetric spike for supersonic inlet was designed. The pressure recovery for which is displayed in the Figure 49 below along with the standard normal shock pressure recovery for a series of Mach numbers.

The total pressure recovery across a normal shock with any upstream Mach number M, can be estimated by using the following equation [16].

$$\frac{P_{t_{exit}}}{P_{t_{entry}}} = \left[\frac{(\gamma+1)M^2}{(\gamma-1)M^2+2}\right]^{\frac{\gamma}{\gamma-1}} \cdot \left[\frac{(\gamma+1)}{2\,\gamma\,M^2-(\gamma-1)}\right]^{\frac{1}{\gamma-1}} \qquad \textit{Eq. 2}$$

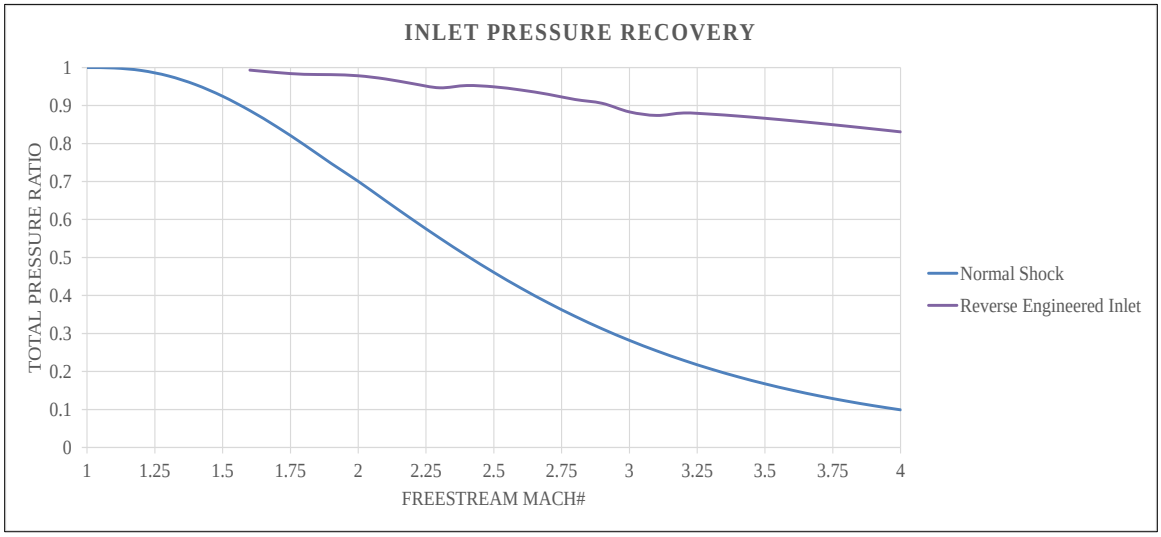

Figure 49 Comparison of Inlet Pressure Recovery of the Reverse Engineered Inlet and That Across a Standard Normal Shock at Different Upstream Mach Numbers

Comparing this with the actual SR 71's J58 turbojet engines pressure recovery displayed below in Figure 50, the data looks quite consistent and the solution looks legitimate.

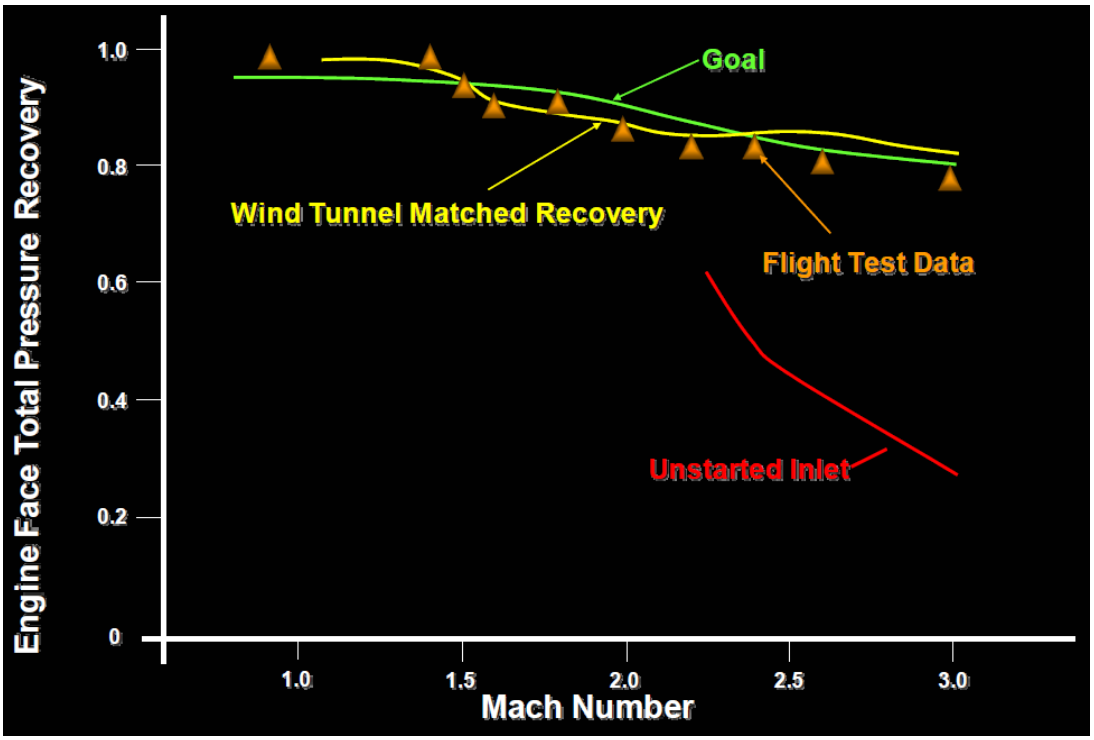

Figure 50 Achieved and Anticipated Engine Inlet Pressure Recovery on SR-71 Across Different Mach Numbers Used as Benchmark for Reverse Engineered Inlet Design [15]

In this thesis, I performed a complete turbojet engine analysis to develop data which will help legitimize the published GE4 report values [12]. Based on concepts of air-breathing propulsion system estimations; the jet, and pressure thrusts were calculated using several combinations of thermodynamic equations involved in each stage and its relationship with the next stage. The data was obtained using a temperature limited Brayton cycle analysis for non-ideal condition.

An important factor which often goes unnoticed during such analysis is “diffusor buoyancy thrust” which at higher Mach number can contribute up to 50% of net thrust based on system configuration. It was calculated using first order principles based on data calculated from designing axisymmetric conical spike for inlet section [17].

5.3. Propulsion Analysis Tool

The core turbojet analysis as performed in Excel VBA tool uses the concepts of air – breathing propulsion taught by Prof. Dahm in his Aircraft Propulsion class at Arizona State University [18]. The final simplified equations are mentioned below. It must be noted that before using the analysis tool, a thorough understanding of each components is essential to provide inputs such as Mach numbers, dimensions, and efficiencies of each component to account for irreversibility associated with engine. The data for freestream conditions must be selected from the standard atmosphere table to get consistent results to that observed in engine performance charts.

5.3.1. Inlet / Diffuser Section

$$T_{t_{inlet}} = T_{t_{freestream}} \qquad \textit{Eq. 3}$$

$$P_{t_{inlet}} = P_{t_{freestream}} \cdot \left[\frac{1 + \eta_d \frac{(\gamma - 1)}{2} M_{freestream}{}^2}{1 + \frac{(\gamma - 1)}{2} M_{freestream}{}^2} \right]^{\frac{\gamma}{\gamma - 1}} \qquad \textit{Eq. 4}$$

$$T_{inlet} = \frac{T_{t_{inlet}}}{\left[1 + \frac{(\gamma - 1)}{2} M_{inlet}{}^2 \right]} \qquad \textit{Eq. 5}$$

$$P_{inlet} = \frac{P_{t_{inlet}}}{\left[1 + \frac{(\gamma - 1)}{2} M_{inlet}{}^2\right]^{\frac{\gamma}{\gamma-1}}} \quad \textit{Eq. 6}$$

5.3.2. Fan Section

$$P_{t_{fan}} = (Fan\ Pressure\ Ratio)\ .\ P_{t_{inlet}} \quad \textit{Eq. 7}$$

$$T_{t_{fan}} = T_{t_{inlet}} . \left\{1 + \frac{1}{\eta_{fan}} \left[\left(\frac{P_{t_{fan}}}{P_{t_{inlet}}}\right)^{\frac{\gamma}{\gamma-1}} - 1\right]\right\} \quad \textit{Eq. 8}$$

$$T_{fan} = \frac{T_{t_{fan}}}{\left[1 + \frac{(\gamma - 1)}{2} M_{fan}{}^2\right]} \quad \textit{Eq. 9}$$

$$P_{fan} = \frac{P_{t_{fan}}}{\left[1 + \frac{(\gamma - 1)}{2} M_{fan}{}^2\right]^{\frac{\gamma}{\gamma-1}}} \quad \textit{Eq. 10}$$

$$|w_{fan}| = C_{p_{\gamma \to 1.4}} \left[T_{t_{fan}} - T_{t_{inlet}}\right] \quad \textit{Eq. 11}$$

5.3.3. Low Pressure Compressor (LPC) Section

$$P_{t_{LPC}} = (Pressure\ Ratio_{LPC}) . P_{t_{fan}} \quad \textit{Eq. 12}$$

$$T_{t_{LPC}} = T_{t_{fan}} . \left\{1 + \frac{1}{\eta_{LPC}} \left[\left(\frac{P_{t_{LPC}}}{P_{t_{fan}}}\right)^{\frac{\gamma}{\gamma-1}} - 1\right]\right\} \quad \textit{Eq. 13}$$

$$T_{LPC} = \frac{T_{t_{LPC}}}{\left[1 + \frac{(\gamma - 1)}{2} {M_{LPC}}^2\right]} \quad \textit{Eq. 14}$$

$$P_{LPC} = \frac{P_{t_{LPC}}}{\left[1 + \frac{(\gamma - 1)}{2} {M_{LPC}}^2\right]^{\frac{\gamma}{\gamma - 1}}} \quad \textit{Eq. 15}$$

$$|w_{LPC}| = C_{p\,\gamma \to 1.4} \left[T_{t_{LPC}} - T_{t_{fan}}\right] \quad \textit{Eq. 16}$$

5.3.4. High Pressure Compressor (HPC) Section

$$P_{t_{HPC}} = (Pressure\ Ratio_{HPC}) \,.\, P_{t_{LPC}} \quad \textit{Eq. 17}$$

$$T_{t_{HPC}} = T_{t_{LPC}} \,.\, \left\{1 + \frac{1}{\eta_{HPC}} \left[\left(\frac{P_{t_{HPC}}}{P_{t_{LPC}}}\right)^{\frac{\gamma}{\gamma - 1}} - 1\right]\right\} \quad \textit{Eq. 18}$$

$$T_{HPC} = \frac{T_{t_{HPC}}}{\left[1 + \frac{(\gamma - 1)}{2} {M_{HPC}}^2\right]} \quad \textit{Eq. 19}$$

$$P_{HPC} = \frac{P_{t_{HPC}}}{\left[1 + \frac{(\gamma - 1)}{2} {M_{HPC}}^2\right]^{\frac{\gamma}{\gamma - 1}}} \quad \textit{Eq. 20}$$

$$|w_{HPC}| = C_{p\,\gamma \to 1.4} \left[T_{t_{HPC}} - T_{t_{LPC}}\right] \quad \textit{Eq. 21}$$

5.3.5. Combustor Section

$$P_{Combustor} = P_{HPC} \quad \textit{Eq. 22}$$

$$T_{t_{Combustor}} = T_{Combustor} \cdot \left[1 + \frac{(\gamma - 1)}{2} M_{Combustor}{}^2\right] \quad \textit{Eq. 23}$$

$$P_{t_{Combustor}} = P_{Combustor} \cdot \left[1 + \frac{(\gamma - 1)}{2} M_{Combustor}{}^2\right]^{\frac{\gamma}{\gamma-1}} \quad \textit{Eq. 24}$$

$$|q_{Combustor}| = C_{p_{\gamma \to 1.3}} \left[T_{t_{Combustor}} - T_{t_{HPC}}\right] \quad \textit{Eq. 25}$$

5.3.6. High Pressure Turbine (HPT) Section

$$|w_{HPT}| = |w_{HPC}| \quad \textit{Eq. 26}$$

$$T_{t_{HPT}} = T_{t_{Combustor}} - \frac{|w_{HPT}|}{C_{p_{\gamma \to 1.3}}} \quad \textit{Eq. 27}$$

$$P_{t_{HPT}} = P_{t_{Combustor}} \cdot \left[1 - \frac{1}{\eta_{HPT}}\left(1 - \frac{T_{t_{HPT}}}{T_{t_{Combustor}}}\right)\right]^{\frac{\gamma}{\gamma-1}} \quad \textit{Eq. 28}$$

$$T_{HPT} = \frac{T_{t_{HPT}}}{\left[1 + \frac{(\gamma - 1)}{2} M_{HPT}{}^2\right]} \quad \textit{Eq. 29}$$

$$P_{HPT} = \frac{P_{t_{HPT}}}{\left[1 + \frac{(\gamma - 1)}{2} M_{HPT}{}^2\right]^{\frac{\gamma}{\gamma-1}}} \quad \textit{Eq. 30}$$

5.3.7. Low Pressure Turbine (LPT) Section

$$\left|\dot{W}_{LPT}\right| = \left|\dot{W}_{LPC}\right| + \left|\dot{W}_{fan}\right| \qquad \textit{Eq. 31}$$

$$\left|w_{LPT}\right| = \left|w_{LPC}\right| + [1 + BPR].\left|w_{fan}\right| \qquad \textit{Eq. 32}$$

$$T_{t_{LPT}} = T_{t_{HPT}} - \frac{|w_{LPT}|}{C_{p\,\gamma\to 1.3}} \qquad \textit{Eq. 33}$$

$$P_{t_{LPT}} = P_{t_{HPT}} \cdot \left[1 - \frac{1}{\eta_{LPT}}\left(1 - \frac{T_{t_{LPT}}}{T_{t_{HPT}}}\right)\right]^{\frac{\gamma}{\gamma-1}} \qquad \textit{Eq. 34}$$

$$T_{LPT} = \frac{T_{t_{LPT}}}{\left[1 + \frac{(\gamma-1)}{2}\, {M_{LPT}}^2\right]} \qquad \textit{Eq. 35}$$

$$P_{LPT} = \frac{P_{t_{LPT}}}{\left[1 + \frac{(\gamma-1)}{2}\, {M_{LPT}}^2\right]^{\frac{\gamma}{\gamma-1}}} \qquad \textit{Eq. 36}$$

5.3.8. Converging Nozzle Section

Choking Check, $$M' = \sqrt{\frac{2}{(\gamma-1)} \cdot \frac{\eta_{nozzle} \cdot \left[1 - \left({P_{freestream}}/{P_{LPT}}\right)^{\frac{\gamma}{\gamma-1}}\right]}{1 - \eta_{nozzle} \cdot \left[1 - \left({P_{freestream}}/{P_{LPT}}\right)^{\frac{\gamma}{\gamma-1}}\right]}} \qquad \textit{Eq. 37}$$

If $M' > 1$ i.e. Choked Nozzle

$$M_{exit} = 1 \qquad \textit{Eq. 38}$$

$$T_{t_{exit}} = T_{t_{LPT}} \quad \textit{Eq. 39}$$

$$P_{exit} = P_{t_{LPT}} \cdot \left\{\left[1 - \frac{1}{\eta_{nozzle}}\left(\frac{\gamma - 1}{\gamma + 1}\right)\right]^{\frac{\gamma}{\gamma - 1}}\right\} \quad \textit{Eq. 40}$$

$$T_{exit} = \frac{T_{t_{exit}}}{\left[1 + \frac{(\gamma - 1)}{2} M_{exit}{}^2\right]} \quad \textit{Eq. 41}$$

$$P_{t_{exit}} = P_{exit} \cdot \left[1 + \frac{(\gamma - 1)}{2} M_{exit}{}^2\right]^{\frac{\gamma}{\gamma - 1}} \quad \textit{Eq. 42}$$

Else $M' \leq 1$ i.e. Unchoked Nozzle

$$M_{exit} = M' \quad \textit{Eq. 43}$$

$$T_{t_{exit}} = T_{t_{LPT}} \quad \textit{Eq. 44}$$

$$P_{exit} = P_{freestream} \quad \textit{Eq. 45}$$

$$T_{exit} = \frac{T_{t_{exit}}}{\left[1 + \frac{(\gamma - 1)}{2} M_{exit}{}^2\right]} \quad \textit{Eq. 46}$$

$$P_{t_{exit}} = P_{exit} \cdot \left[1 + \frac{(\gamma - 1)}{2} M_{exit}{}^2\right]^{\frac{\gamma}{\gamma - 1}} \quad \textit{Eq. 47}$$

5.3.9. Thrust Estimation

$$V_{exit} = M_{exit} \cdot \sqrt{\gamma R T_{exit}} \qquad \textit{Eq. 48}$$

$$\dot{m}_{exit} = \frac{P_{exit}}{R\, T_{exit}} \cdot V_{exit} \cdot A_{nozzle} \qquad \textit{Eq. 49}$$

Jet Thrust, $$F_{Jet} = \dot{m}_{exit} \cdot \left(V_{exit} - V_{freestream}\right) \qquad \textit{Eq. 50}$$

Pressure Thrust, $$F_{Pressure} = \left(P_{exit} - P_{freestream}\right) \cdot A_{nozzle} \qquad \textit{Eq. 51}$$

Now, to calculate the aerodynamic force due to high pressure changes in inlet section, we need to estimate inlet buoyancy force.

Inlet Buoyancy Thrust as explained in the inlet buoyancy thrust estimation paper [17],

$$\begin{aligned} F_{buoyancy} \approx & \left[\frac{1}{2}\left(P_{throat} + P_{cowl}\right) - P_{shock}\right]\left(A_{cowl} - A_{throat}\right) \\ & + \left[\frac{1}{2}\left(P_{fan} - P_{throat}\right) - P_{shock}\right]\left(A_{fan} - A_{throat}\right) \end{aligned} \qquad \textit{Eq. 52}$$

Where, P_{shock} is the static pressure at upstream flow of the inlet where, in the case of flight at supersonic speeds, a normal or oblique shockwave may form. At subsonic speeds, flow conditions do not change here. To visually understand where this points are located on the turbojet engine, the flow path analysis has been displayed in figure 51 which illustrates the nomenclature used in buoyancy force estimation.

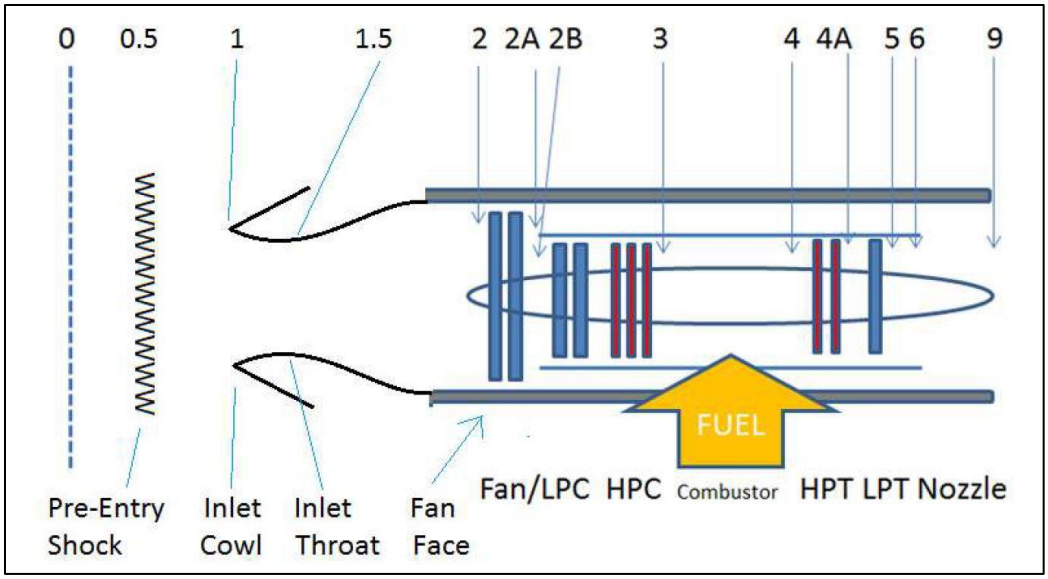

Figure 51 Illustration of station point's nomenclature for turbojet engine buoyancy force estimation [17]

The inlet buoyancy term used here is not part of the classic airbreathing propulsion equation, but it is an additional term which needs to be used to account for the huge pressure difference thrust that is generated at higher Mach number in the inlet. Hence it becomes necessary to add such quantity while estimating the thrust of the entire system. This term falls under the aerodynamics side of the thrust estimation. The Net thrust can be estimated by in the following way.

Net Thrust, $F_{Net} = F_{Jet} + F_{Pressure} + F_{buoyancy}$ *Eq. 53*

This Net thrust which could also be called as Regenerated thrust since, it has been obtained by reverse engineering the turbojet engine, has been compared against the published thrust values in verification section following this.

5.4. Verification Results

The Table 4 below shows the relative difference between the regenerated data and thrust value mentioned in the report. A total of 46 different points were used for calculating the military thrust (maximum thrust under non-augmentation condition) for this verification purpose.

Altitude / ***Difference(%)***	***Sea Level***	***5,000 ft***	***15,000 ft***	***36,089 ft***	***45,000 ft***	***55,000 ft***	***65,000 ft***	***75,000 ft***	***Total***
x > 20	0	0	0	0	1	0	0	0	*1*
15 < x < 20	0	0	1	2	0	0	0	0	*3*
10 < x < 15	0	0	0	1	0	0	2	0	*3*
5 < x < 10	0	2	3	2	4	3	4	0	*18*
x < 5	3	1	1	1	2	6	1	6	*21*

Table 4 Classification of Difference Between Published and Regenerated Military Thrust at Different Altitudes

It becomes clearer from observing the relative difference in Table 4, that the turbojet engine developed performs similarly to the engine from which the data has been presented in the report. The differences in the value is due to the fact that the dimensions used for redeveloping the engine might be different from those that define the actual engine.

Moreover, the buoyancy thrust estimated and then used to calculated net thrust might vary since, the inlet in this case was designed such that it would perform external compression and all the shocks will be sitting on the cowl lip with diffusion occurring once the throat is crossed with a diffusion ratio of 1.65:1. The diffusion ratio is very important in designing the inlet, since it helps to roughly approximate Mach number needed before diffusion, which would be the Mach number after the normal shock for design condition. The method mentioned above was primarily used for designing the supersonic inlet for this case. It could also be the case that the diffusion ratio for GE4 engine be different than the one used for this case. Moreover, the TIT and SPR also were not available and hence were approximated based on preexisting knowledge. Along with factors such as bypass leakage and component efficiencies, there could be many other contributing factors that might be the difference between the calculated and published thrust values.

Since more than 80% of the thrust values that were examined has a relative thrust difference less than 10%, it could help validate the thrust ratings mentioned in the performance reports.

The net thrust value (F_N) as obtained from calculating jet, pressure and inlet buoyancy force and net thrust presented in the performance report published by the General Electric's Flight Propulsion Division for GE4/J4C turbojet engine are displayed below. Figures 52 through 59 compares the two military thrust values at each test altitude and using the values at Mach number given in published report without applying any complex regression method to alter the readings in between.

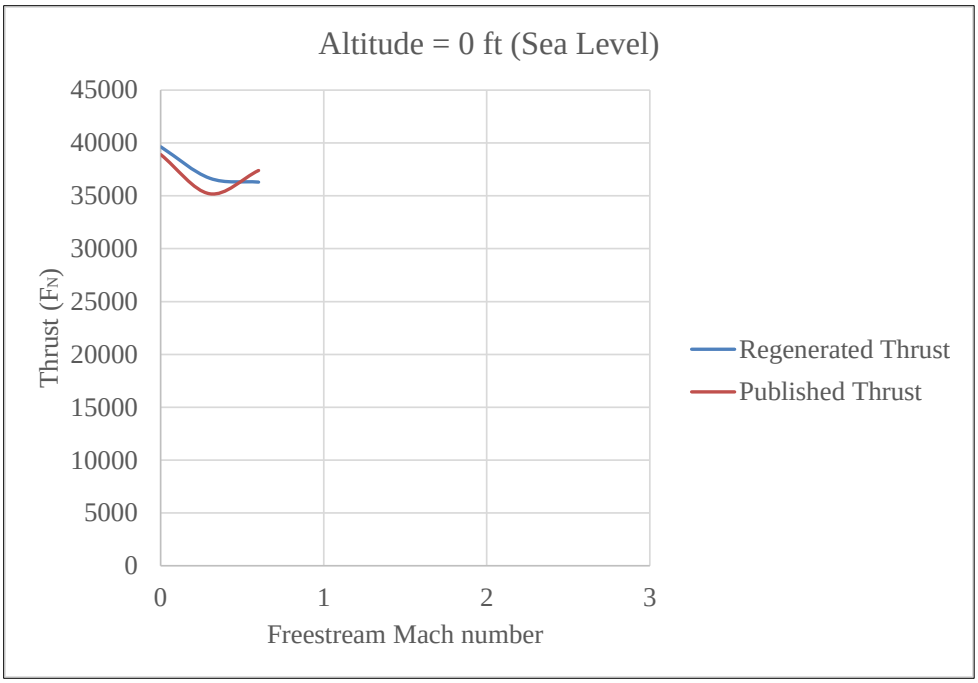

Figure 52 Regenerated and Published Military Thrust Comparisons at Sea Level

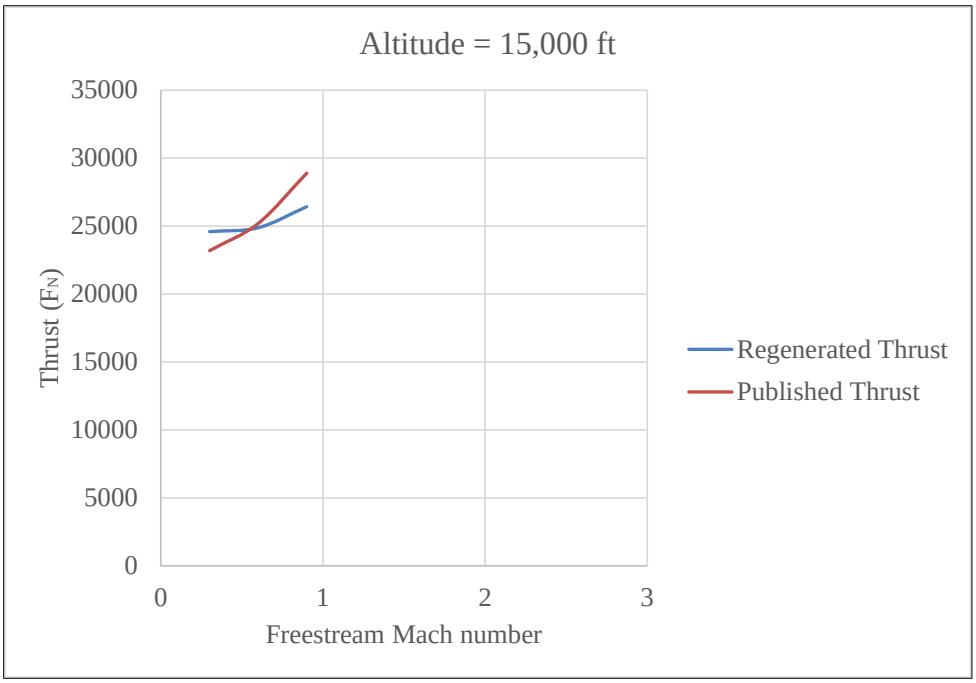

Figure 53 Regenerated and Published Military Thrust Comparisons at 15,000 ft

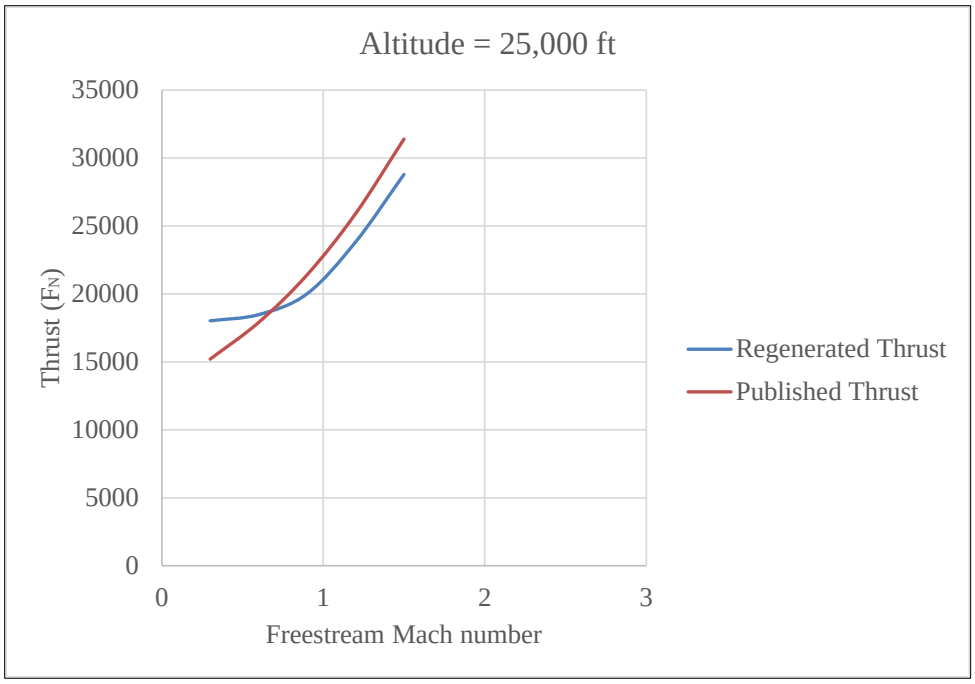

Figure 54 Regenerated and Published Military Thrust Comparisons at 25,000 ft

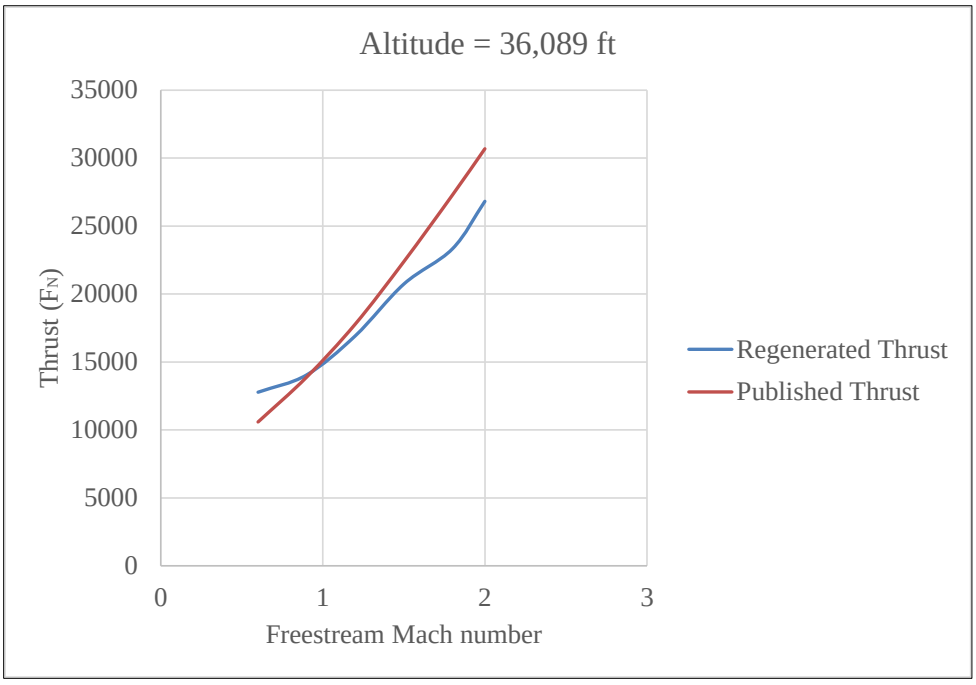

Figure 55 Regenerated and Published Military Thrust Comparisons at 36,089 ft

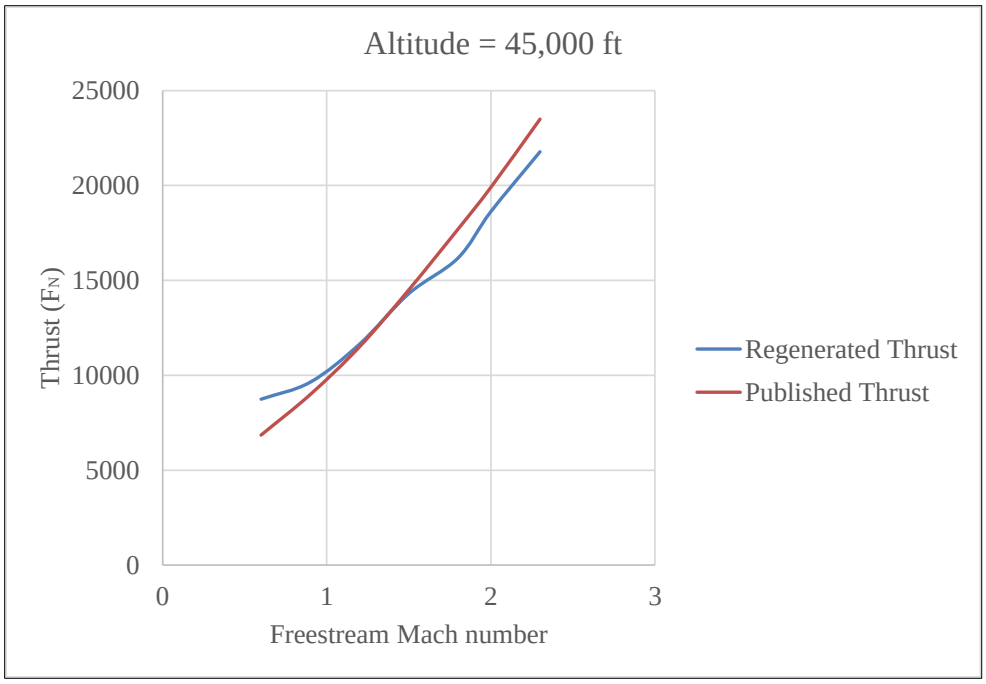

Figure 56 Regenerated and Published Military Thrust Comparisons at 45,000 ft

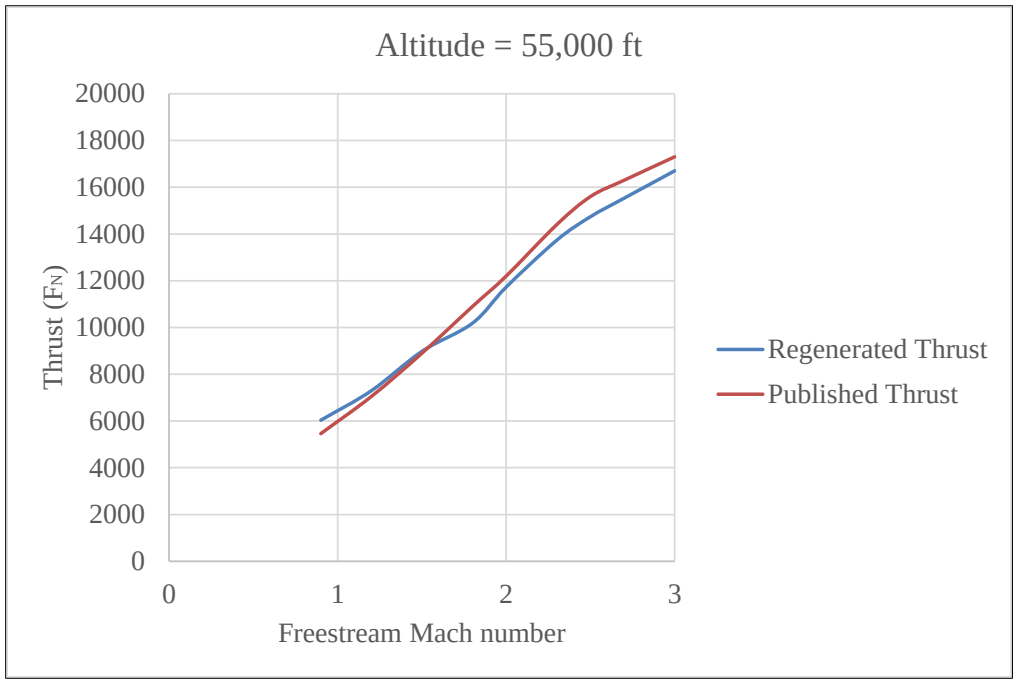

Figure 57 Regenerated and Published Military Thrust Comparisons at 55,000 ft

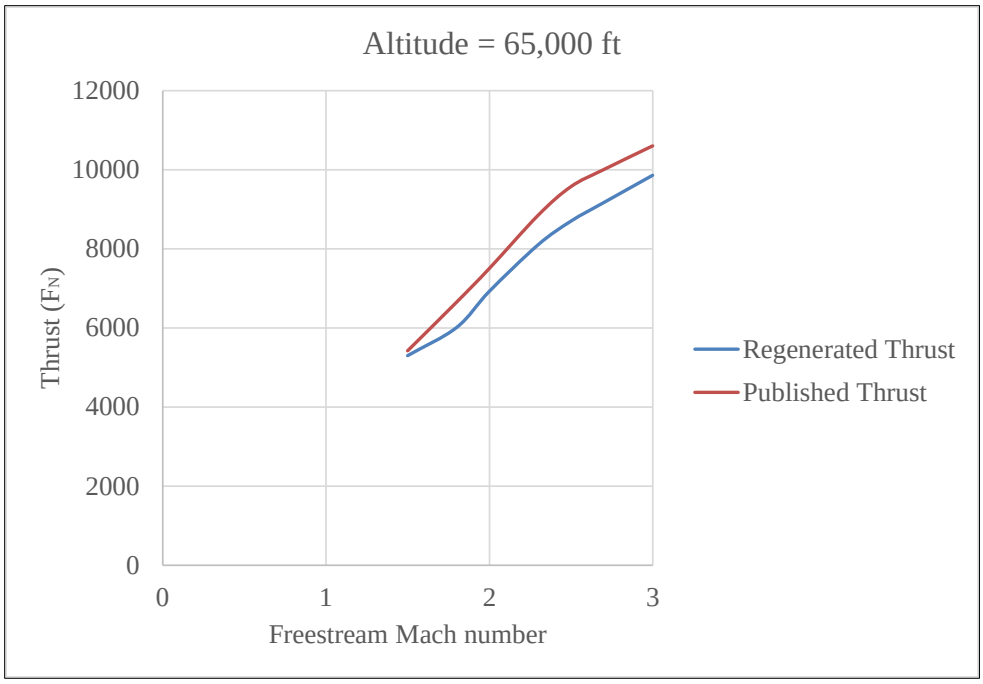

Figure 58 Regenerated and Published Military Thrust Comparisons at 65,000 ft

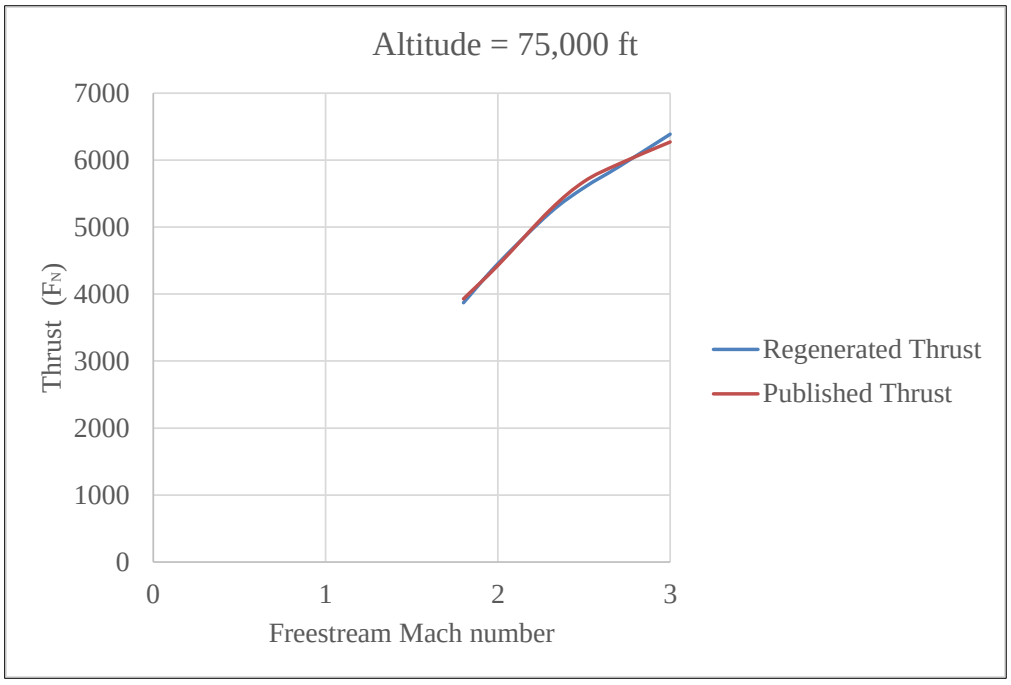

Figure 59 Regenerated and Published Military Thrust Comparisons at 75,000 ft

6. RESULTS

The research work was divided into different analysis weight and each weight analyzed with different wing sweep orientation of the aircraft in order to gain as much data as possible to reach conclusion. The analysis weight used will be based on the standard defined design flight weight (666,000 lb.), design landing weight (430,000 lb.) and an arbitrary intermediate weight (525,000 lb.) to act as nexus between the two.

The engine thrust has been used in such a way that it would replicate a very close approximate of the 4 engines of GE4/J5P turbojet engine at maximum PLA ratings. Hence, for this case to be true, each engine table used needs to be scaled to 1.1875 times each to produce enough maximum thrust in augmented condition to replicate the engine model that was supposed to be used. As was mentioned in the energy-maneuverability overview section, the engine database along with the aerodynamic database is fed to the Excel VBA solver where it computes specific range, aerodynamic efficiency, and aerodynamic performance parameter in following way.

$$Specific\ Range\ (M, Alt)\ = \frac{Cruise\ Mach\ \ X\ \ Speed\ of\ Sound\ (Alt)\ \ X\ \ 3600}{TSFC(M, Alt)\ \ X\ \ Thrust(M, Alt)\ \ X\ \ 6080} \quad \textit{Eq. 54}$$

$$Aerodynamic\ Efficiency\ (M, Alt) = \frac{C_L(\ M, Alt)}{C_D(\ M, Alt)} \quad \textit{Eq. 55}$$

$$Aerodynamic\ Performance\ Efficiency\ (M, Alt) = \ M\ .\ \frac{C_L(\ M, Alt)}{C_D(\ M, Alt)} \quad \textit{Eq. 56}$$

where, $$C_L(\ M, Alt) = \frac{Weight}{Sref\ X\ q(\ Mach, Alt)} \quad \textit{Eq. 57}$$

and, $$C_D(\ M, Alt) = \ C_{D0}(M) + \frac{C_L(M, Alt)^2}{\pi\ .\ AR\ .\ e} \quad \textit{Eq. 58}$$

6.1. Maximum Design Flight Weight (666,000 lbm.)

6.1.1. Wing Sweep Angle = 20^{o}

For this case of sweep, the specific range performance representation for the aforementioned analysis weight is as shown below in the Figure 60. The point performance plot which uses energy maneuverability theory shows a very good specific range for such a high analysis weight in the subsonic region and just under 40,000 ft altitude range.

On the flip side, at such a lower sweep angle of the wing, the supersonic performance of the aircraft seems to be rather less useful when compared with that in subsonic region. The maximum value of specific range is 0.0173 nM/lbm in subsonic region whereas it decreases sharply to just above 0.0131 nM/lbm in supersonic region which shows its wastefulness above sonic speeds in this configuration.

By observing the specific range contours, one could see that at this sweep, the transonic performance is very poor, since the specific range value near sonic speed is almost negligible. This poor specific range section can be seen shaded in red color. It seems to stand consistent with previous knowledge of poor mileage of aircraft near sonic speed with lower sweep angles.

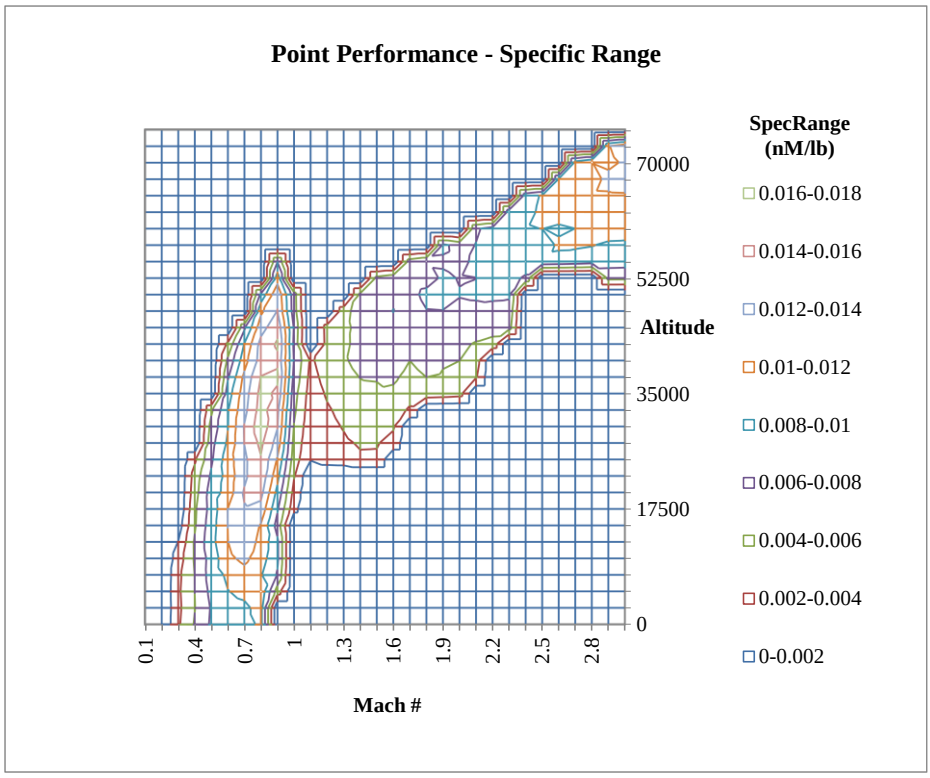

Figure 60 Specific Range Point Performance Contours at 20º Sweep and 666,000 lbm.

Analysis Weight

The aerodynamic performance parameter *M(L/D)* shows a rather different trend as compared to specific range. The maximum *M(L/D)* in subsonic region is 22.994 whereas in supersonic region it stands at 29.875.

The aerodynamic efficiency on the other hand provides enough evidence that the sweep angle is not suitable for supersonic speeds by giving higher *(L/D)* values in subsonic regions compared to supersonic region. The maximum *(L/D)* in subsonic region is 28.781 whereas it drops to almost a half in supersonic region to 9.958.

6.1.2. Wing Sweep Angle = 25º

The point performance as estimated using the flight envelope approach is similar to the previous case due to its almost identical aircraft geometry. The maximum specific range for the subsonic condition is 0.0178 nM/lbm observed at around 35,000 ft altitude whereas for supersonic case, the value of specific range displays similar pattern as the previous case and decreases to 0.0141 nM/lbm. The contour plot in Figure 61 displays the specific range distribution along throughout the tested Mach speed and altitudes for this particular case.

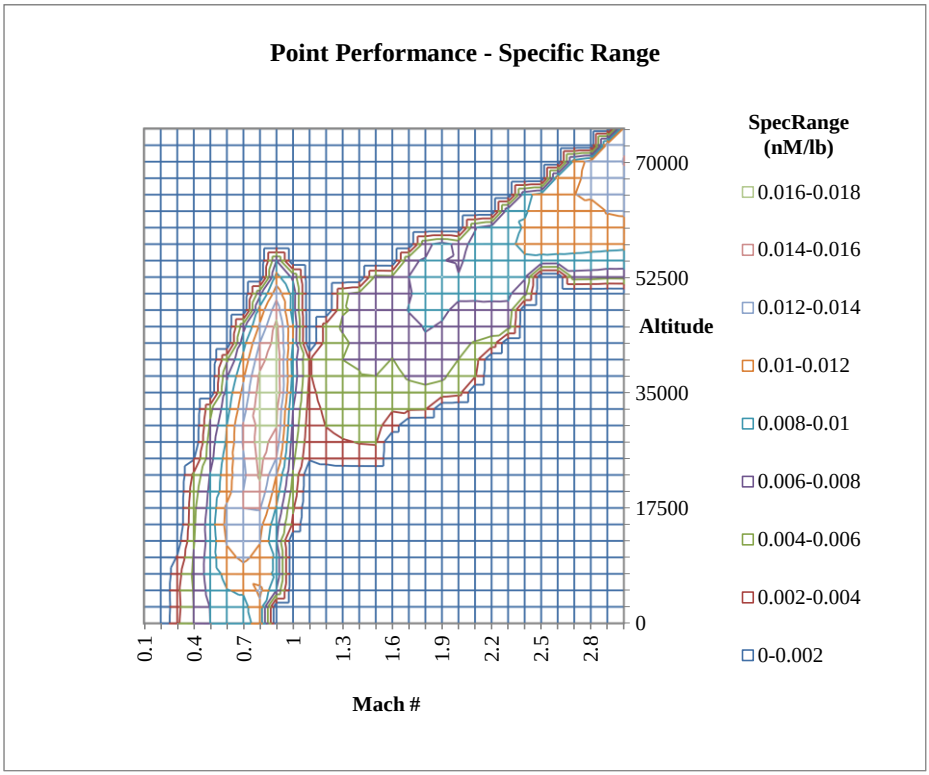

Figure 61 Specific Range Point Performance Contours at 25º Sweep and 666,000 lbm. Analysis Weight

The aerodynamic efficiency of the aircraft under this specifications of sweep angle and analysis weight leads to a higher *(L/D)* value in subsonic conditions compared to supersonic conditions. The maximum *(L/D)* is subsonic region is 29.414 whereas it slashes to almost 1/3rd in supersonic region where the maximum *(L/D)* is 10.515, leading to a no-brainer use of this configuration primarily in subsonic conditions.

The aerodynamic performance efficiency *M(L/D)* has a maximum value of 23.521 in subsonic condition and 31.545 in supersonic condition, showing the consistency with the pattern observed in previous case.

6.1.3. Wing Sweep Angle = 30^{o}

For wing sweep angle of 30^{o} and using maximum analysis weight of the three, the maximum specific range is observed around Mach 0.8 and the highest spectrum is observed to be within the range of 32,500 ft to 37,500 ft. The value of maximum specific range is 0.0193 nM/lbm in subsonic region and 0.0129 nM/lbm in supersonic condition.

The increase in the magnitude of the specific range value in subsonic condition could be related directly to the improvements in the lift to drag ratio and reduction in several components of drag. The maximum *(L/D)* in subsonic condition is 29.345 and it reduces to 10.124 in supersonic condition.

The *M(L/D)* values in subsonic speed regimes are comparatively higher when compared with previous cases. In subsonic condition the maximum value obtained is 24.906, which increases to 29.906 in supersonic speed region.

Below Figure 62 is the plot of specific range distribution representing the point performance value at different iterations of Mach number and altitude values.

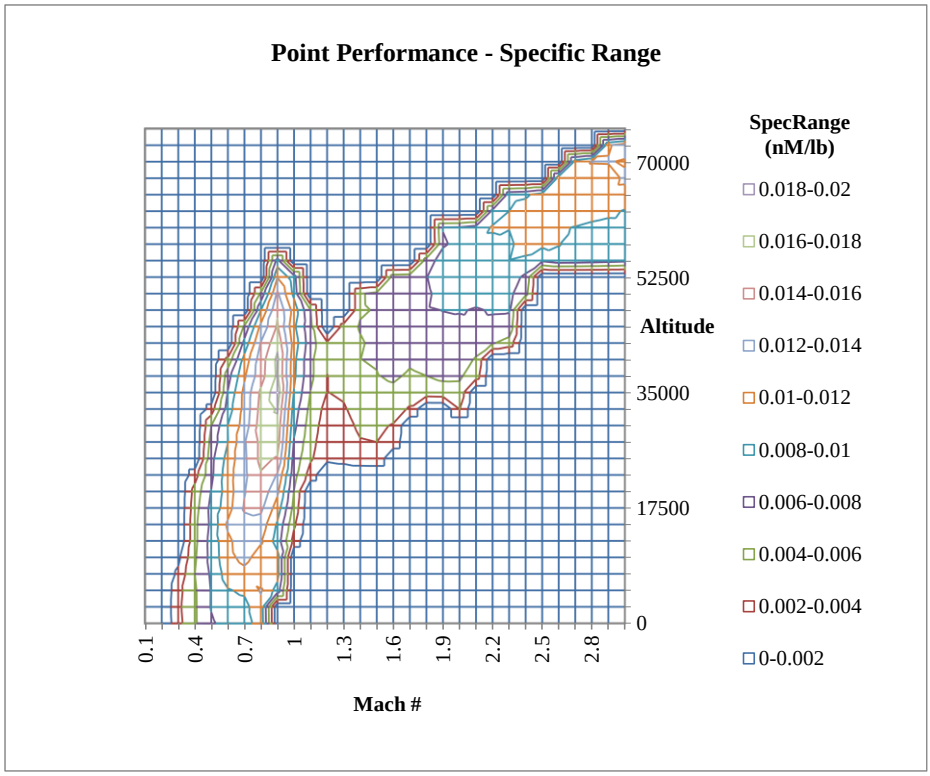

Figure 62 Specific Range Point Performance Contours at 30º Sweep and 666,000 lbm. Analysis Weight

6.1.4. Wing Sweep Angle = 35º

The maximum value of specific range for subsonic conditions under this specific configurations of wing and weight is 0.0192 nM/lbm which is observed at

nearly Mach 0.9 and at an altitude circa 35,000 ft as can be observed from the distribution plot of specific range in Figure 63. On the other side, for the supersonic condition the aircraft under this geometrical changes can at the most amass around 0.0119 nM/lbm which could be observed to be at the extremes of both the Mach speed of the flight and the altitude.

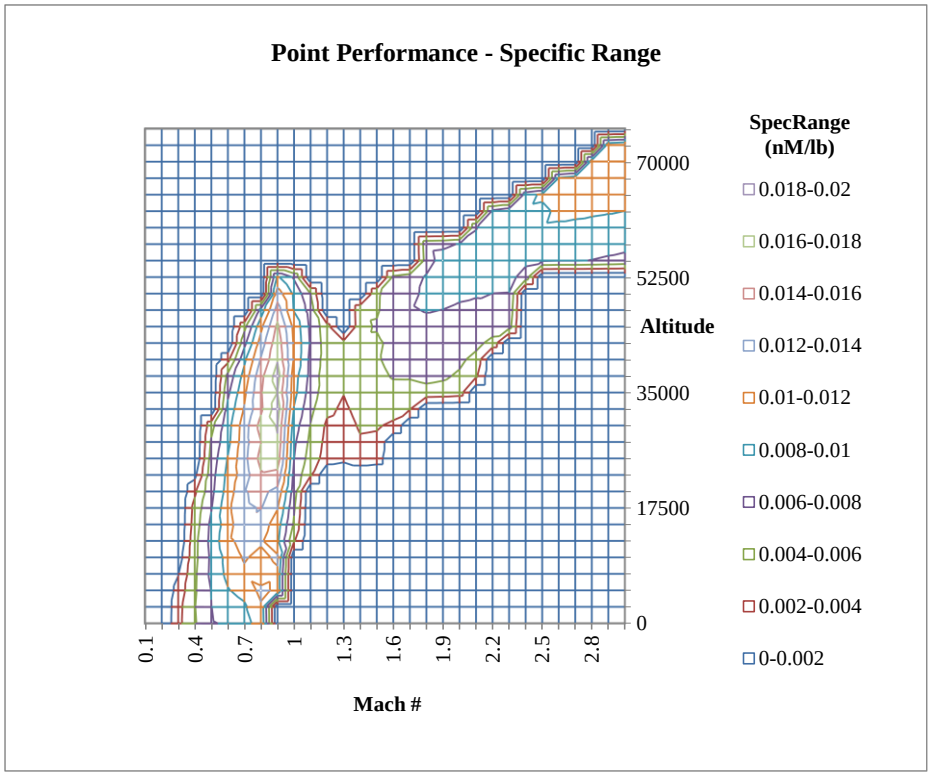

Figure 63 Specific Range Point Performance Contours at 35º Sweep and 666,000 lbm.

Analysis Weight

The aerodynamic performance efficiency *M(L/D)* has the maximum value for the subsonic region of 25.271 which also happens to be the best aerodynamic performance efficiency that could be extracted from the analyzed weight. On the

supersonic front, the *M(L/D)* has a maximum value of 28.743, which is relatively lower the preceding cases.

The aerodynamic efficiency *(L/D)* is observed to have maximum value in subsonic region. The maximum *(L/D)* is subsonic region is 28.333 whereas it reduces to just 11.13 when aircraft goes supersonic.

6.1.5. Wing Sweep Angle = 40º

The results obtained for this configuration are as could be expected from observing the trend from previous cases. The maximum specific range in subsonic condition is 0.0176 nM/lbm and it decreases to 0.0134 nM/lbm in supersonic speed region.

The maximum value of *(L/D)* in subsonic condition is obtained to be 26.88 and it decreases to 12.334 across sonic speed line. On the other side, the maximum value of *M(L/D)* in subsonic condition is 23.176 which is relatively lower than 31.519 which is observed in supersonic speed region.

Figure 64 below illustrates the specific range distribution along with the maximum point regions throughout the envelope of flight.

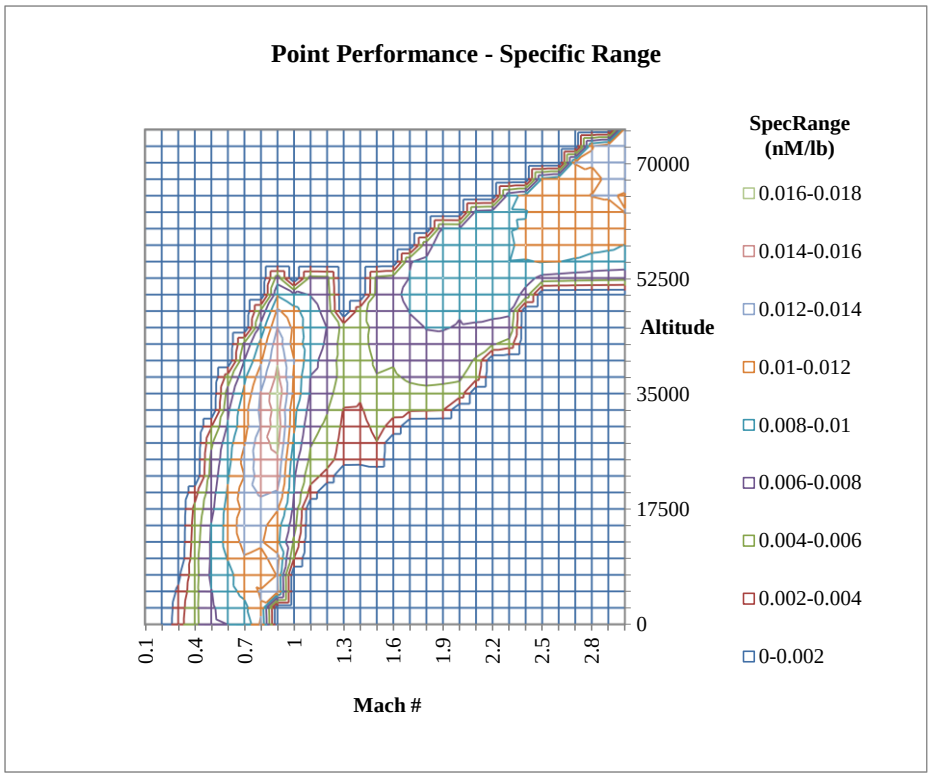

Figure 64 Specific Range Point Performance Contours at 40º Sweep and 666,000 lbm. Analysis Weight

6.1.6. Wing Sweep Angle = 45º

The maximum specific range observed for a sweep angle of 45 degrees at the highest test weight is 0.0164 nM/lbm at subsonic condition and 0.013 nM/lbm in supersonic speed region.

The plot as displayed in Figure 65 below represents the specific range distribution for the given geometry at 666,000 lbm of analysis weight.

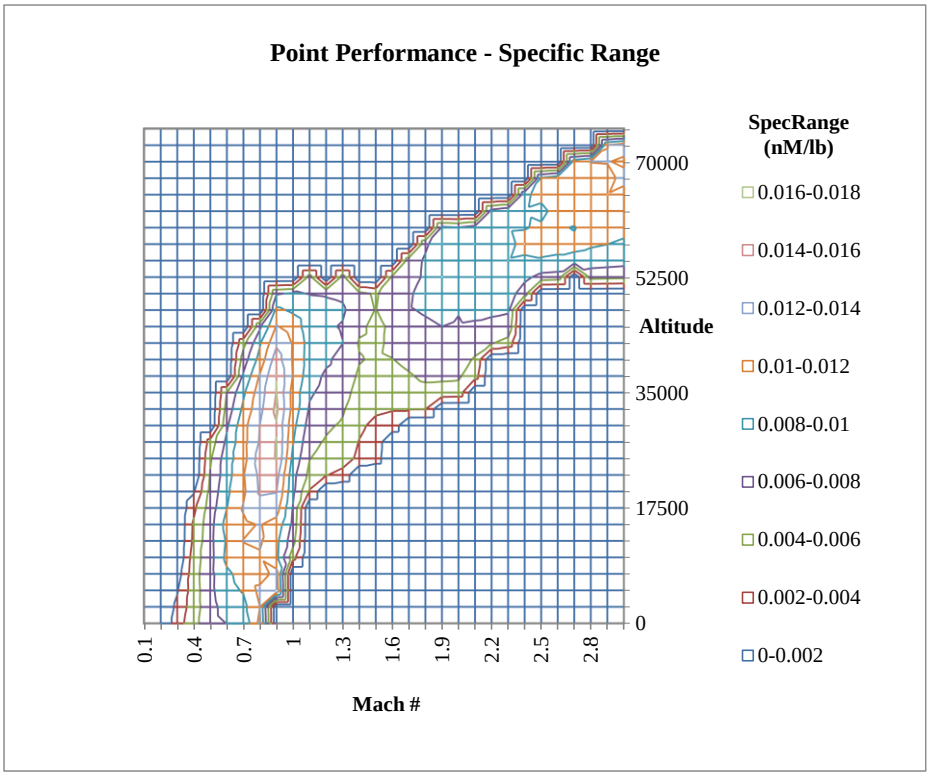

Figure 65 Specific Range Point Performance Contours at 45º Sweep and 666,000 lbm. Analysis Weight

The aerodynamic performance efficiency *M(L/D)* has a maximum value of 22.459 in subsonic region and it increases to 29.6 in supersonic region. The other performance parameter, the aerodynamic efficiency, *(L/D)* has a maximum value of 25.97 below sonic speed, and it decreases to 12.366 upon crossing speed of the sound.

6.1.7. Wing Sweep Angle = 50º

The maximum value of specific range for subsonic conditions under this specific configurations of wing and weight is 0.0158 nM/lbm which is observed at nearly Mach 0.9 and at an altitude just below 35,000 ft as can be observed from the

distribution plot of specific range. On the other side, for the supersonic condition the aircraft can at the most amass around 0.0134 nM/lbm which could be observed as the light navy blue section in the upper echelon of the altitude level and Mach speed.

The Figure 66 below represent the specific range distribution along the entire test range of the aircraft at the above mentioned specification.

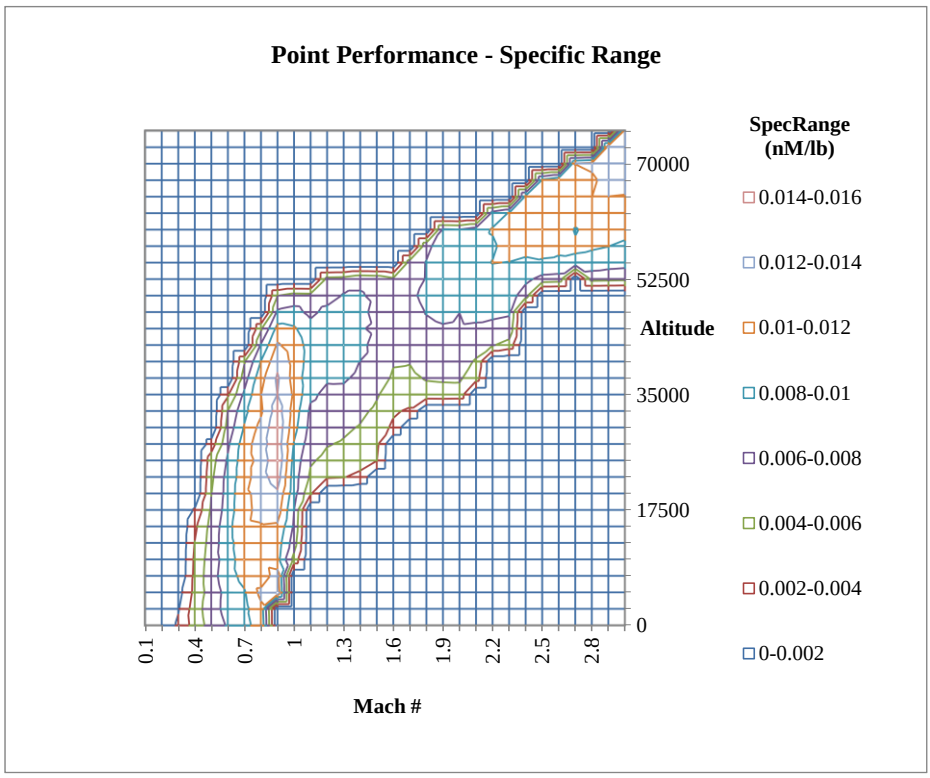

Figure 66 Specific Range Point Performance Contours at 50º Sweep and 666,000 lbm.

Analysis Weight

The maximum value of *(L/D)* in subsonic condition is obtained to be 24.681 and it decreases to 11.883 across sound speed line. On the other side, the maximum

value of *M(L/D)* in subsonic condition is 22.017 which is relatively lower than 30.687 which is observed in supersonic speed region.

6.1.8. Wing Sweep Angle = 55º

The maximum specific range observed for a sweep angle of 55 degrees at the maximum design flight weight is 0.0149 nM/lbm at subsonic condition and 0.0134 nM/lbm in post-sonic speed region.

The plot as displayed in Figure 67 below depicts the specific range distribution at analyzed specifications of aircraft.

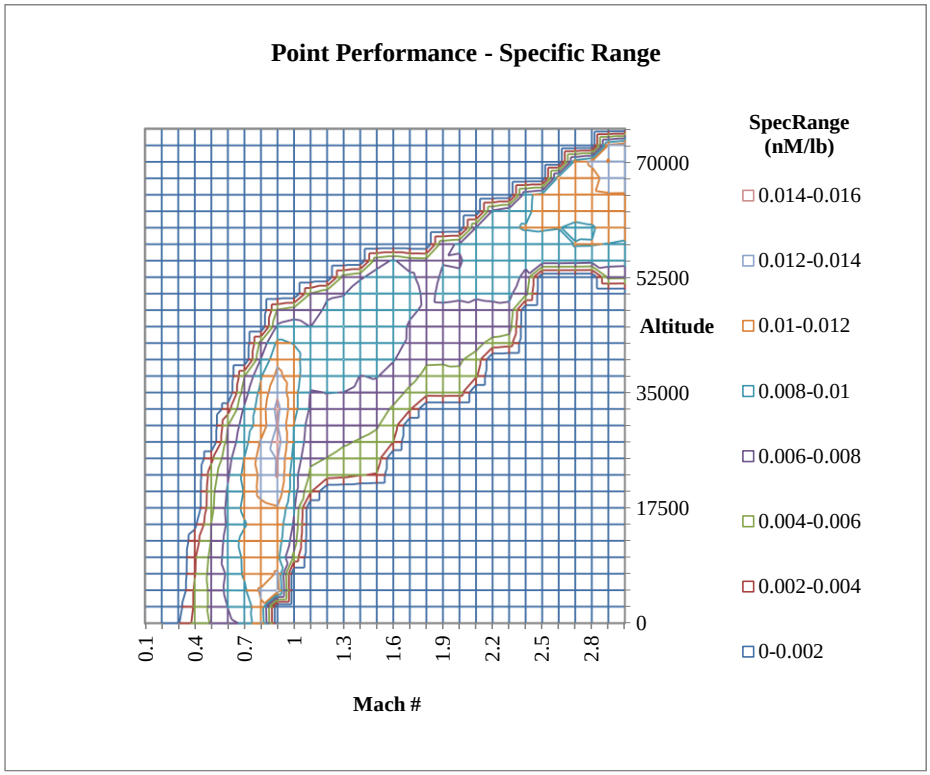

Figure 67 Specific Range Point Performance Contours at 55º Sweep and 666,000 lbm. Analysis Weight

The aerodynamic performance efficiency *M(L/D)* has a maximum value of 20.806 in subsonic region and it increases to 30.506 in supersonic region. The other performance parameter, the aerodynamic efficiency, *(L/D)* has a maximum value of 23.435 below sonic speed, and it decreases to 11.302 upon flying at supersonic speed.

6.1.9. Wing Sweep Angle = 60º

The maximum value of specific range for subsonic conditions under this specific configurations of wing and weight is 0.0138 nM/lbm which is observed at nearly Mach 0.9 and at an altitude ranging between 30,00 ft to 35,000 ft as can be observed from the distribution of specific range in Figure 68.

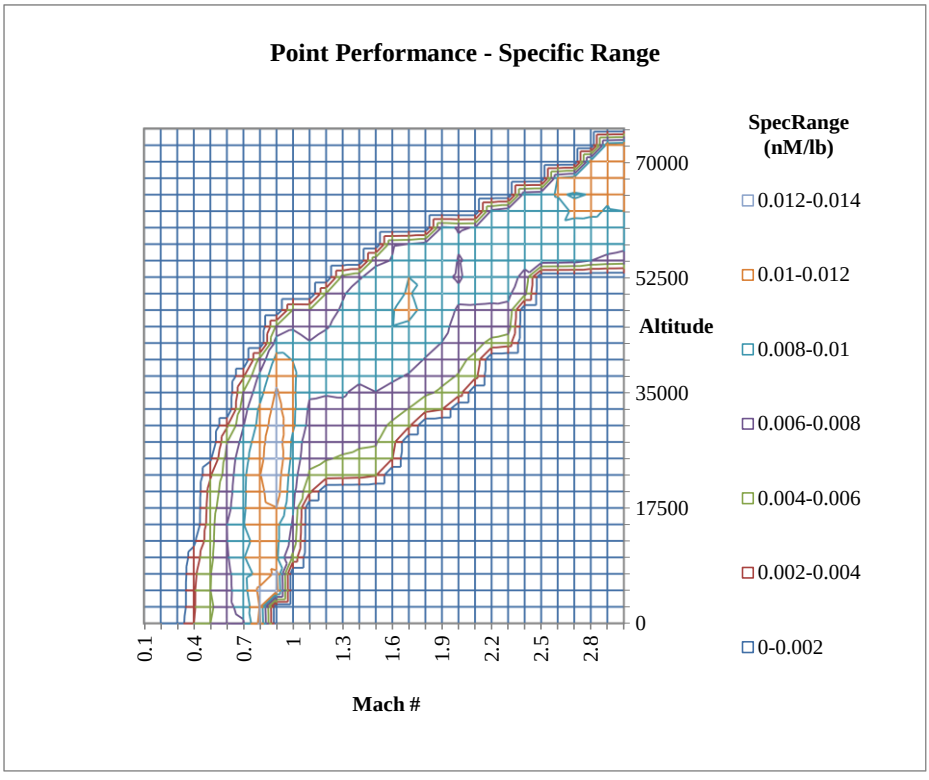

Figure 68 Specific Range Point Performance Contours at 60º Sweep and 666,000 lbm.

On the other side, for the supersonic condition the aircraft can at the most amass around 0.0115 nM/lbm which could be observed as the orange section in the higher magnitudes of the altitude level (from 65,000 ft to 72,500 ft) and Mach speeds (from Mach 2.5 to Mach 3).

The aerodynamic performance efficiency parameter, *M(L/D)* has a maximum value of 20.151 in subsonic region and it increases to 27.824 in supersonic region. The other performance parameter, the aerodynamic efficiency, *(L/D)* has a maximum value of 22.39 below sonic speed, and it decreases to 10.75 upon flying at supersonic speed.

6.1.10. Wing Sweep Angle = 65^{o}

For wing sweep angle of 65^{o} and using maximum analysis weight of the three, the maximum specific range is observed around Mach 0.85 and this highest spectrum of specific range is observed to be within the range of 22,500 ft to 27,500 ft. The value of maximum specific range is 0.0135 nM/lbm in subsonic region and 0.0121 nM/lbm in supersonic condition.

The aerodynamic performance efficiency *M(L/D)* has a maximum value of 17.933 in subsonic region and it increases to 25.286 in supersonic region. The other performance parameter, the aerodynamic efficiency, *(L/D)* has a maximum value of 21.006 below sonic speed, and it decreases to 10.042 upon flying at supersonic speed. Below is in Figure 69 is specific range distribution representing the point performance value at different iterations of Mach number and altitude values.

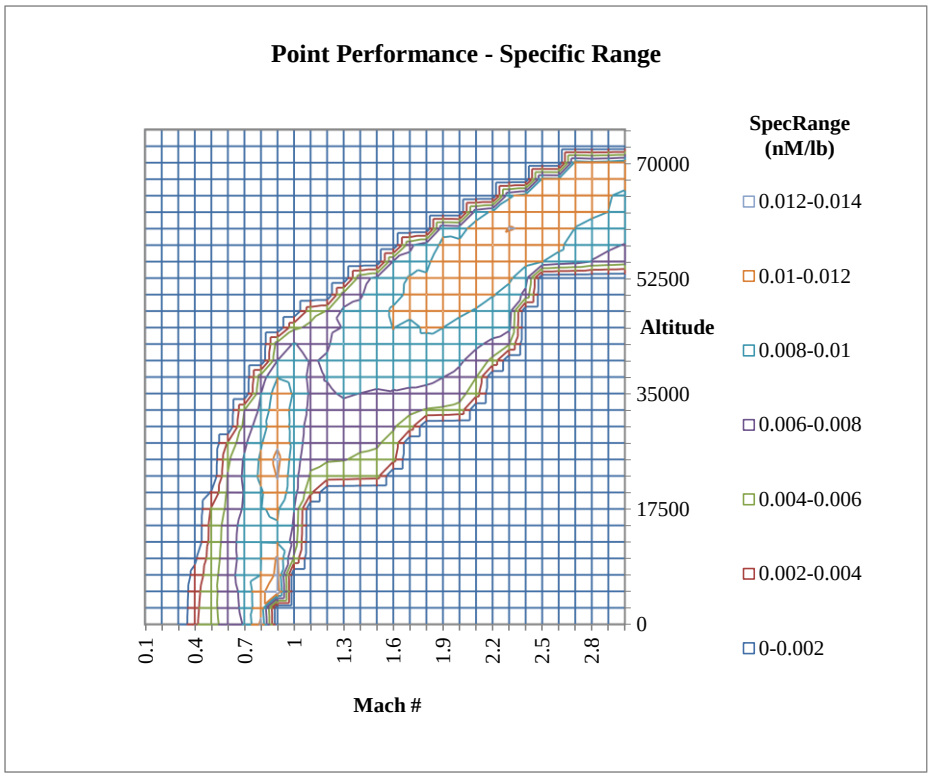

Figure 69 Specific Range Point Performance Contours at 65º Sweep and 666,000 lbm. Analysis Weight

If it is decided to utilize the maximum specific range point for this particular orientation, flying might lead to all sorts of trouble because the transonic speed of flight along with proximity to surface may create a series of shock waves which creates enormous noise which may disturb underneath environment and may also be against the governing regulations.

6.1.11. Wing Sweep Angle = 72º

The maximum value of specific range for subsonic conditions at the most aft wing condition and weight configurations is 0.0126 nM/lbm which is observed at nearly Mach 0.8 and at an altitude ranging between 25,00 ft to 30,000 ft as can

be observed from the distribution of specific range in Figure 70. On the other side, for the supersonic condition the aircraft can at the most amass around 0.0113 nM/lbm which could be observed as the orange section in the higher magnitudes of the altitude level and Mach speed. Flying subsonic at maximum specific range point may raise concerns of supersonic boom due to shock wave generation and its impact on the surrounding and proximity to the surface of Earth.

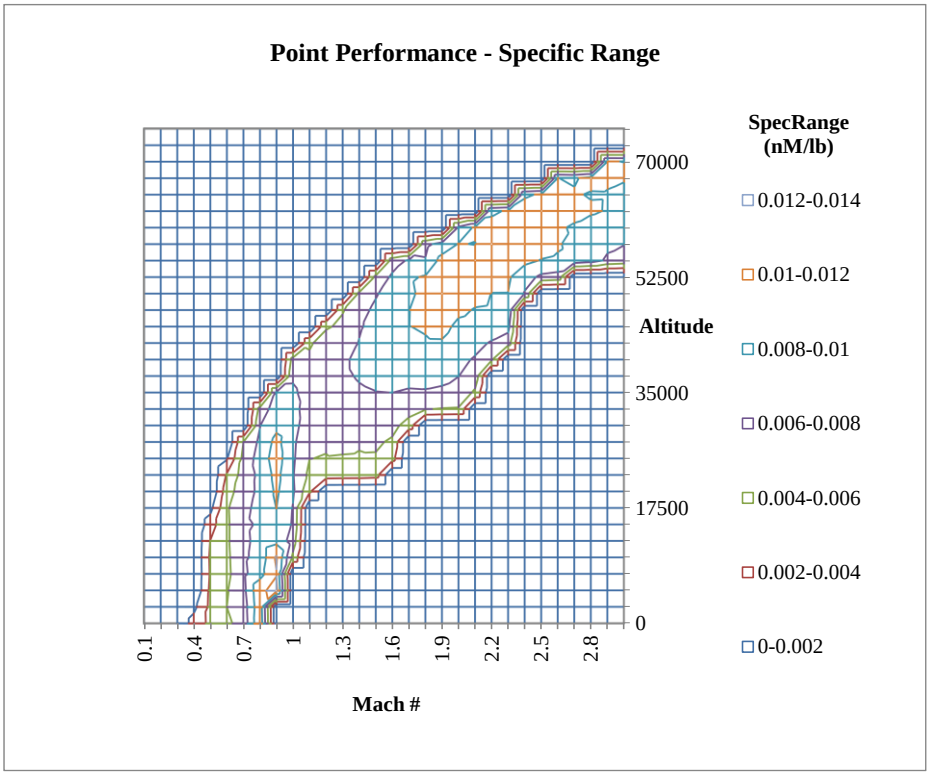

Figure 70 Specific Range Point Performance Contours at 72º Sweep and 666,000 lbm.

Analysis Weight

The aerodynamic performance efficiency *M(L/D)* has the maximum value for the subsonic region of 16.882 which also happens to be the worst aerodynamic performance efficiency that could be extracted from the analyzed weight. On the

supersonic front, the *M(L/D)* has a maximum value of 24.098, which is relatively lower the preceding cases. Hence, flying subsonic or supersonic at this weight and orientation is a bad strategy.

The aerodynamic efficiency *(L/D)* is observed to have maximum value in subsonic region. The maximum *(L/D)* is subsonic region is 19.413 whereas it reduces to just 9.368 when aircraft goes supersonic, leaving with another reason to avoid flying with such high weight at this orientation of wing

6.2. Maximum Design Landing Weight (430,000 lbm.)

6.2.1. Wing Sweep Angle = 20^{o}

The specific range point performance chart is displayed below in Figure 71 for the 20^{o} wing sweep and design landing weight orientation. It can be observed from just viewing the chart that although the trend of contours remains the same for different analysis weight, the magnitude changes inversely with the analysis weight. It can be seen here that the specific range is much better for landing weight analysis compared to maximum flight weight.

The maximum specific range value is obtained in subsonic region around Mach 0.8 and an altitude window of 35,000 ft and 37,500 ft where it reaches almost 0.0266 nM/lbm. Whereas in the supersonic region, the maximum specific range could just be 0.017 nM/lbm.

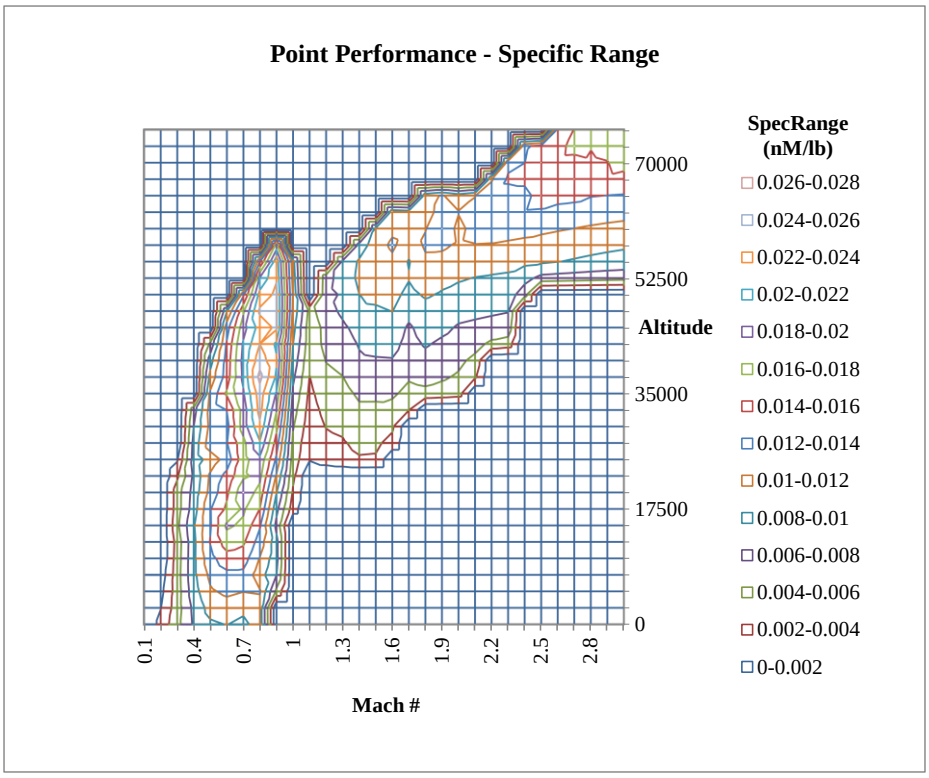

Figure 71 Specific Range Point Performance Contours at 20º Sweep and 430,000 lbm. Analysis Weight

The aerodynamic efficiency *(L/D)* supports the fact that at such orientation, it would be logical and advantageous to fly below the speed of sound. The maximum *(L/D)* in subsonic region is 28.697 and in supersonic region it falls to 8.788 which shows poor lift to drag relation above sonic speed.

The trends of *M(L/D)* is however completely opposite to the two performance parameters mentioned above. The maximum *M(L/D)* in subsonic region is 22.728 whereas it reaches 24.594 in supersonic region.

6.2.2. Wing Sweep Angle = 25º

The point performance as estimated using the flight envelope approach is similar to the previous case due to its almost identical aircraft geometry. The maximum specific range for the subsonic condition is 0.0269 nM/lbm observed just above 35,000 ft altitude whereas for the value of specific range displays similar pattern as the previous case and decreases to 0.019 nM/lbm. The contour plot in Figure 72 below displays the specific range distribution along throughout the tested Mach speed and altitudes for this particular case.

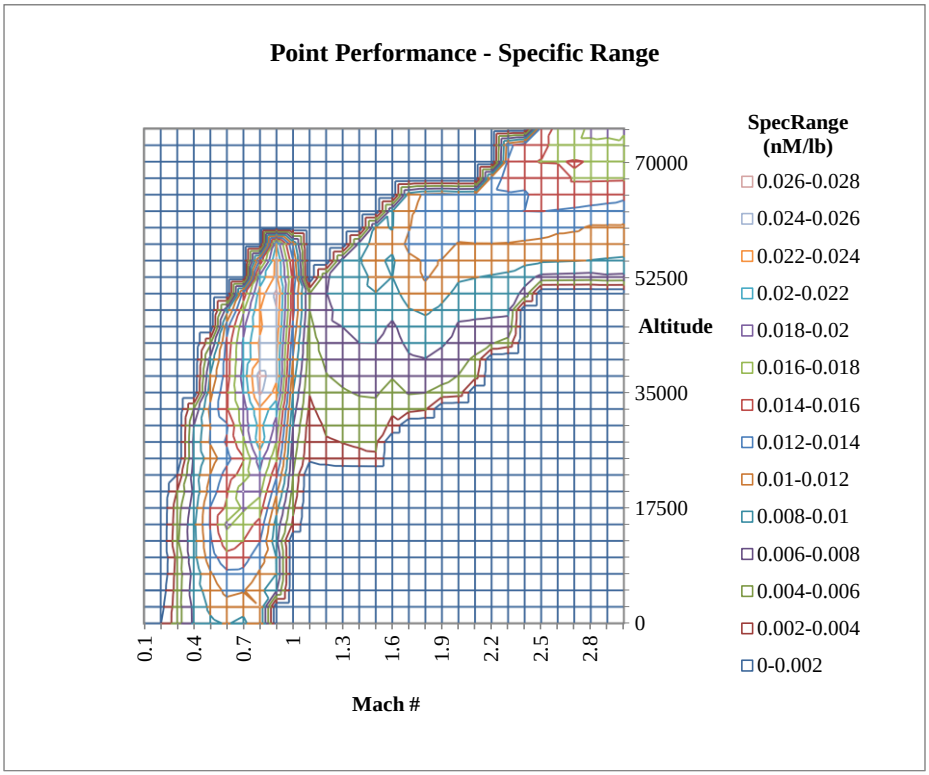

Figure 72 Specific Range Point Performance Contours at 25º Sweep and 430,000 lbm. Analysis Weight

The aerodynamic efficiency of the aircraft under this specifications of sweep angle and analysis weight leads to a higher *(L/D)* value in subsonic conditions compared to supersonic conditions. The maximum *(L/D)* in the subsonic region is 28.713 whereas it slashes to almost $1/3^{rd}$ in supersonic region where the maximum *(L/D)* is 9.012, making this configuration very useful primarily in subsonic conditions.

The aerodynamic performance efficiency *M(L/D)* has maximum value of 22.97 in subsonic condition and 26.107 in supersonic condition, showing the consistency with the pattern observed in previous case.

6.2.3. Wing Sweep Angle = 30^o

For wing sweep angle of 30^o and using the minimum analysis weight of the three, the maximum specific range is observed around Mach 0.9 and the highest spectrum is observed to be within the range of 45,000 ft to 50,000 ft. The value of maximum specific range is 0.0273 nM/lbm in subsonic region and 0.0166 nM/lbm in supersonic condition.

The increase in the magnitude of the specific range value in subsonic condition could be related directly to the improvements in the lift to drag ratio and reduction in several components of drag. The maximum *(L/D)* in subsonic condition is 28.934 and it reduces to 9.948 in supersonic condition.

The *M(L/D)* values in subsonic speed regimes are comparatively higher when compared with previous cases. In subsonic condition the maximum value obtained is 24.237, which decreases slightly to 24.089 in supersonic speed region.

Below is the plot as displayed in Figure 73 of specific range distribution representing the point performance value at different iterations of Mach number and altitude values.

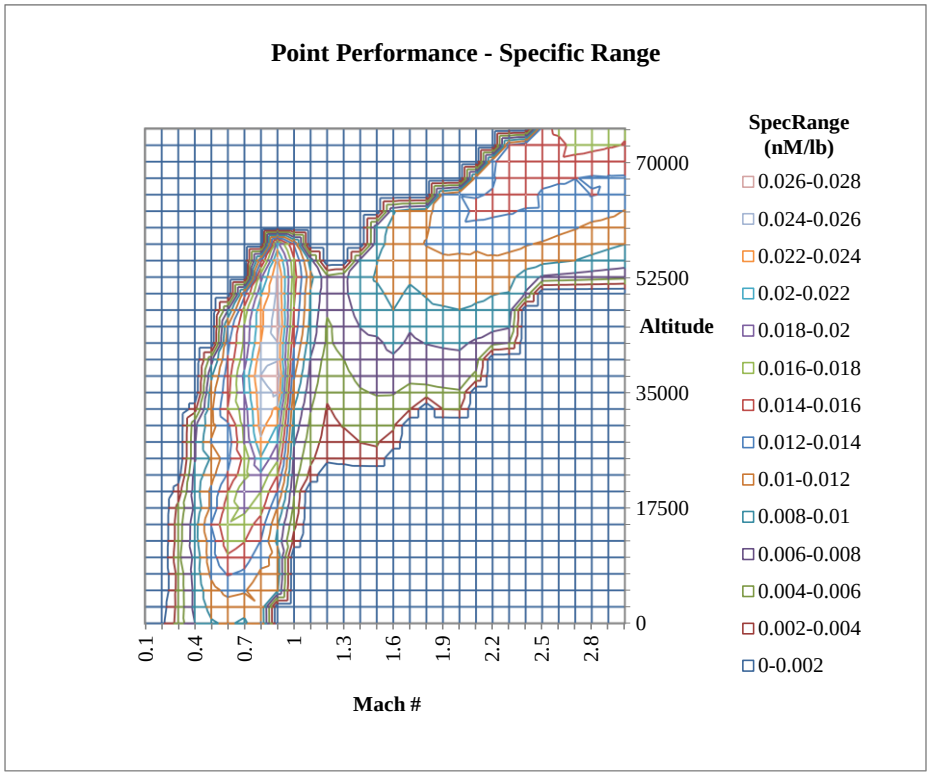

Figure 73 Specific Range Point Performance Contours at 30º Sweep and 430,000 lbm. Analysis Weight

6.2.4. Wing Sweep Angle = 35º

The maximum value of specific range for subsonic conditions under this specific configurations of wing and weight is 0.0268 nM/lbm which is observed at nearly Mach 0.9 and at an altitude circa 45,000 ft as can be observed from the distribution plot of specific range in Figure 74. On the other side, for the supersonic condition the aircraft under this geometrical changes can at the most amass around 0.016 nM/lbm which could be observed to be at the extremes of both the Mach speed of the flight and the altitude.

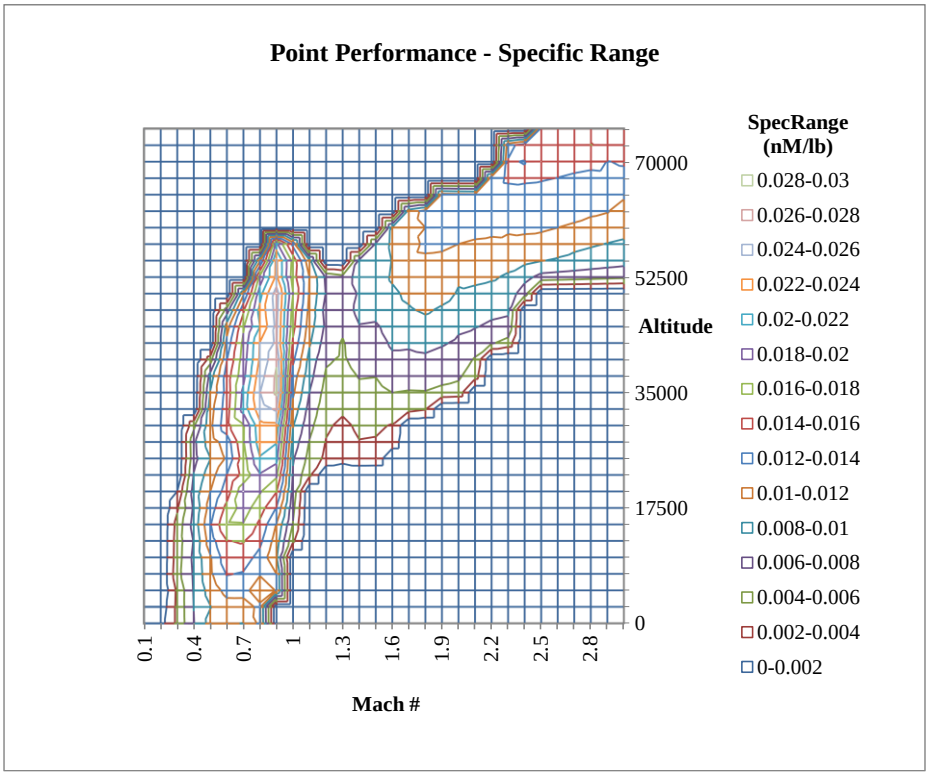

Figure 74 Specific Range Point Performance Contours at 35º Sweep and 430,000 lbm. Analysis Weight

The aerodynamic performance efficiency *M(L/D)* has the maximum value for the subsonic region of 24.472 which also happens to be the best aerodynamic performance efficiency that could be extracted from the analyzed weight. On the supersonic front, the *M(L/D)* has a maximum value of 23.493, which is relatively lower than the preceding cases.

The aerodynamic efficiency *(L/D)* is observed to have maximum value in subsonic region. The maximum *(L/D)* in subsonic region is 27.907 whereas it reduces to just 10.57 when aircraft goes supersonic.

6.2.5. Wing Sweep Angle = 40º

The results obtained for this configuration are as could be expected from observing the trend from previous cases. The maximum specific range in subsonic condition is 0.0268 nM/lbm and it decreases to 0.0185 nM/lbm in supersonic speed region.

The maximum value of *(L/D)* in subsonic condition is obtained to be 26.428 and it decreases to 12.086 across sonic speed line. On the other side, the maximum value of *M(L/D)* in subsonic condition is 22.592 which is relatively lower than 25.798 which is observed in supersonic speed region.

The contours as displayed in Figure 75 below illustrates the specific range distribution along with the maximum point regions throughout the envelope of flight.

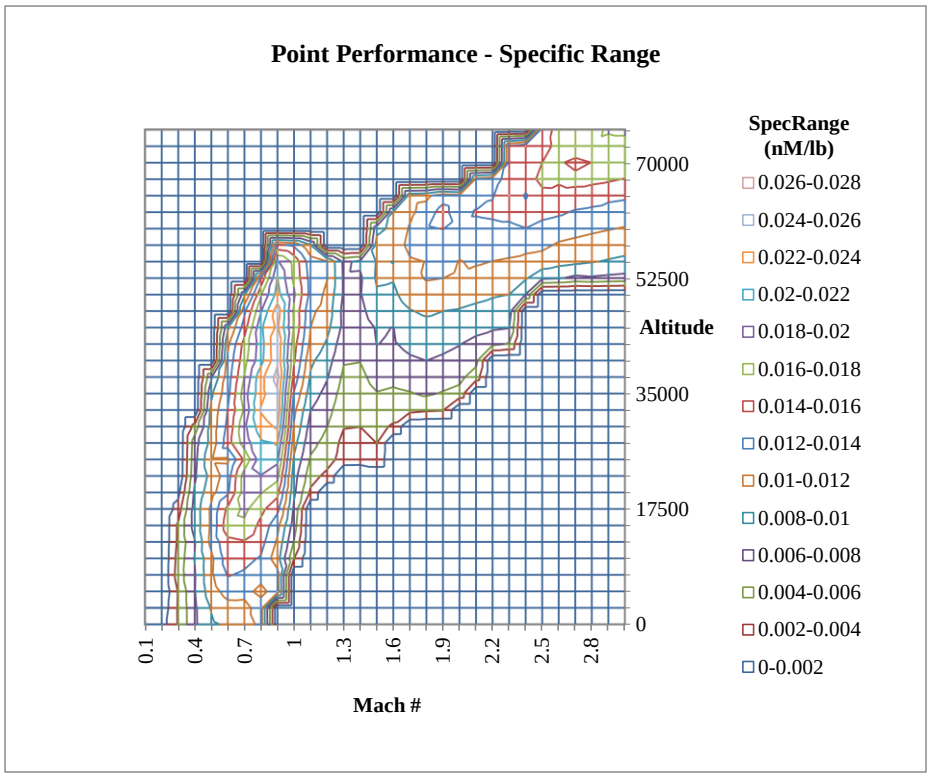

Figure 75 Specific Range Point Performance Contours at 40º Sweep and 430,000 lbm. Analysis Weight

6.2.6. Wing Sweep Angle = 45º

The maximum specific range observed for a sweep angle of 45 degrees at the lowest test weight is 0.0266 nM/lbm at subsonic condition and 0.0179 nM/lbm in supersonic speed region.

The Figure 76 below represents the specific range distribution for the given geometry at 430,000 lbm of analysis weight.

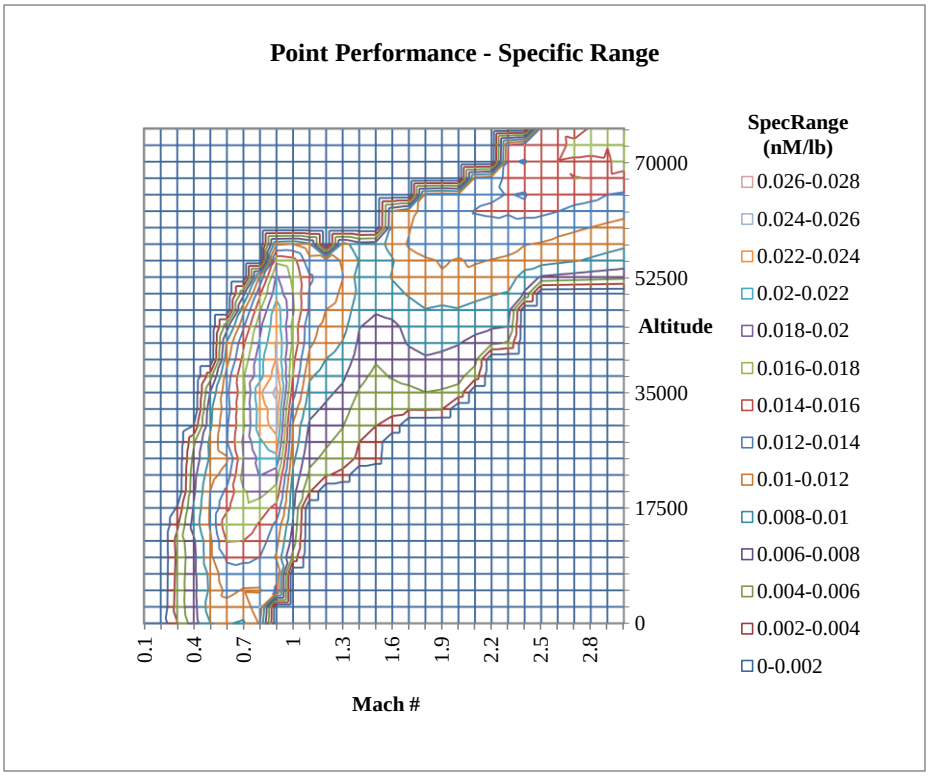

Figure 76 Specific Range Point Performance Contours at 45º Sweep and 430,000 lbm. Analysis Weight

The aerodynamic performance efficiency *M(L/D)* has a maximum value of 22.158 in subsonic region and it increases to 24.941 in supersonic region. The other performance parameter, the aerodynamic efficiency, *(L/D)* has a maximum value of 25.522 below sonic speed, and it decreases to 12.392 upon crossing speed of the sound.

6.2.7. Wing Sweep Angle = 50º

The maximum value of specific range for subsonic conditions under this specific configurations of wing and weight is 0.0257 nM/lbm which is observed at nearly Mach 0.9 and at an altitude around 35,000 ft as can be observed from the

distribution of specific range in Figure 77. On the other side, for the supersonic condition the aircraft can at the most amass around 0.0182 nM/lbm which could be observed as the faded purple section in the upper echelon of the altitude level and Mach speed.

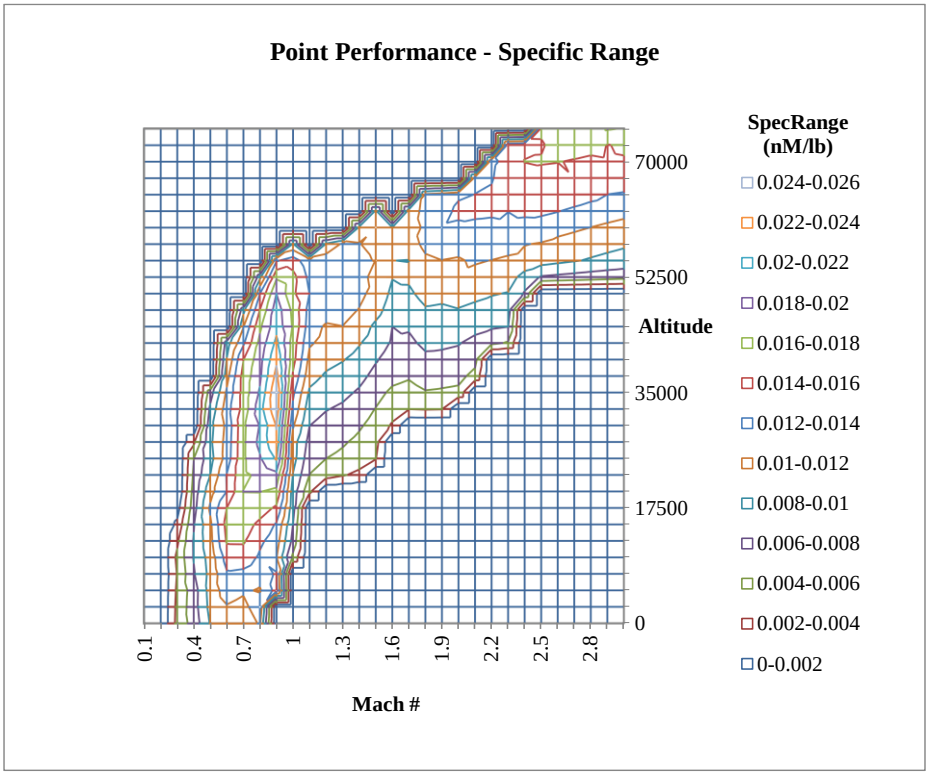

Figure 77 Specific Range Point Performance Contours at 50º Sweep and 430,000 lbm.

Analysis Weight

The maximum value of *(L/D)* in subsonic condition is obtained to be 24.377 and it decreases to 11.642 across sound speed line. On the other side, the maximum value of *M(L/D)* in subsonic condition is 21.667 which is relatively lower than 25.043 which is observed in supersonic speed region.

6.2.8. Wing Sweep Angle = 55º

The maximum specific range observed for a sweep angle of 55 degrees at the maximum design landing weight is 0.024 nM/lbm at subsonic condition and 0.018 nM/lbm in post-sonic speed region. The Figure 78 below depicts the specific range distribution at analyzed specifications of aircraft.

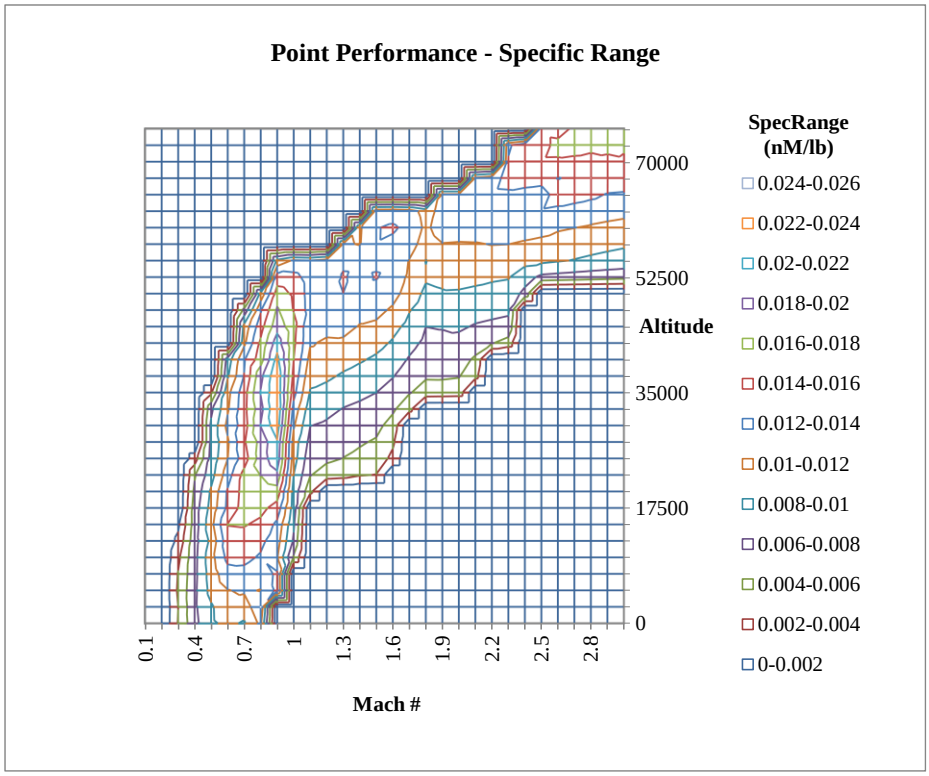

Figure 78 Specific Range Point Performance Contours at 55º Sweep and 430,000 lbm. Analysis Weight

The aerodynamic performance efficiency *M(L/D)* has a maximum value of 20.423 in subsonic region and it increases to 25.068 in supersonic region. The other performance parameter, the aerodynamic efficiency, *(L/D)* has a maximum value

of 22.979 below sonic speed, and it decreases to 11.199 upon flying at supersonic speed.

6.2.9. Wing Sweep Angle = 60º

The maximum value of specific range for subsonic conditions under this specific configurations of wing and weight is 0.0228 nM/lbm which is observed at nearly Mach 0.9 and at an altitude ranging between 32,000 ft to 35,000 ft as can be observed from the distribution plot of specific range in the Figure 79. On the other side, for the supersonic condition the aircraft can at the most accumulate just under 0.016 nM/lbm.

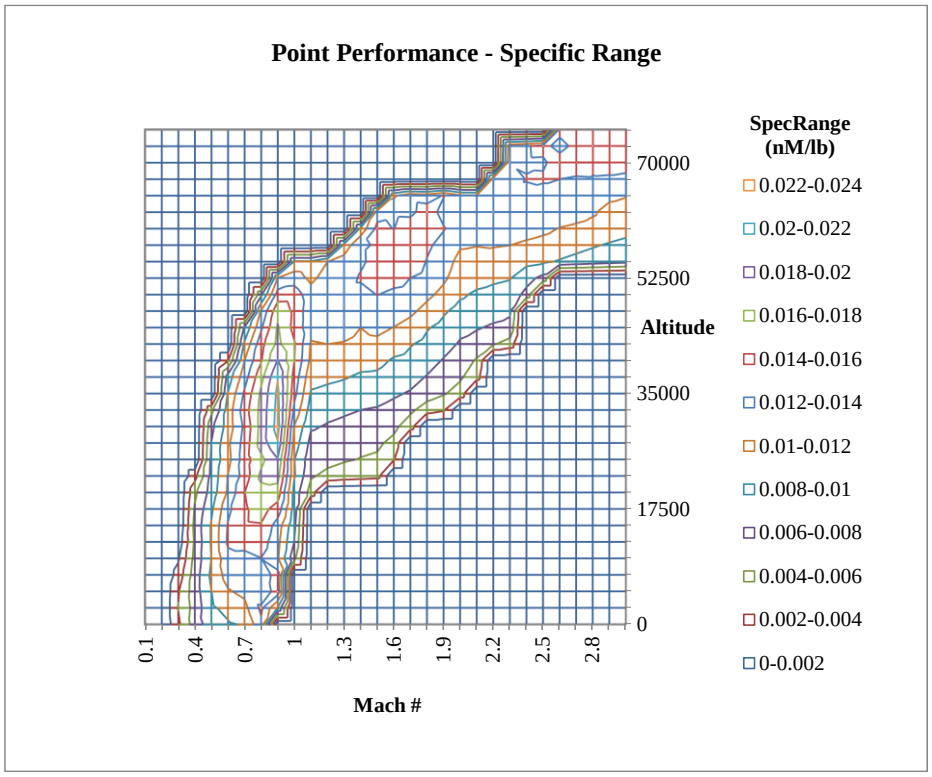

Figure 79 Specific Range Point Performance Contours at 60º Sweep and 430,000 lbm.

The aerodynamic performance efficiency parameter, *M(L/D)* has a maximum value of 19.795 in subsonic region and it increases to 23.485 in supersonic region. The other performance parameter, the aerodynamic efficiency, *(L/D)* has a maximum value of 21.994 below sonic speed, and it decreases to 10.681 upon flying at supersonic speed.

6.2.10. Wing Sweep Angle = 65º

For wing sweep angle of 65º and using smallest analysis weight of the three, the maximum specific range is observed around Mach 0.9 and this highest spectrum of specific range is observed to be around 35,000 ft. The value of maximum specific range is 0.0208 nM/lbm in subsonic region and 0.0176 nM/lbm in supersonic condition.

The aerodynamic performance efficiency *M(L/D)* has a maximum value of 17.643 in subsonic region and it increases to 23.095 in supersonic region. The other performance parameter, the aerodynamic efficiency, *(L/D)* has a maximum value of 20.833 below sonic speed, and it decreases to 9.884 upon flying at supersonic speed.

Figure 80 following this is the specific range distribution representing the point performance value at different iterations of Mach number and altitude values.

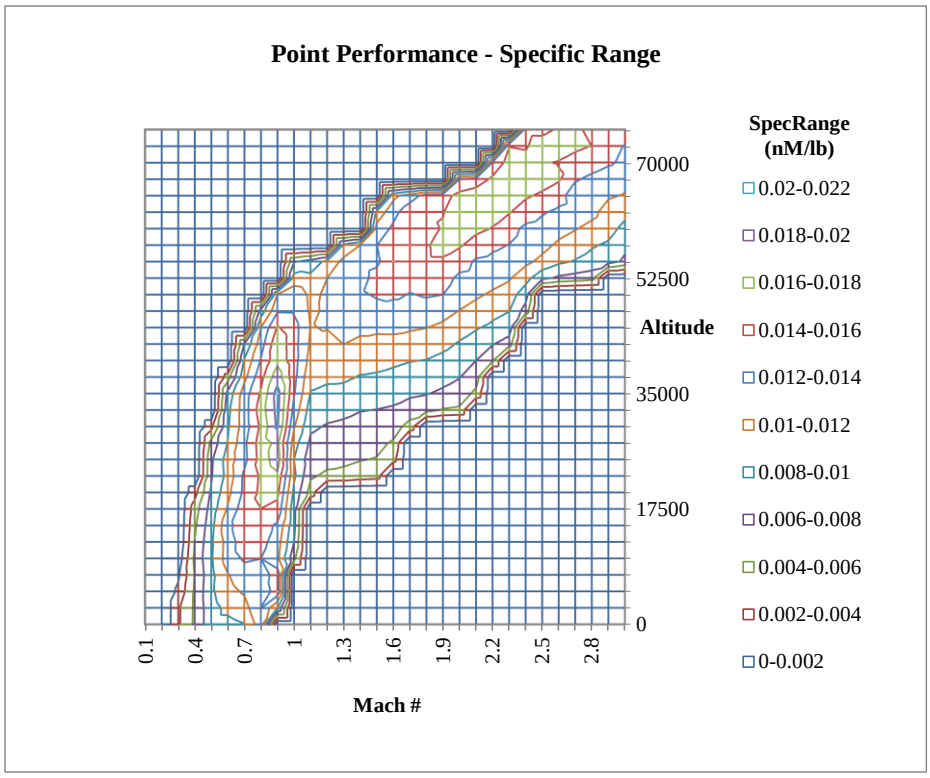

Figure 80 Specific Range Point Performance Contours at 65º Sweep and 430,000 lbm. Analysis Weight

6.2.11. Wing Sweep Angle = 72º

The maximum value of specific range for subsonic conditions at the most aft wing condition and smallest analyzed weight configurations is 0.0186 nM/lbm which is observed at nearly Mach 0.8 and at an altitude ranging between 25,00 ft to 35,000 ft as can be observed from the distribution plot of specific range in Figure 81. On the other side, for the supersonic condition the aircraft can at the most amass around 0.017 nM/lbm which could be observed as the light green section in the higher magnitudes of the altitude level and Mach speed. Flying subsonic at maximum specific range point may raise concerns of supersonic boom due to shock

wave generation and its impact on the surrounding and proximity to the surface of Earth.

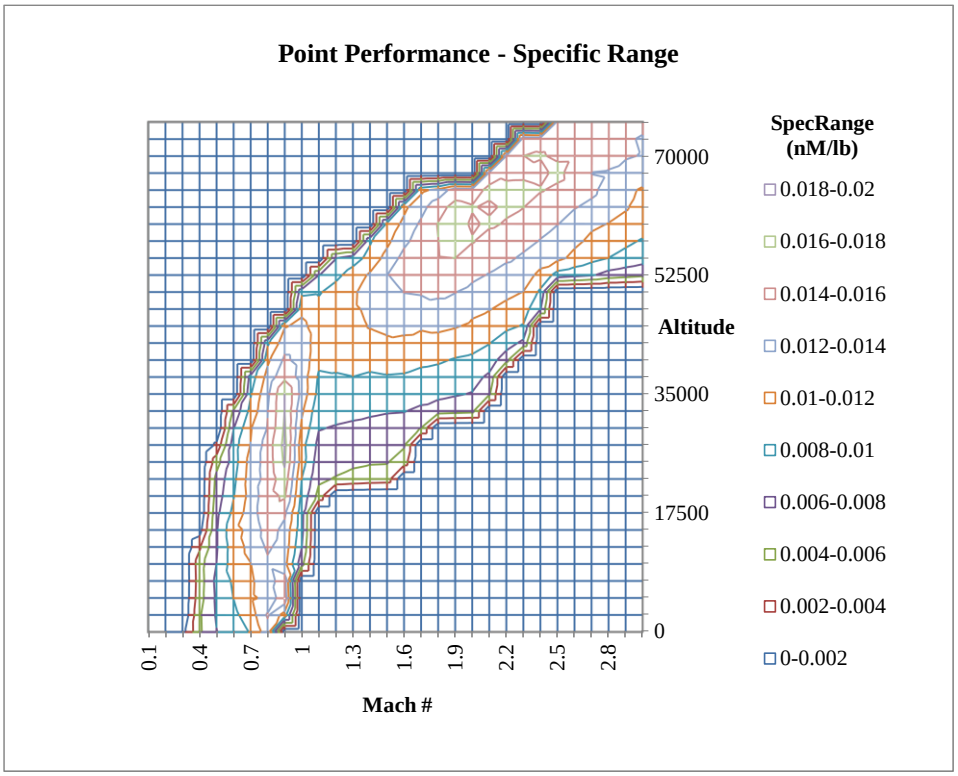

Figure 81 Specific Range Point Performance Contours at 72º Sweep and 430,000 lbm. Analysis Weight

The aerodynamic performance efficiency *M(L/D)* has the maximum value for the subsonic region of 16.467 which also happens to be the worst aerodynamic performance efficiency that could be extracted from the analyzed weight. On the supersonic front, the *M(L/D)* has a maximum value of 22.12, which is relatively lower the preceding cases.

This could eventually turn out to be a good option for supersonic cruising only if the weight associated with the instance of flight is anywhere near the analyzed weight in this section.

The aerodynamic efficiency *(L/D)* is observed to have maximum value in subsonic region. The maximum *(L/D)* is subsonic region is 19.075 whereas it reduces to just 9.411 when aircraft goes supersonic.

6.3. Intermediate Flight Weight (525,000 lbm.)

6.3.1. Wing Sweep Angle = 20º

For this sweep, the specific range performance representation for the aforementioned analysis weight is as shown below in Figure 82. The skymap plot which uses energy maneuverability theory shows a very good specific range for such a high analysis weight in the subsonic region at just around 37,500 - 40,000 ft altitude range.

On the other side of sonic boom, at such a lower sweep angle of the wing, the mileage performance of the aircraft seems to be similar to that when examined at maximum design flight weight condition. However, due to almost 100,000 lbm reduction in analysis weight the maximum value of specific range seems to have been elevated to 0.0219 nM/lbm in subsonic region whereas it stands at 0.0159 nM/lbm in supersonic region which still gives no solid reason to go above sonic speeds in this configuration.

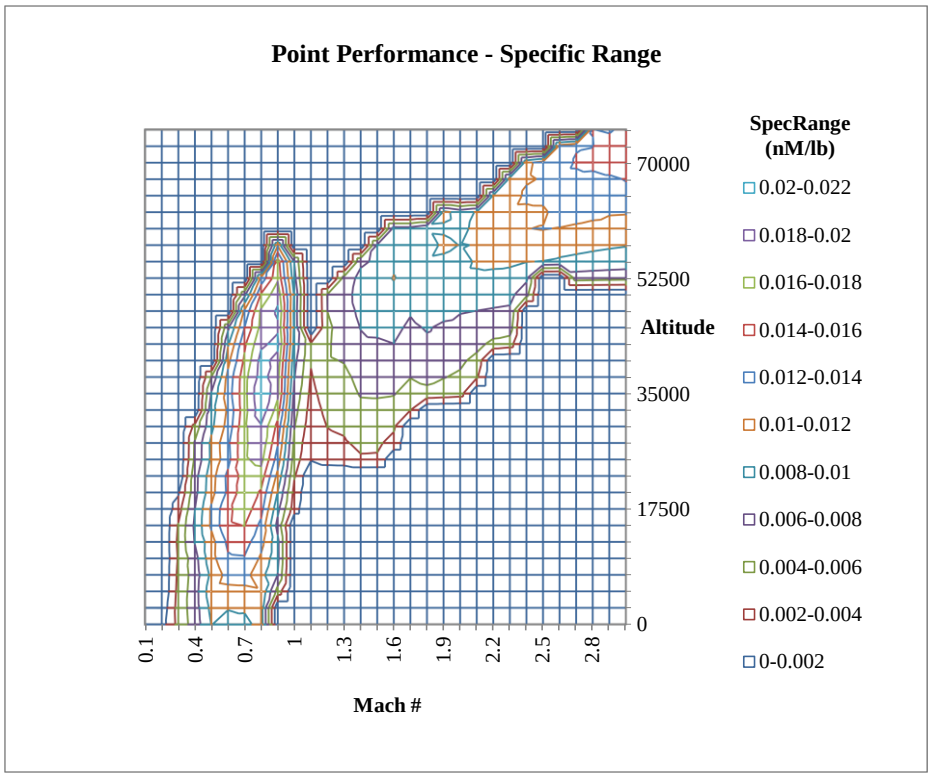

Figure 82 Specific Range Point Performance Contours at 20º Sweep and 525,000 lbm. Analysis Weight

The aerodynamic efficiency *(L/D)* values seems to be showing similar signs as to specific range in terms of performance of the aircraft at such low sweep angle. The maximum *(L/D)* in subsonic speed is 28.856 whereas in supersonic region it decreases to almost a third of its subsonic region performance where the maximum value of *(L/D)* is estimated to be 9.321.

The maximum *M(L/D)* value in this configuration was estimated to be 27.636 in supersonic region and 22.721 in subsonic region.

6.3.2. Wing Sweep Angle = 25º

The point performance as estimated using the flight envelope approach is similar to the previous case due to its almost similar aircraft geometry. The maximum specific range for the subsonic condition is 0.022 nM/lbm observed at around 40,000 ft altitude whereas for the value of specific range displays similar pattern as the previous case and decreases to 0.017 nM/lbm. Figure 83 below displays the contour plot of specific range distribution throughout the tested Mach speed and altitudes for this particular case.

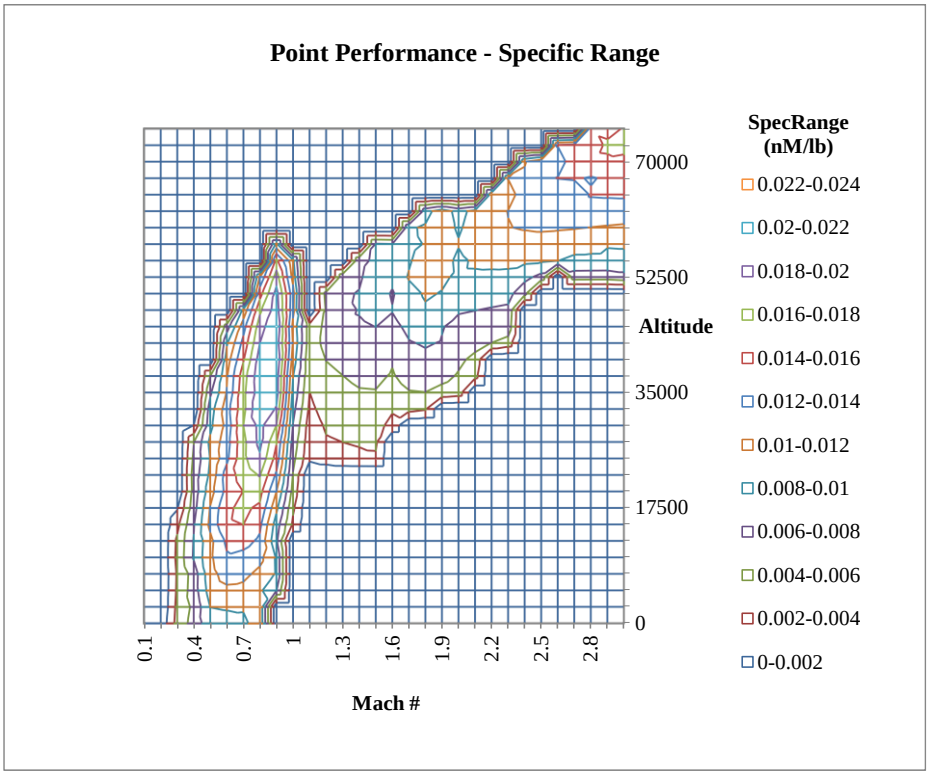

Figure 83 Specific Range Point Performance Contours at 25º Sweep and 525,000 lbm. Analysis Weight

The aerodynamic efficiency of the aircraft under this specifications of sweep angle and analysis weight leads to a higher *(L/D)* value in subsonic conditions compared to supersonic conditions. The maximum *(L/D)* is subsonic region is 29.173 whereas it slashes to almost 1/3rd in supersonic region where the maximum *(L/D)* is 9.787, making it a considerable fit in subsonic flight conditions.

The aerodynamic performance efficiency *M(L/D)* has a maximum value of 23.338 in subsonic condition and 29.359 in supersonic condition, showing the consistency with the pattern observed in previous case.

6.3.3. Wing Sweep Angle = 30^{o}

For wing sweep angle of 30^{o} and using intermediate analysis weight, the maximum specific range is observed around Mach 0.85 and the highest spectrum is observed to be within the range of 42,500 ft to 47,500 ft. The value of maximum specific range is 0.0239 nM/lbm in subsonic region and 0.015 nM/lbm in supersonic condition.

Below in Figure 84 is the specific range distribution representing the point performance value at different iterations of Mach number and altitude values.

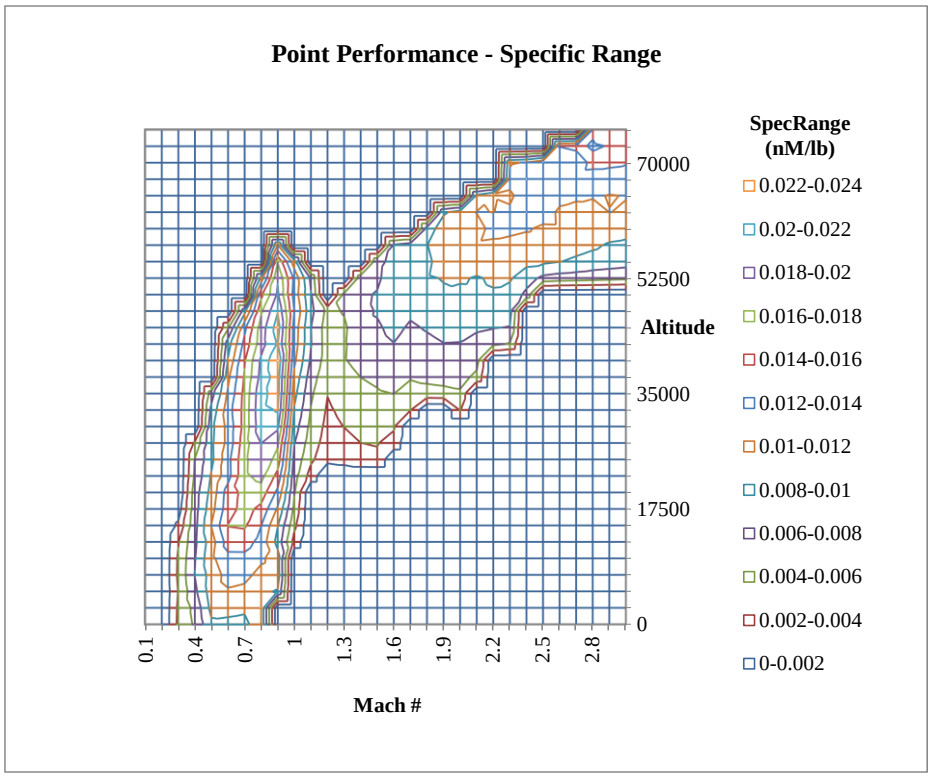

Figure 84 Specific Range Point Performance Contours at 30º Sweep and 525,000 lbm. Analysis Weight

The increase in the magnitude of the specific range value in subsonic condition could be related directly to the improvements in the lift to drag ratio and reduction in several components of drag. The maximum *(L/D)* in subsonic condition is 28.934 and it reduces to 10.102 in supersonic condition.

The *M(L/D)* values in subsonic speed regimes are comparatively higher when compared with previous cases. In subsonic condition the maximum value obtained is 24.674, which increases to 26.858 in supersonic speed region.

6.3.4. Wing Sweep Angle = 35º

The maximum value of specific range for subsonic conditions under this specific configurations of wing and weight is 0.0243 nM/lbm which is observed at nearly Mach 0.9 and at an altitude circa 40,000 ft as can be observed from the distribution plot of specific range in Figure 85. On the other side, for the supersonic condition the aircraft under this geometrical changes can at the most amass around 0.014 nM/lbm which could be observed to be at the extremes of both the Mach speed of the flight and the altitude.

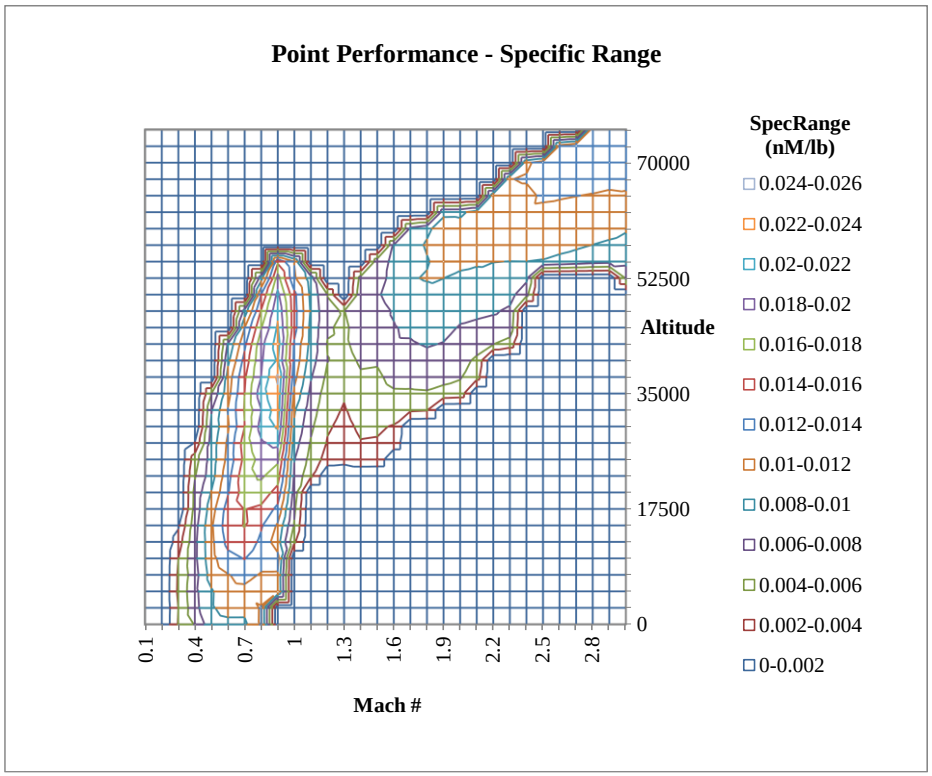

Figure 85 Specific Range Point Performance Contours at 35º Sweep and 525,000 lbm. Analysis Weight

The aerodynamic performance efficiency *M(L/D)* has the maximum value for the subsonic region of 25.034 which also happens to be the best aerodynamic performance efficiency that could be extracted from the analyzed weight. On the supersonic front, the *M(L/D)* has a maximum value of 26.241, which is relatively lower the preceding cases.

The aerodynamic efficiency *(L/D)* is observed to have maximum value in subsonic region. The maximum *(L/D)* is subsonic region is 28.233 whereas it reduces to just 11.095 when aircraft goes supersonic.

6.3.5. Wing Sweep Angle = 40º

The results obtained for this configuration are as could be expected from observing the trend from previous cases. The maximum specific range in subsonic condition is 0.0226 nM/lbm and it decreases to 0.0163 nM/lbm in supersonic speed region.

The maximum value of *(L/D)* in subsonic condition is obtained to be 26.701 and it decreases to 12.301 across sonic speed line. On the other side, the maximum value of *M(L/D)* in subsonic condition is 22.99 which is relatively lower than 26.853 which is observed in supersonic speed region.

The Figure 86 below illustrates the specific range distribution along with the maximum point regions throughout the envelope of flight.

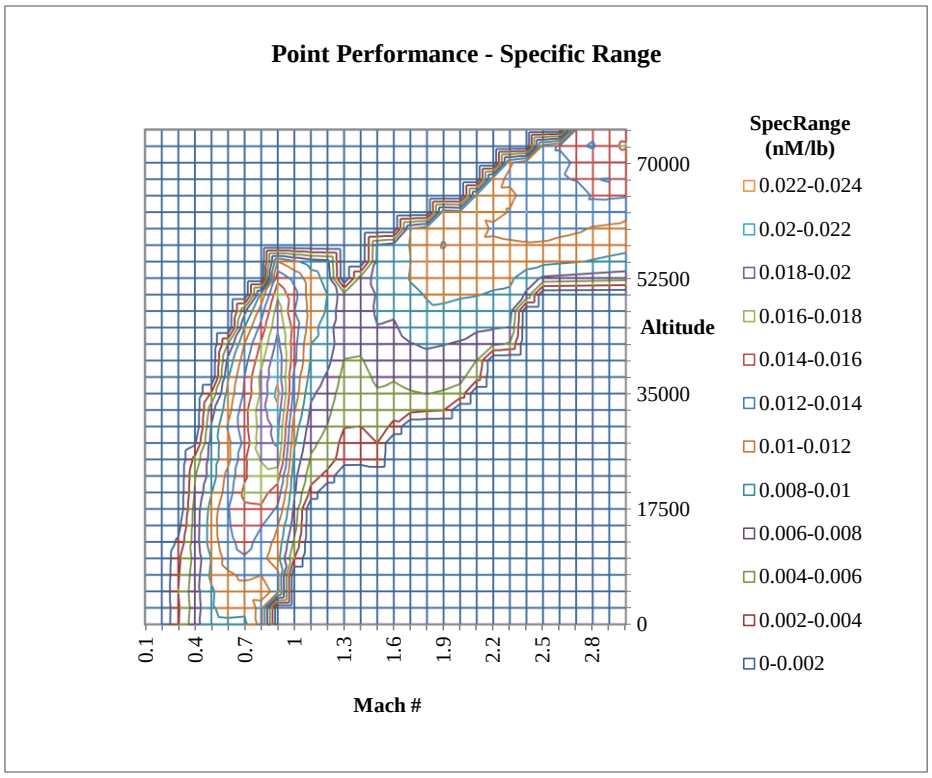

Figure 86 Specific Range Point Performance Contours at 40º Sweep and 525,000 lbm. Analysis Weight

6.3.6. Wing Sweep Angle = 45º

The maximum specific range observed for a sweep angle of 45 degrees at the highest test weight is 0.0212 nM/lbm at subsonic condition and 0.0156 nM/lbm in supersonic speed region.

The Figure 87 below represents the specific range distribution for the given geometry at 525,000 lbm of analysis weight.

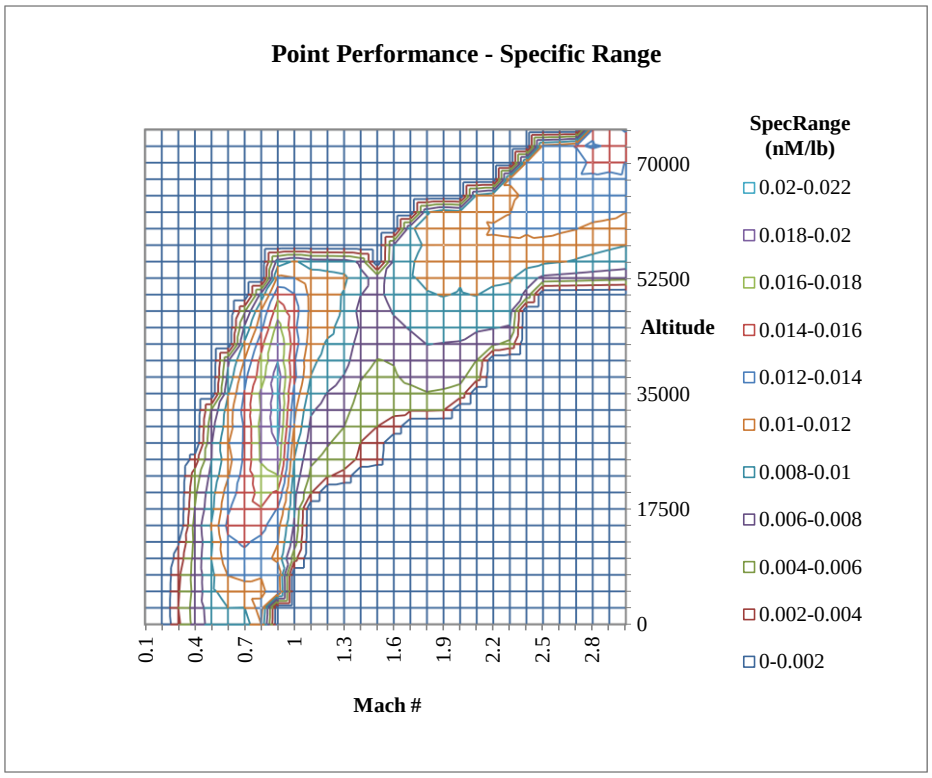

Figure 87 Specific Range Point Performance Contours at 45º Sweep and 525,000 lbm. Analysis Weight

The aerodynamic performance efficiency *M(L/D)* has a maximum value of 22.101 in subsonic region and it increases to 26.853 in supersonic region. The other performance parameter, the aerodynamic efficiency, *(L/D)* has a maximum value of 26.701 below sonic speed, and it decreases to 12.301 upon crossing speed of the sound.

6.3.7. Wing Sweep Angle = 50º

The maximum value of specific range for subsonic conditions under this specific configurations of wing and weight is 0.0207 nM/lbm which is observed at nearly Mach 0.9 and at an altitude just below 35,000 ft as can be observed from the distribution plot of specific range in Figure 88. On the other side, for the supersonic condition the aircraft can at the most amass around 0.016 nM/lbm which could be observed in the upper echelon of the altitude level and Mach speed.

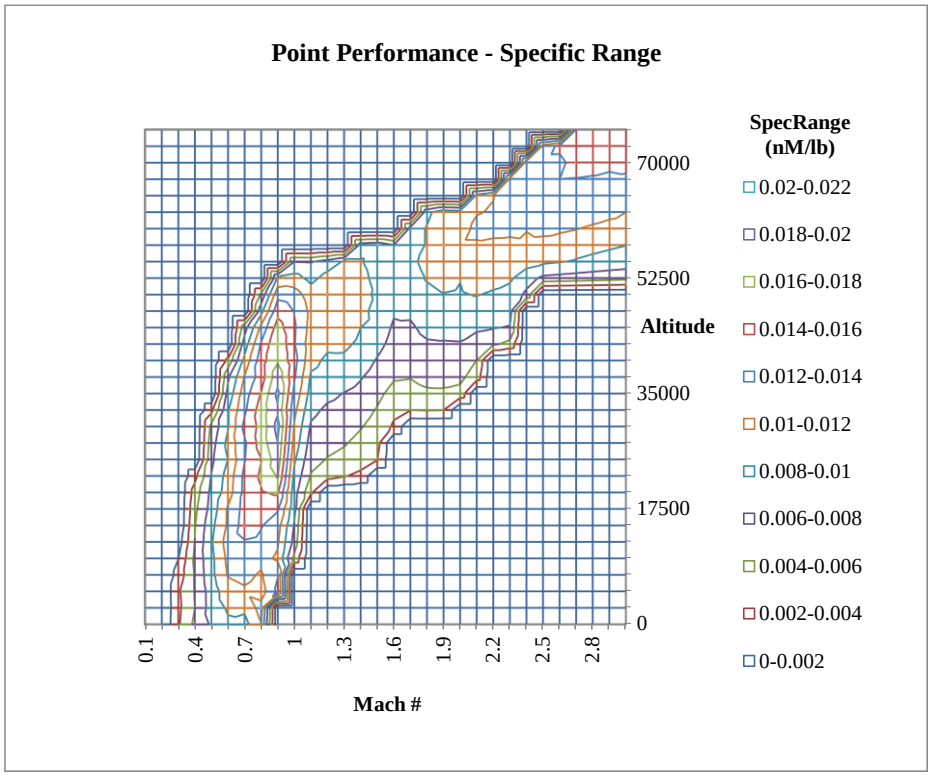

Figure 88 Specific Range Point Performance Contours at 50º Sweep and 525,000 lbm. Analysis Weight

The maximum value of *(L/D)* in subsonic condition is obtained to be 24.598 and it decreases to 11.835 across sound speed line. On the other side, the maximum value of *M(L/D)* in subsonic condition is 21.885 which is relatively lower than 28.162 which is observed in supersonic speed region.

6.3.8. Wing Sweep Angle = 55º

The maximum specific range observed for a sweep angle of 55 degrees at the maximum design flight weight is 0.0196 nM/lbm at subsonic condition and 0.0159 nM/lbm in post-sonic speed region. The contours depicted below in Figure 89 are of the specific range distribution at analyzed specifications of aircraft.

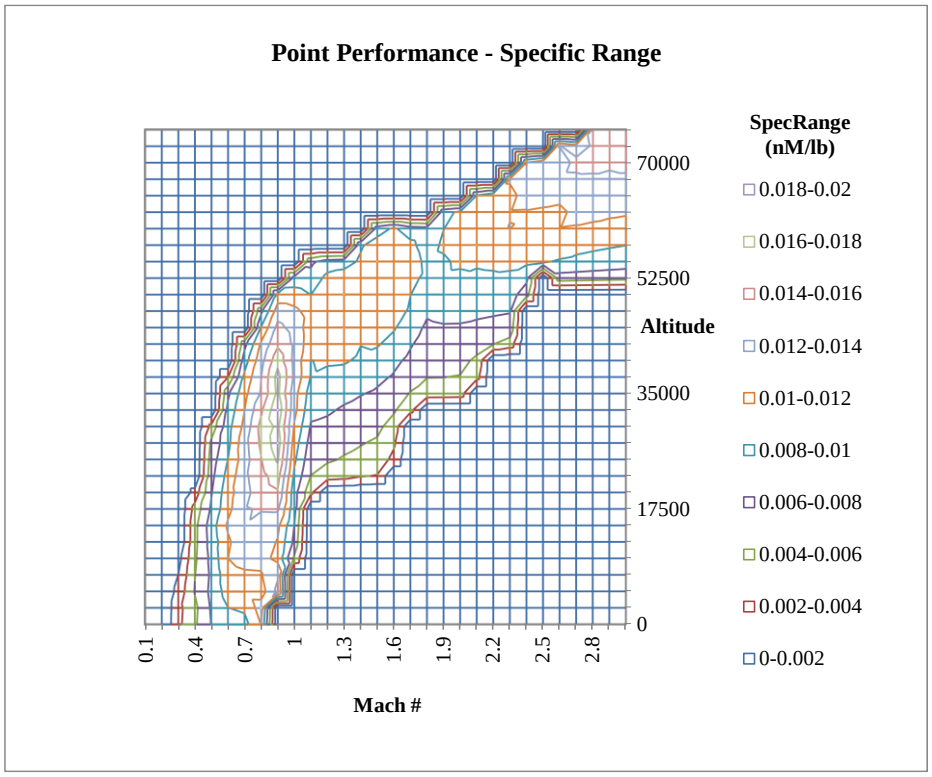

Figure 89 Specific Range Point Performance Contours at 55º Sweep and 525,000 lbm.

The aerodynamic performance efficiency *M(L/D)* has a maximum value of 20.692 in subsonic region and it increases to 27.966 in supersonic region. The other performance parameter, the aerodynamic efficiency, *(L/D)* has a maximum value of 23.202 below sonic speed, and it decreases to 11.264 upon flying at supersonic speed.

6.3.9. Wing Sweep Angle = 60º

The maximum value of specific range for subsonic conditions under this specific configurations of wing and weight is 0.0184 nM/lbm which is observed at nearly Mach 0.9 and at an altitude ranging between 30,00 ft to 35,000 ft as can be observed from the distribution plot of specific range below in Figure 90. On the other side, for the supersonic condition the aircraft can at the most amass around 0.0139 nM/lbm.

The aerodynamic performance efficiency parameter, *M(L/D)* has a maximum value of 19.057 in subsonic region and it increases to 25.729 in supersonic region.

The other performance parameter, the aerodynamic efficiency, *(L/D)* has a maximum value of 22.175 below sonic speed, and it decreases to 10.712 upon flying at supersonic speed.

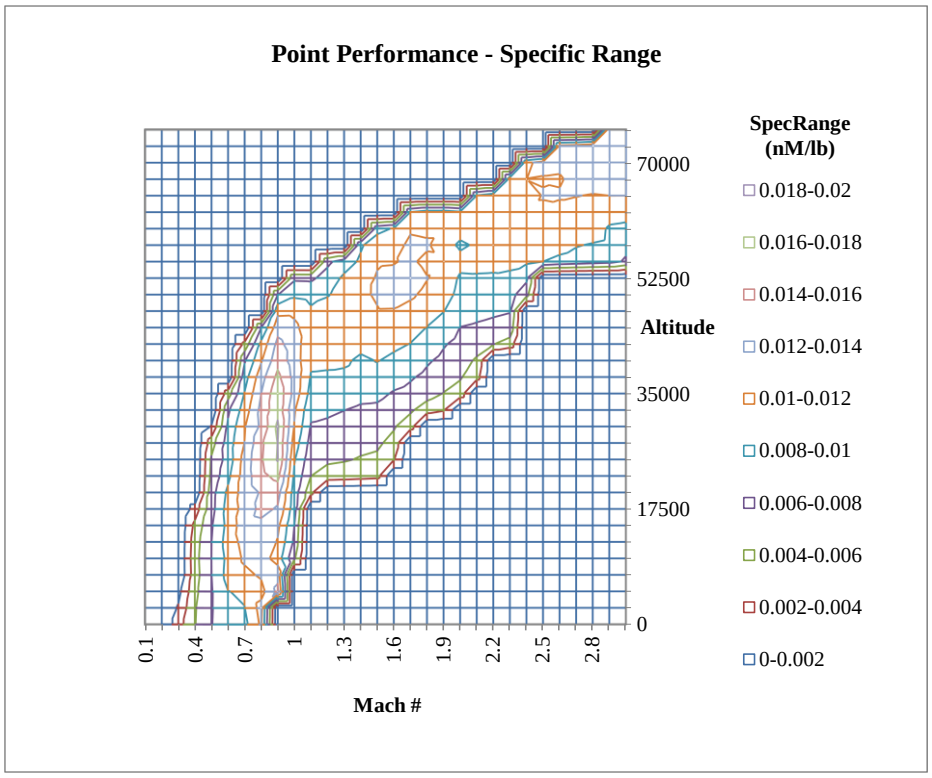

Figure 90 Specific Range Point Performance Contours at 60º Sweep and 525,000 lbm. Analysis Weight

6.3.10. Wing Sweep Angle = 65º

For wing sweep angle of 65º and using maximum analysis weight of the three, the maximum specific range is observed around Mach 0.87 and this highest spectrum of specific range is observed to be within the range of 25,000 ft to 30,000 ft. The value of maximum specific range is 0.0165 nM/lbm in subsonic region and 0.0146 nM/lbm in supersonic condition.

The aerodynamic performance efficiency *M(L/D)* has a maximum value of 17.799 in subsonic region and it increases to 25.127 in supersonic region. The other

performance parameter, the aerodynamic efficiency, *(L/D)* has a maximum value of 20.861 below sonic speed, and it decreases to 10.004 upon flying at supersonic speed.

Below in Figure 91 is the specific range distribution representing the point performance value at different iterations of Mach number and altitude values.

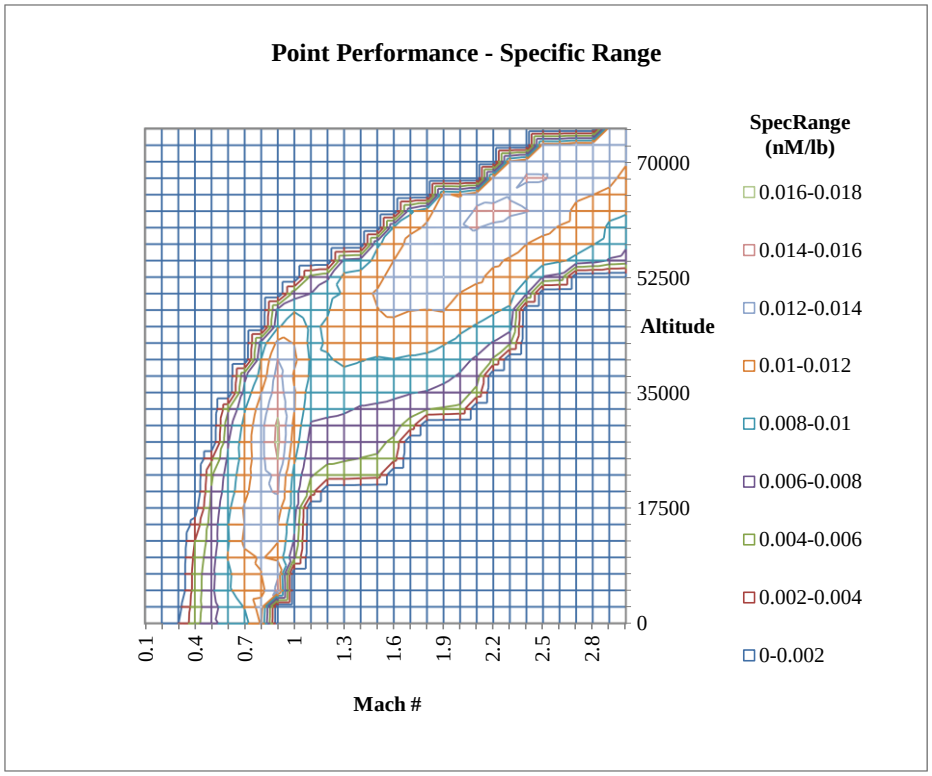

Figure 91 Specific Range Point Performance Contours at 65º Sweep and 525,000 lbm. Analysis Weight

6.3.11. Wing Sweep Angle = 72º

The maximum value of specific range for subsonic conditions at the most aft wing condition and weight configurations is 0.0147 nM/lbm which is observed

at nearly Mach 0.9 and at an altitude ranging between 25,00 ft to 30,000 ft as can be observed from the distribution plot of specific range as displayed in Figure 92. On the other side, for the supersonic condition the aircraft can at the most amass around 0.0141 nM/lbm which could be observed as the relatively smaller pink section in the higher magnitudes of the altitude level(~ 65,000 ft) and Mach speed (~ Mach 2.2).

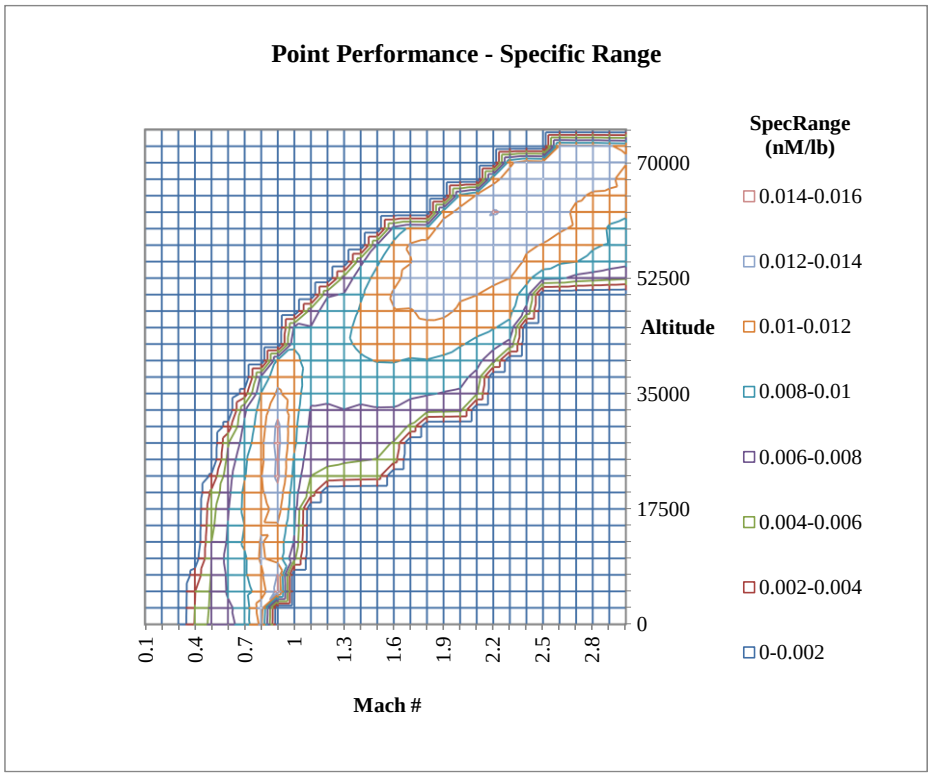

Figure 92 Specific Range Point Performance Contours at 72º Sweep and 525,000 lbm.

Analysis Weight

The aerodynamic performance efficiency *M(L/D)* has the maximum value for the subsonic region of 16.71 which also happens to be the worst aerodynamic performance efficiency that could be extracted from the analyzed weight. On the

supersonic front, the *M(L/D)* has a maximum value of 22.912, which is relatively lower the preceding cases. Hence, flying subsonic at this weight, previously mentioned altitude and orientation is a bad strategy.

The aerodynamic efficiency *(L/D)* is observed to have maximum value in subsonic region. The maximum *(L/D)* is subsonic region is 19.241 whereas it reduces to just 9.329 when aircraft goes supersonic, leaving with another reason to avoid flying with such high weight at this orientation of wing.

Hence, flying subsonic at maximum specific range point may raise concerns of supersonic boom due to shock wave generation and its impact on the surrounding and proximity to the surface of Earth.

However, it should be an excellent option of using this sweep geometry for flying supersonic speeds at high altitude near the service ceiling of the aircraft, as the effects of shock wave would be reduced drastically, and the specific range doesn't seem to be too bad to fly for a supersonic airliner.

6.4. Aerodynamic Performance Parameter's Summary

The Table 5 below summarizes the specific range of the aircraft when tested against different analysis weight for both subsonic and supersonic speeds.

Sweep Angles	***Specific Range - Subsonic***			***Specific Range - Supersonic***		
	430,000 lbm.	***525,000 lbm.***	***666,000 lbm.***	***430,000 lbm.***	***525,000 lbm.***	***666,000 lbm.***
20º	0.0266	0.0219	0.0173	0.0170	0.0159	0.0131
25º	0.0269	0.0220	0.0178	0.0190	0.0170	0.0141
30º	0.0273	0.0239	0.0193	0.0166	0.0150	0.0129
35º	0.0283	0.0243	0.0192	0.0160	0.0140	0.0119
40º	0.0268	0.0226	0.0176	0.0185	0.0163	0.0134
45º	0.0266	0.0212	0.0164	0.0179	0.0156	0.0130
50º	0.0257	0.0207	0.0158	0.0182	0.0160	0.0134
55º	0.0240	0.0196	0.0149	0.0180	0.0159	0.0134
60º	0.0228	0.0184	0.0138	0.0160	0.0139	0.0115
65º	0.0208	0.0165	0.0135	0.0176	0.0146	0.0121
72º	0.0186	0.0147	0.0126	0.0170	0.0141	0.0113

Table 5 Comparison of Results Obtained for Specific Range Across All Test Sweep Angles at Different Analysis Weight

The Table 6 below summarizes the aerodynamic efficiency of the aircraft when tested against different analysis weight for both subsonic and supersonic speeds.

Sweep Angles	***Aerodynamic Efficiency - Subsonic***			***Aerodynamic Efficiency - Supersonic***		
	430,000 lbm.	***525,000 lbm.***	***666,000 lbm.***	***430,000 lbm.***	***525,000 lbm.***	***666,000 lbm.***
20º	28.697	28.856	22.217	8.788	9.321	9.958
25º	28.713	29.173	29.414	9.012	9.787	10.515
30º	28.934	28.934	29.345	9.948	10.102	10.124
35º	27.907	28.233	28.333	10.570	11.095	11.130
40º	26.428	26.701	26.880	12.086	12.301	12.334
45º	25.522	25.638	25.970	12.392	12.285	12.366
50º	24.377	24.598	24.681	11.642	11.835	11.883
55º	22.979	23.202	23.435	11.199	11.264	11.302
60º	21.994	22.175	22.390	10.681	10.712	10.750
65º	20.833	20.861	21.006	9.884	10.004	10.042
72º	19.075	19.241	19.413	9.411	9.329	9.368

Table 6 Comparison of Results Obtained for Aerodynamic Efficiency Across All Test Sweep Angles at Different Analysis Weight

The Table 7 below summarizes the aerodynamic performance efficiency of the aircraft when tested against different analysis weight for subsonic and supersonic speeds.

Sweep Angles	***Aerodynamic Performance Efficiency - Subsonic***			***Aerodynamic Performance Efficiency - Supersonic***		
	430,000 lbm.	***525,000 lbm.***	***666,000 lbm.***	***430,000 lbm.***	***525,000 lbm.***	***666,000 lbm.***
20º	22.728	22.721	22.994	24.594	27.636	29.875
25º	22.970	23.338	23.521	26.107	29.359	31.545
30º	24.237	24.674	24.906	24.089	26.858	29.449
35º	24.472	25.034	25.271	23.493	26.241	28.743
40º	22.592	22.990	23.176	25.798	27.521	31.519
45º	22.158	22.101	22.459	24.941	26.853	29.600
50º	21.667	21.885	22.017	25.043	28.162	30.687
55º	20.423	20.692	20.806	25.068	27.966	30.506
60º	19.795	19.957	20.151	23.485	25.729	27.824
65º	17.643	17.799	17.933	23.095	25.127	25.286
72º	16.467	16.710	16.882	22.120	22.912	24.098

Table 7 Comparison of Results Obtained for Aerodynamic Performance Efficiency Across All Test Sweep Angles at Different Analysis Weight

7. FLIGHT MISSION COMPARISON

This section contains data from the flight mission approach that has been used to understand the impact of swing wing aircraft over standard delta wing aircraft with no variable sweep capabilities for a complete flight mission from takeoff to landing.

The flight mission starts with the mission objective, where all the sweep angles of aircraft that are used are described along with other relevant specifications such as speed, altitude, distance, etc. It later delves into the results obtained from analysis of the flight mission across all the database available on different sweep angles used along with the propulsion system.

For better understanding the impact of the performance in real life situation, the thrust value published in the General Electric's report has been scaled by 15% as a safety margin. This is done to achieve the necessary aircraft thrust performance which would closely relate to that of GE4/J5P turbojet engine which was supposed to be installed on B2707 aircraft.

Moreover, the number of engine to be used to power the flight has been decided by estimating the ratio of total thrust that was supposed to be used in dry weight condition (i.e. Maximum non-augmented thrust) to the maximum non-augmented thrust currently available from the engine after scaling.

7.1. Variable Sweep Flight Mission

The Figure 93 below is the sample mission approach used for assessing the performance of the aircraft based on understanding and implementing suitable sweep geometry from the previous results of specific range, aerodynamic efficiency, and aerodynamic performance efficiency. On analyzing those results, it becomes clearer and more logical to select a specific wing orientation to serve the object at any given point during the flight mission of the aircraft. For the variable sweep analysis, the aircraft is supposed to use 20^o, 45^o, 55^o, 60^o, and 72^o orientations of wing geometry.

For understanding effects and advantage of using variable sweep geometry during mission, the initial weight of the aircraft has been changed to replicate different scenarios which the aircraft may face in real-life situation in terms of demand and payload.

```
W_START   635000
W_END     360000
NENG      4.75

SET
AERO_FILE C:\Users\chaud\OneDrive\Desktop\MAE_564\PROJECT\Research_Papers\THESIS_FILES\b2707_20_database_rn.dat
DELTA_CD 0.0000

* TAKEOFF
GROUND_RUNUP
PLA 0.97
STOP TIME> 60.

MACH 0.25
ALTITUDE  400

* CLIMB W/O AFTERBURNER
CLIMB_CONST_KIAS
PLA 0.95
STOP ALT> 10000

* SWEEP WINGS
SET
AERO_FILE C:\Users\chaud\OneDrive\Desktop\MAE_564\PROJECT\Research_Papers\THESIS_FILES\b2707_45_database_rn.dat

* CLIMB W/O AFTERBURNER
ACCEL
PLA 0.95
STOP KIAS> 310.

* CLIMB W/O AFTERBURNER TO FL400 / M0.9
CLIMB_CONST_KIAS
PLA 0.95
STOP ALT> 25000 MACH> 0.9
```

```
CLIMB_CONST_MACH
PLA 0.95
STOP ALT> 40000

* LEVEL FLIGHT FOR FIRST 100 MILES
LEVEL
STOP DIST> 100

* SWEEP WINGS AND MAKE JUMP TO SUPERSONIC
SET
AERO_FILE C:\Users\chaud\OneDrive\Desktop\MAE_564\PROJECT\Research_Papers\THESIS_FILES\b2707_60_database_rn.dat

* ACCEL TO SUPERSONIC W/ AFTERBURNERS
ACCEL
PLA 0.98
STOP MACH> 1.5

CLIMB_CONST_KIAS
PLA 0.98
STOP MACH> 2.1 ALT> 62500

* SWEEP WINGS  FOR MACH 2.7 CRUISE
SET
AERO_FILE C:\Users\chaud\OneDrive\Desktop\MAE_564\PROJECT\Research_Papers\THESIS_FILES\b2707_72_database_rn.dat

ACCEL
PLA 0.98
STOP MACH> 2.7

CLIMB_CONST_MACH
PLA 0.98
STOP ALT> 70000

LEVEL
STOP DIST> 2600

CLIMB_CONST_KIAS
PLA 0.85
STOP ALT< 40000


* SWEEP WINGS  FOR DESCENT
SET
AERO_FILE C:\Users\chaud\OneDrive\Desktop\MAE_564\PROJECT\Research_Papers\THESIS_FILES\b2707_60_database_rn.dat

ACCEL
PLA 0.85
STOP MACH< 1.8

* SWEEP WINGS  FOR SUBSONIC
SET
AERO_FILE C:\Users\chaud\OneDrive\Desktop\MAE_564\PROJECT\Research_Papers\THESIS_FILES\b2707_55_database_rn.dat

LEVEL
STOP RELATIVE_DIST> 150.

ACCEL
PLA 0.85
STOP MACH< 0.95

CLIMB_CONST_MACH
PLA 0.85
STOP KIAS< 310 ALT< 20000

CLIMB_CONST_KIAS
PLA 0.85
STOP ALT< 7000

* SWEEP WINGS  FOR LANDING
SET
AERO_FILE C:\Users\chaud\OneDrive\Desktop\MAE_564\PROJECT\Research_Papers\THESIS_FILES\b2707_20_database_rn.dat

ACCEL
PLA 0.85
STOP KIAS< 250

CLIMB_CONST_KIAS
PLA 0.85
STOP ALT< 400
```

Figure 93 Sample Flight Mission Input File for Variable Sweep Geometry Operation of B2707 Over the Flight Span with Max Weight Of 635,000 lbm.

Moreover, the altitude and Mach numbers selected were based on a detailed study carried out to study the variation on the *M(L/D)* and *(L/D)* values at different points on the contours of the selected sweep conditions over a varying analysis weight. The weight will vary at different sweep configurations due to the amount of fuel burned being removed from the initial weight. For this, an initial guess was used to understand the weight variation throughout the flight to use as a benchmark for selecting best possible region on the flight envelope to use for flight mission. Below in Figure 94 is the weight variation over the span of the flight used for the flight mission input data to estimate the *M(L/D)* and *(L/D)* graphs to get optimal regions of travel.

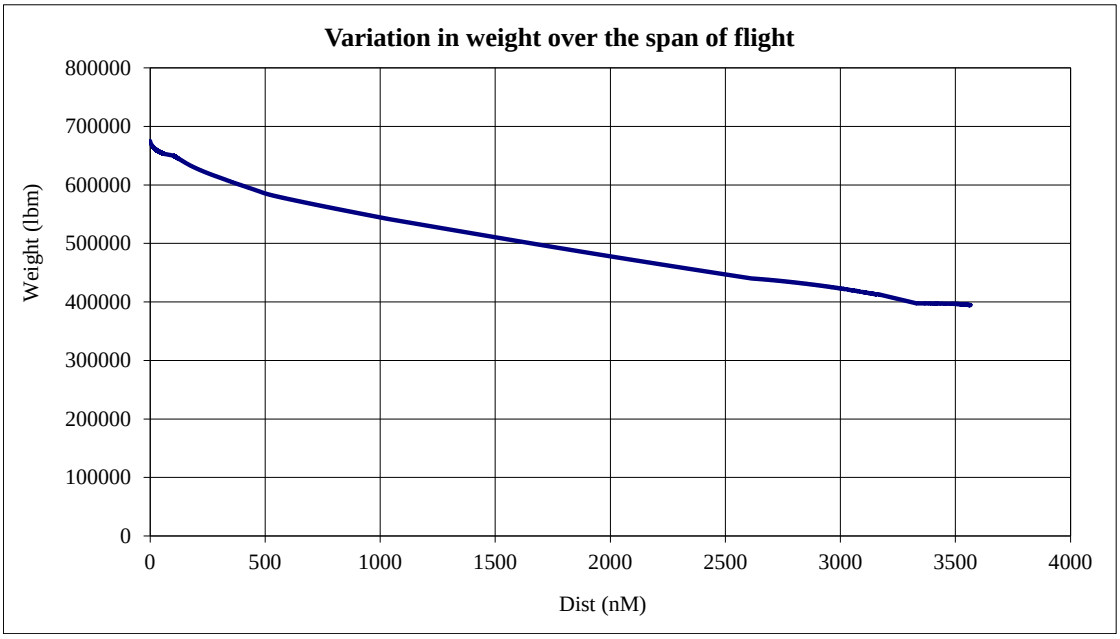

Figure 94 Plot of Variation in Weight Over the Span of Flight

Based on the information on hand, below are the *M(L/D)* charts at corresponding analysis weight obtained from the above displayed weight variation data as could be interpreted from crosschecking time and miles on flight.

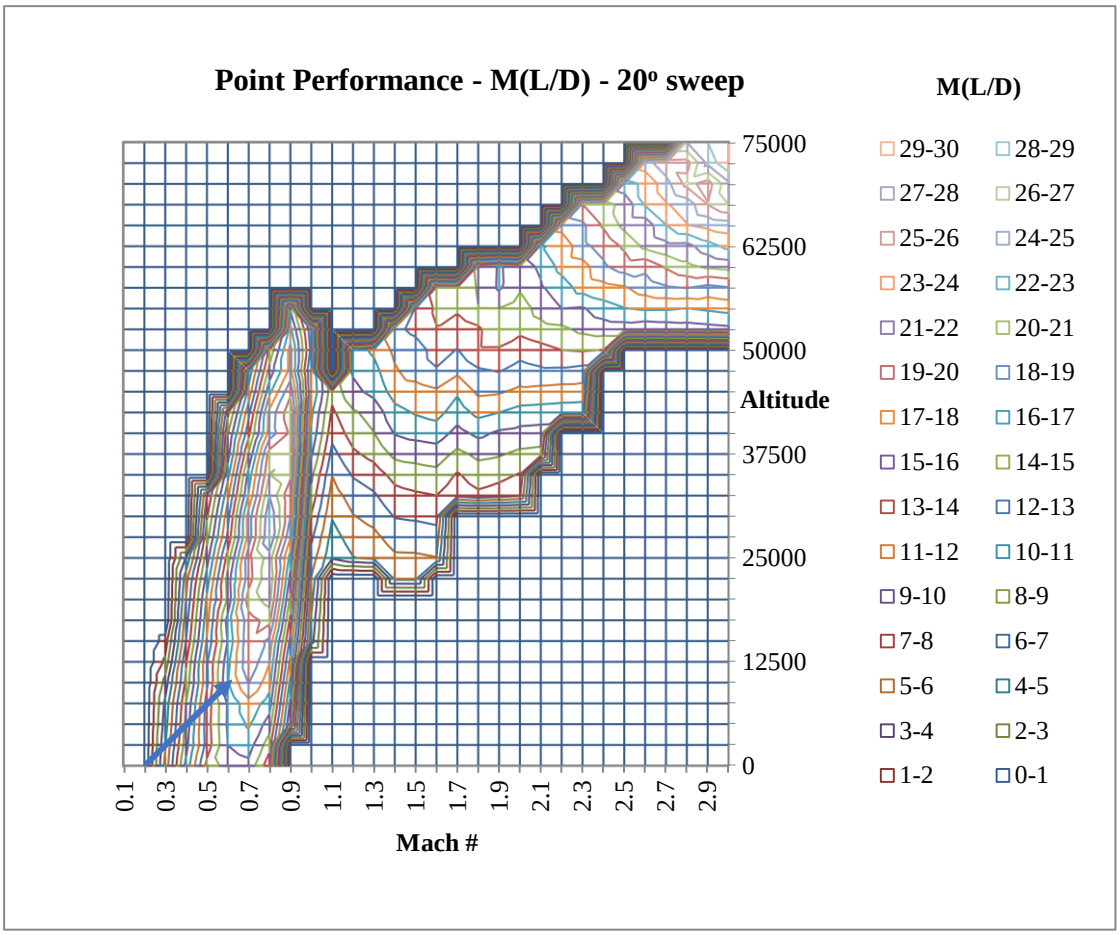

Figure 95 *M(L/D)* Plot at 20º sweep angle and 670,000 lbs Analysis Weight with Flight Direction

Based on the weight observations along the span of the flight, the average weight of flight when under the sweep angle of 20º comes out to be 670,000 lbs. Upon using this weight, the variation in *M(L/D)* as displayed in Figure 95, is not much when compared to the MTOW of 675,000 lbs. Since, the aircraft will primarily perform the duties of takeoff and climbing, the *M(L/D)* must be higher in the lower Mach numbers and at lower altitudes for such high weight. Hence, upon observing the above contours, 20º sweep looks to be the best of all if compared with data available at MTOW.

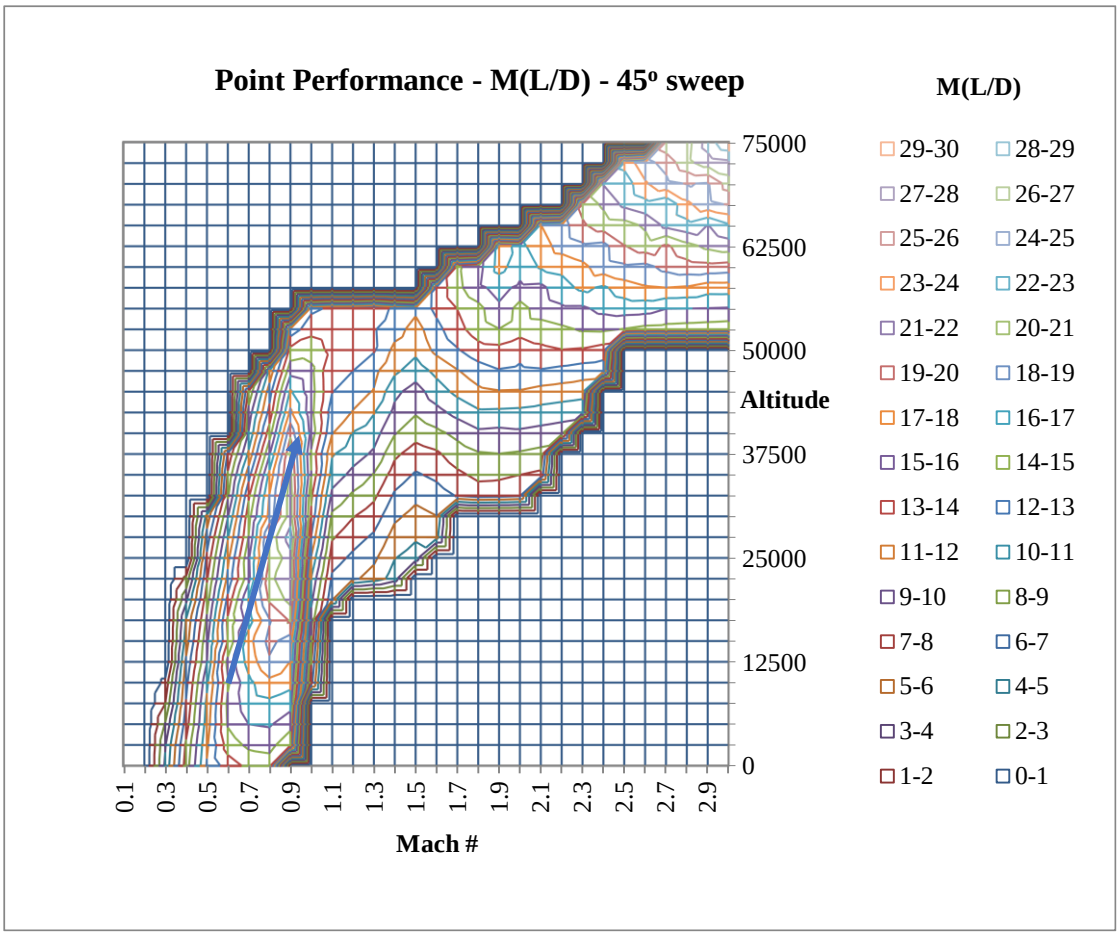

Figure 96 *M(L/D)* Plot at 45º Sweep Angle and 610,000 lbs Analysis Weight with Flight Direction

The aircraft at 45º sweep angle will mostly be cruising at subsonic speed for the time it clears the coastal shores, before jumping to supersonic speed to avoid effects of sonic booms on the ground. Along with the data available at this stage of subsonic cruising, Figure 96 illustrates the *M(L/D)* distribution at the analysis weight of 610,000 lbm. since the weight during subsonic cruising will vary around this mean point. The *M(L/D)* values at subsonic cruising Mach of 0.9 at around 40,000 ft are very convincing for 45º swept wing aircraft configuration for this specifications of operation.

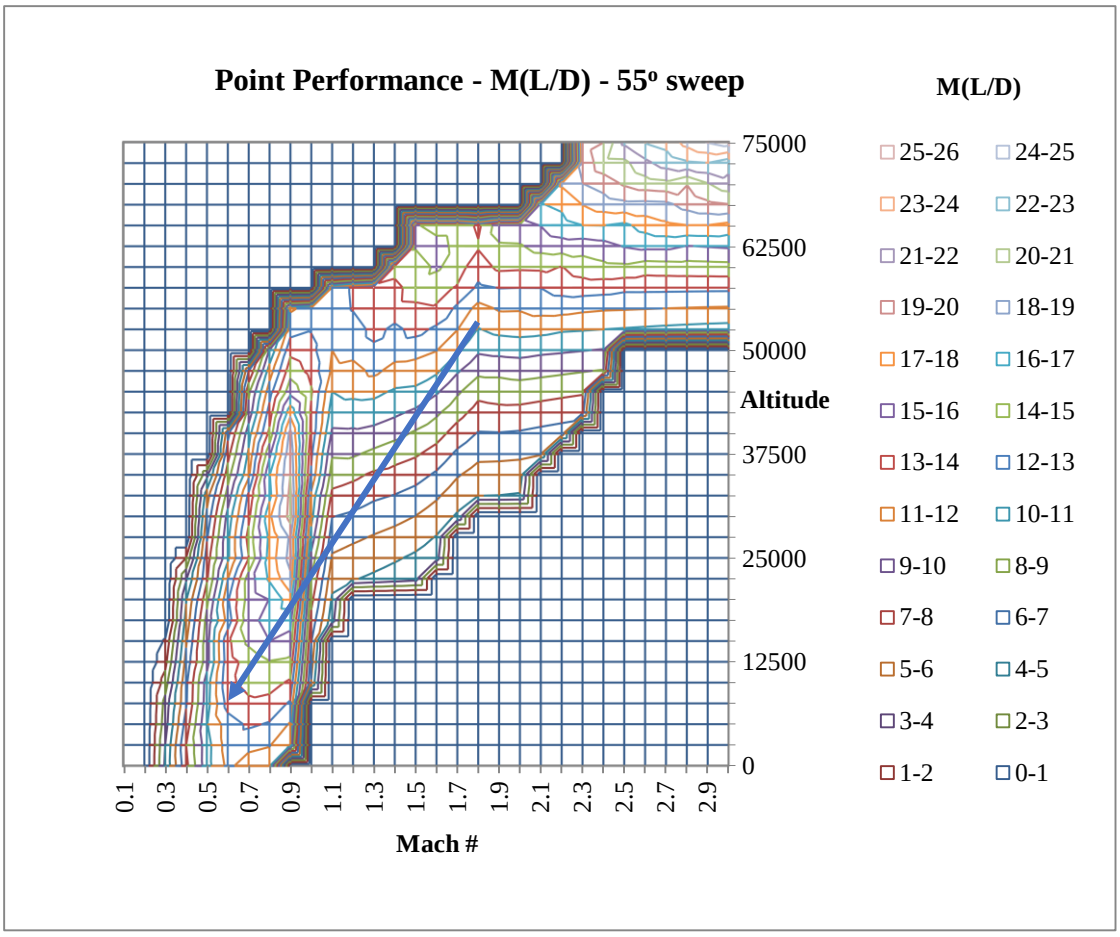

Figure 97 *M(L/D)* Plot at 55º Sweep Angle and 440,000 lbs Analysis Weight with Flight Direction

The aircraft when it sweeps back at 55º angle will be trying to descent and jump back to subsonic cruising altitude of 40,000 ft. However, since the aircraft will still be jumping in steps from Mach 2.7 to Mach 1.8 and then to Mach 0.9, hence, 45º sweep angle would not be ideal fit. Hence, if the flight will be supersonic partially before switching to subsonic, the sweep angle of 45º does not provide good results of *M(L/D)* and *(L/D)* ratios at the average weight of 440,000 lbs in the transonic region. However, the *M(L/D)* results obtained from using 55º sweep angles as displayed in Figure 97, prove superior to both the 50º and 45º sweep angle.

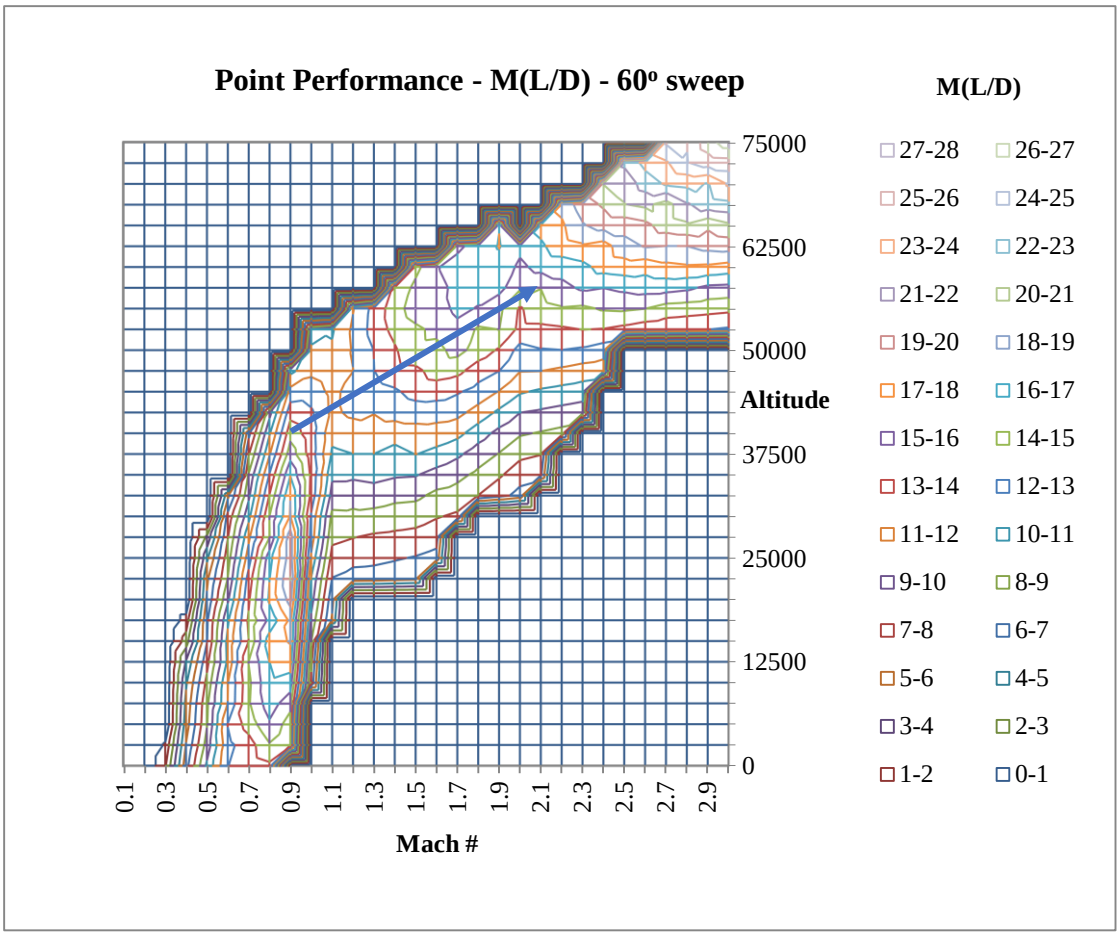

Figure 98 *M(L/D)* Plot at 60º Sweep Angle and 585,000 lbs Analysis Weight with Flight Direction

The aircraft before starting its supersonic cruise at 70,000 ft altitude, will need to reach an intermediate stage to avoid any stability issues from changing the altitude very quickly from 40,000 ft to 70,000 ft and associated transonic effects. Hence, the best guess would be for it to switch to an intermediate altitude of around 60,000 ft where it will be bearing a mean weight of almost 585,000 lbs. Hence, for this specifications, upon calculating *M(L/D)* and *(L/D)* values at several sweep angles, the sweep angle of 60º seems to provide reasonable results on both front without impacting the specific range too much for sake of flight viability as seen in Figure 98 for *M(L/D)*.

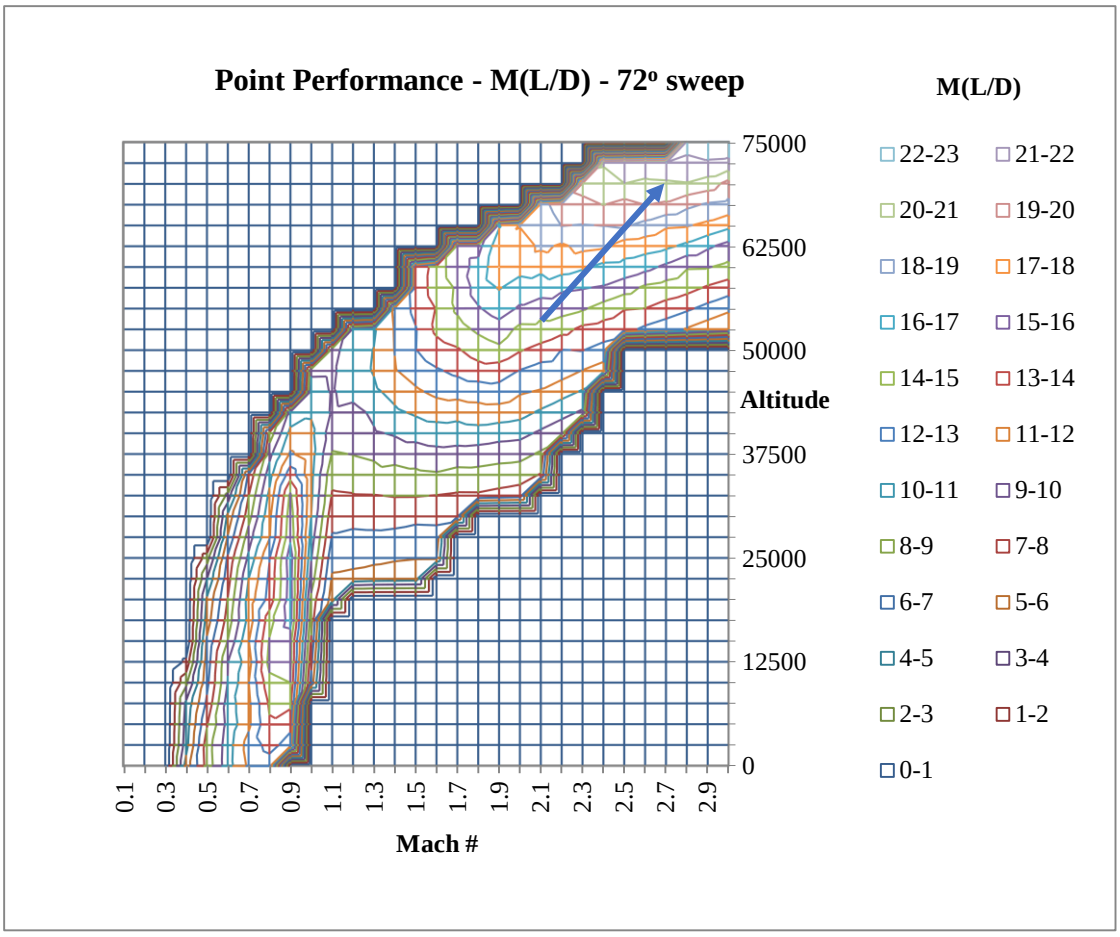

Figure 99 *M(L/D)* Plot at 72º Sweep Angle and 475,000 lbs Analysis Weight with Flight Direction

The aircraft had been designed to fly at Mach 2.7 supersonic cruise in full aft configuration. The available cruising altitude ceiling would be circa 70,000 ft. Hence, for this case, the *M(L/D)* values were extracted from Figure 99 at flight weight of 475,000 lbm, which would be the mean weight during the supersonic cruise stage.

The results obtained for this flight mission procedure have been plotted in the Figure 100 through Figure 114 for altitude, aerodynamic efficiency, aerodynamic performance efficiency, and thrust specific fuel consumption during the flight mission.

7.1.1. Initial Weight of Aircraft = 675,000 lbm.

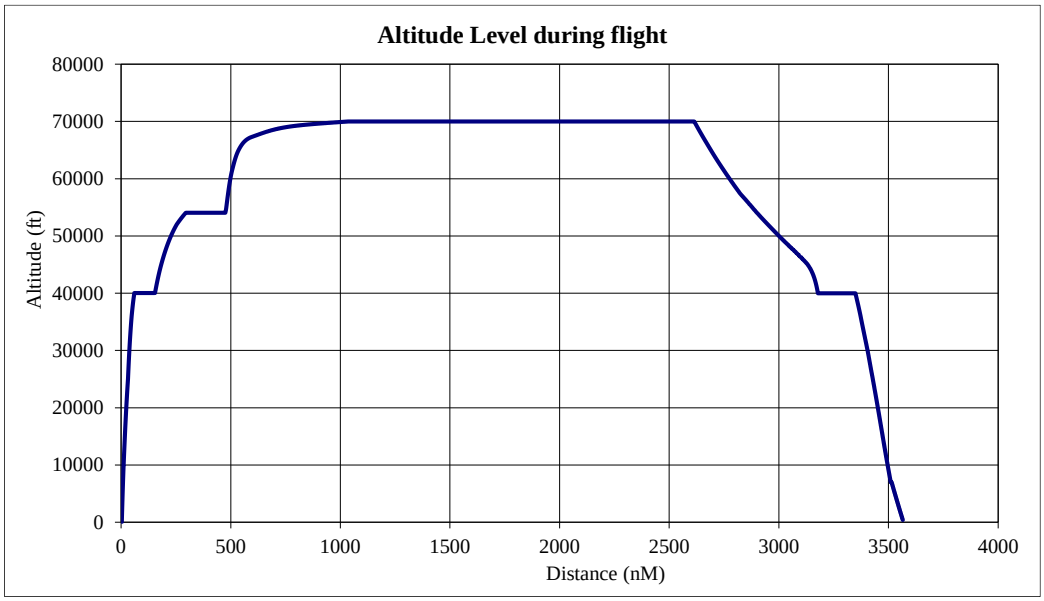

Figure 100 Line Plot of Altitude Variation with Respect to Distance Flown for Variable Sweep Aircraft with Maximum Weight of 675,000 lbm.

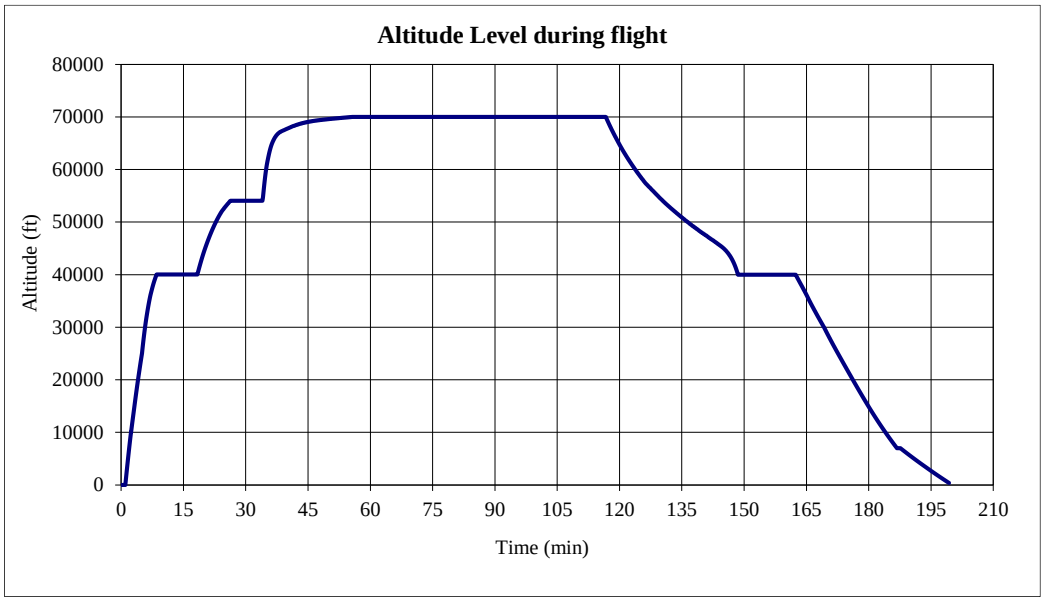

Figure 101 Line Plot of Altitude Level Variation with Respect to Time of Flight for Variable Sweep Aircraft with Maximum Weight of 675,000 lbm.

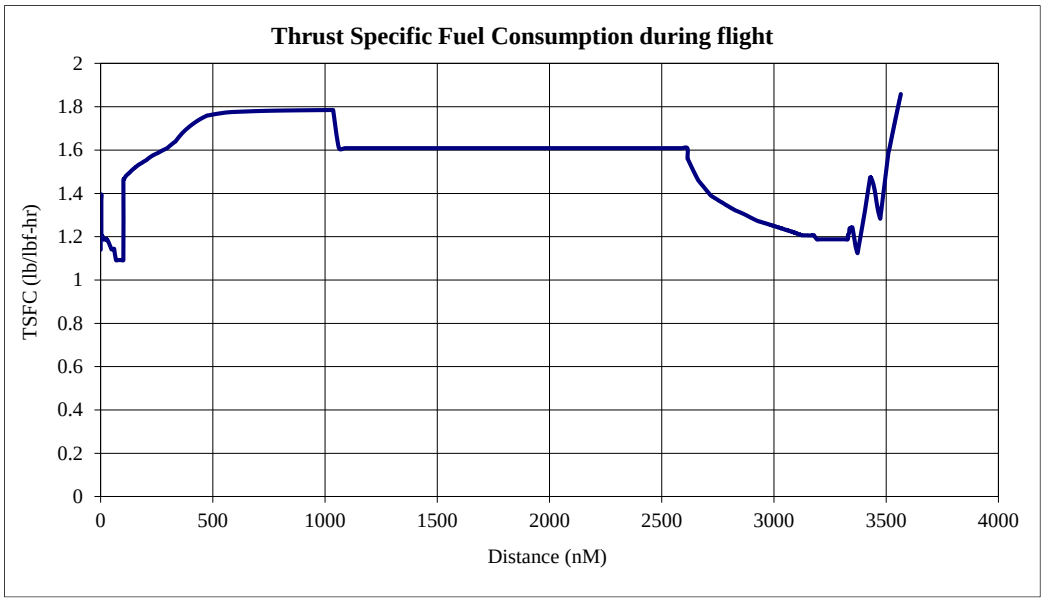

Figure 102 Line Plot of Variation of TSFC with Respect to Distance Covered on Flight for Variable Sweep Aircraft with Maximum Weight of 675,000 lbm.

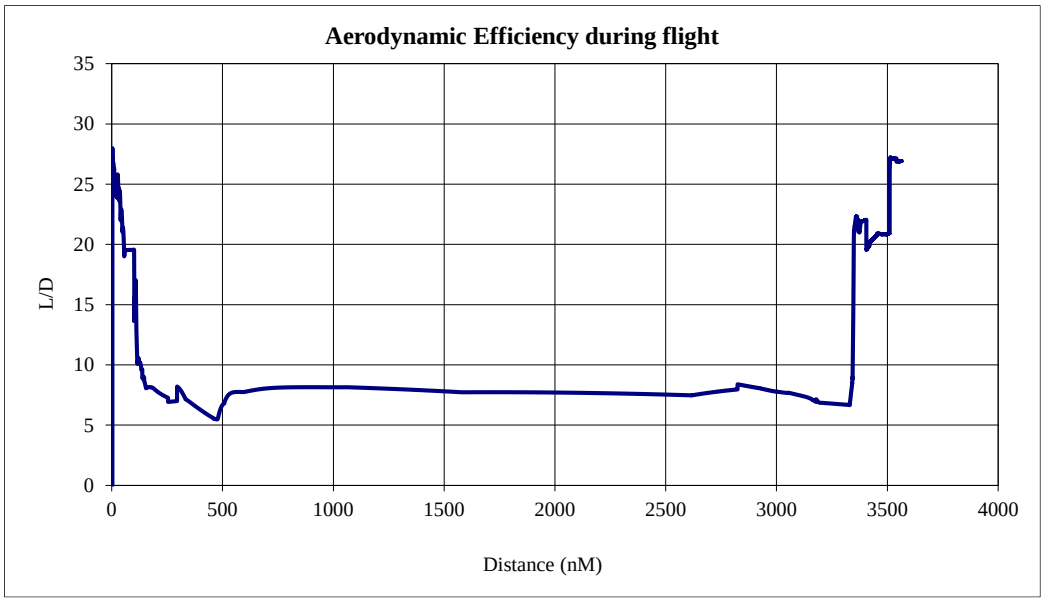

Figure 103 Variation of Aerodynamic Efficiency of The Aircraft with Respect to Distance Flown for Variable Sweep Aircraft with Maximum Weight of 675,000 lbm.

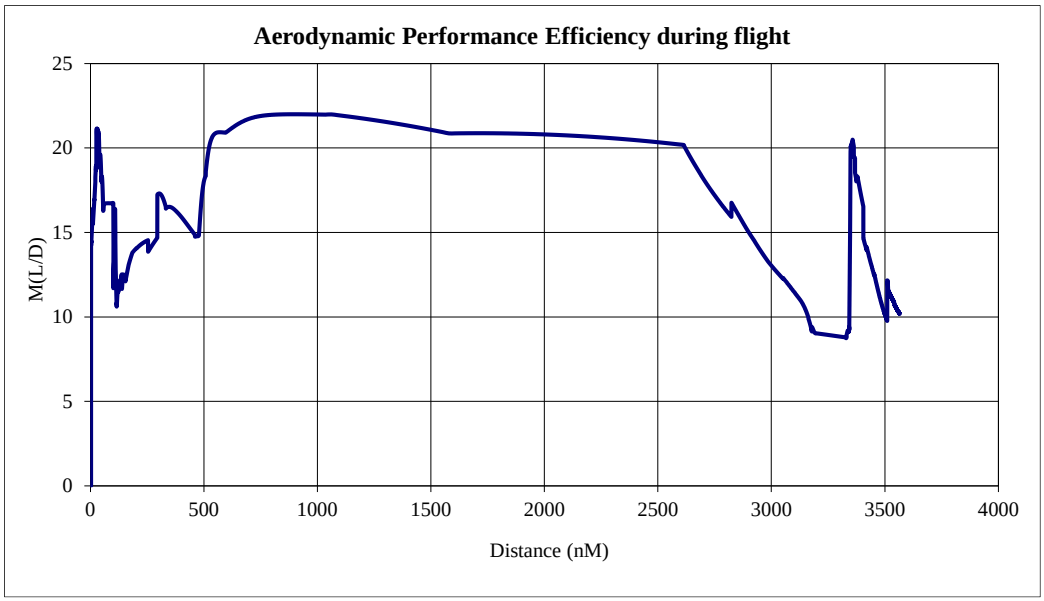

Figure 104 Variation of Aerodynamic Performance Efficiency of Aircraft with Respect to Distance Flown for Variable Sweep Aircraft with Maximum Weight of 675,000 lbm.

The flight performance results obtained for the B2707 flight analysis with variable sweep and the initial weight of 675,000 lbm are as mentioned in Table 8 below.

Flight Range	3,565 nM
Fuel Burned	280,506 lbm
Flight Time	3 hrs 19 min
Supersonic Cruise Altitude at Mach 2.7	70,000 ft
Subsonic Cruise Altitude at Mach 0.9	40,000 ft
Mean Thrust Specific Fuel Consumption	1.48 lb/lbf-hr
Mean Specific Range	0.0151 nM/lbm
Mean Subsonic Cruise Aerodynamic Efficiency	21.98

Mean Supersonic Cruise Aerodynamic Efficiency	7.76
Mean Subsonic Cruise Aerodynamic Performance Efficiency	18.81
Mean Supersonic Cruise Aerodynamic Performance Efficiency	20.95

Table 8 Flight Performance Results for Variable Sweep Operation for Maximum Analysis Weight of 675,000 lbm.

7.1.2. Initial Weight of Aircraft = 650,000 lbm.

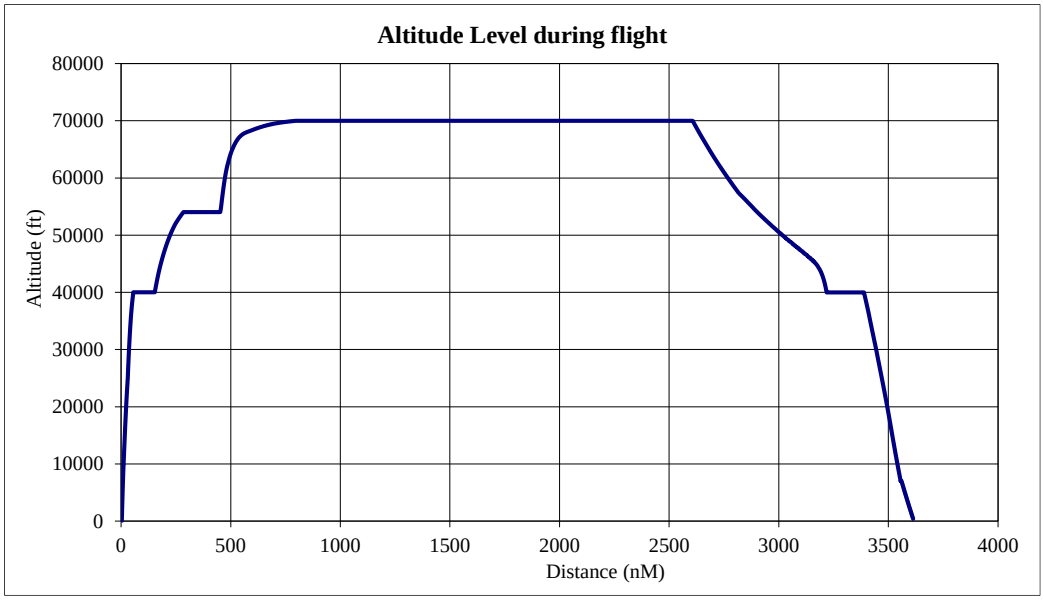

Figure 105 Line Plot of Altitude Variation with Respect to Distance Flown for Variable Sweep Aircraft with Maximum Weight of 650,000 lbm.

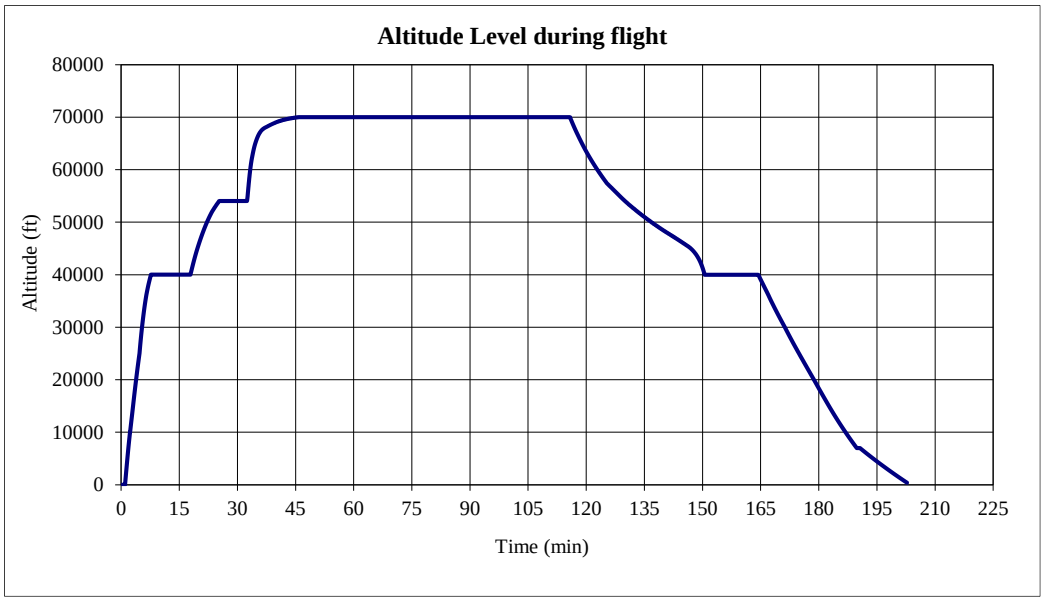

Figure 106 Line Plot of Altitude Level Variation with Respect to Time of Flight for Variable Sweep Aircraft with Maximum Weight of 650,000 lbm.

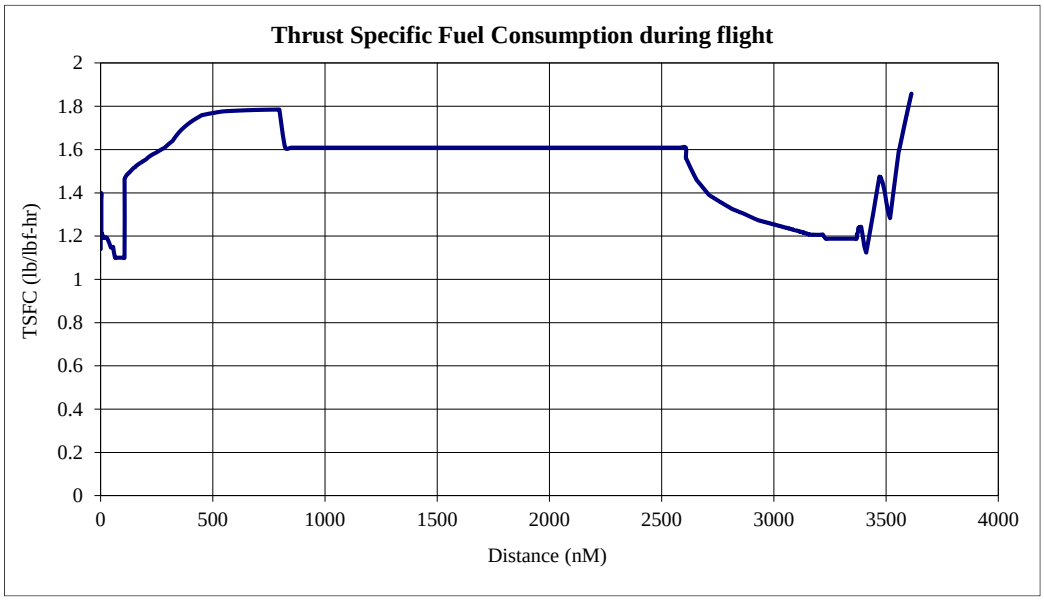

Figure 107 Line Plot of Variation of TSFC with Respect to Distance Covered on Flight for Variable Sweep Aircraft with Maximum Weight of 650,000 lbm.

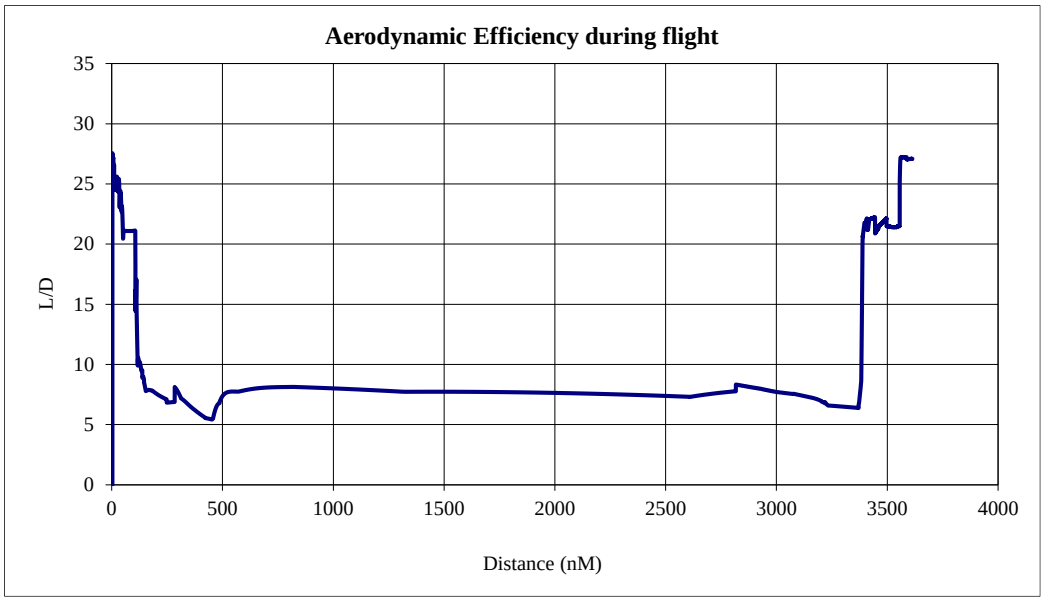

Figure 108 Variation of Aerodynamic Efficiency of The Aircraft with Respect to Distance Flown for Variable Sweep Aircraft with Maximum Weight of 650,000 lbm.

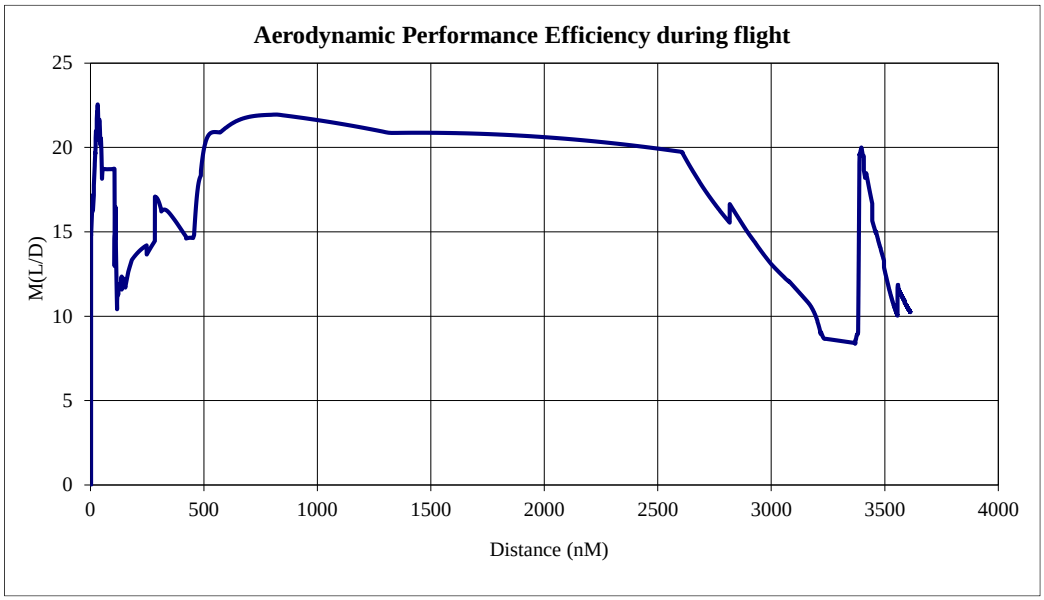

Figure 109 Variation of Aerodynamic Performance Efficiency of Aircraft with Respect to Distance Flown for Variable Sweep Aircraft with Maximum Weight of 675,000 lbm.

The flight performance results obtained for the B2707 flight analysis with variable sweep and the initial weight of 650,000 lbm are as mentioned in Table 9 below.

Flight Range	3,613 nM
Fuel Burned	273,672 lbm
Flight Time	3 hrs 22 min
Supersonic Cruise Altitude at Mach 2.7	70,000 ft
Subsonic Cruise Altitude at Mach 0.9	40,000 ft
Mean Thrust Specific Fuel Consumption	1.45 lb/lbf-hr
Mean Specific Range	0.0156 nM/lbm
Mean Subsonic Cruise Aerodynamic Efficiency	23.04
Mean Supersonic Cruise Aerodynamic Efficiency	7.72
Mean Subsonic Cruise Aerodynamic Performance Efficiency	20.44
Mean Supersonic Cruise Aerodynamic Performance Efficiency	20.86

Table 9 Flight Performance Results for Variable Sweep Operation for Maximum Analysis Weight of 650,000 lbm.

7.1.3. Initial Weight of Aircraft = 635,000 lbm.

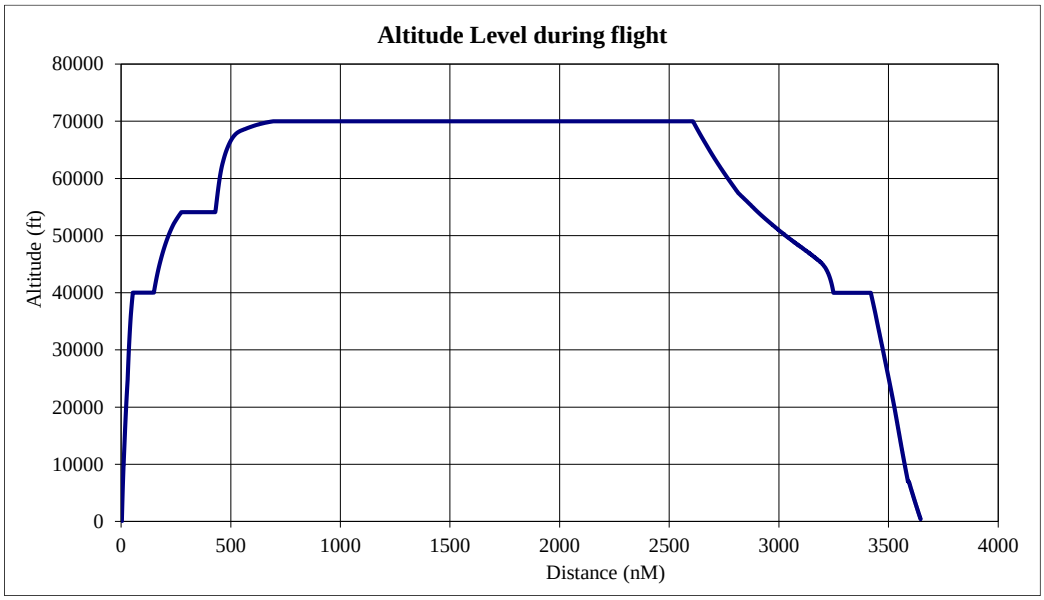

Figure 110 Line Plot of Altitude Variation with Respect to Distance Flown for Variable Sweep Aircraft with Maximum Weight of 635,000 lbm.

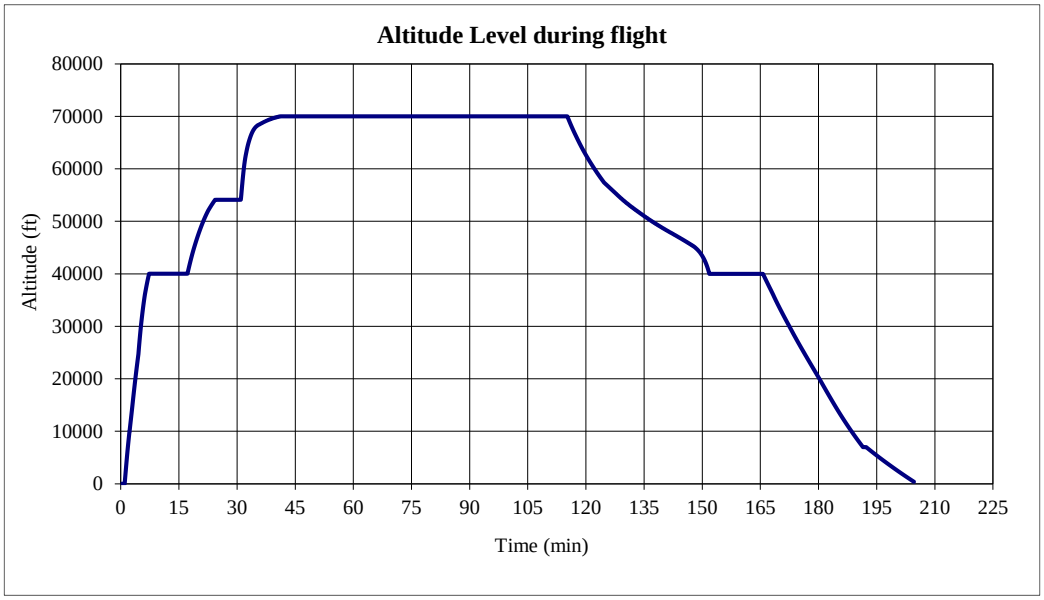

Figure 111 Line Plot of Altitude Level Variation with Respect to Time of Flight for Variable Sweep Aircraft with Maximum Weight of 635,000 lbm.

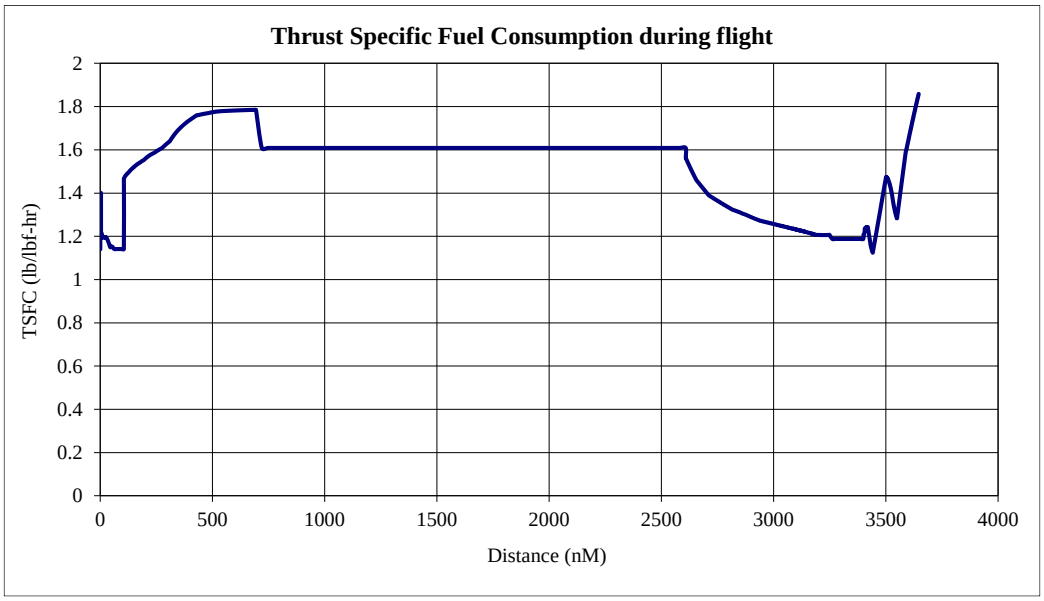

Figure 112 Line Plot of Variation of TSFC with Respect to Distance Covered on Flight for Variable Sweep Aircraft with Maximum Weight of 635,000 lbm.

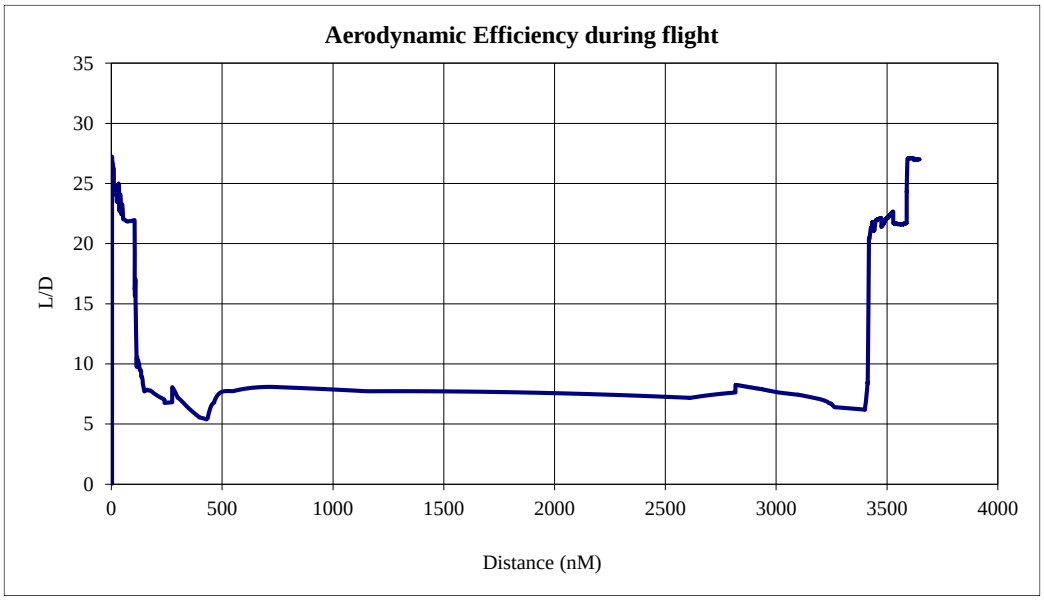

Figure 113 Variation of Aerodynamic Efficiency of The Aircraft with Respect to Distance Flown for Variable Sweep Aircraft with Maximum Weight of 635,000 lbm.

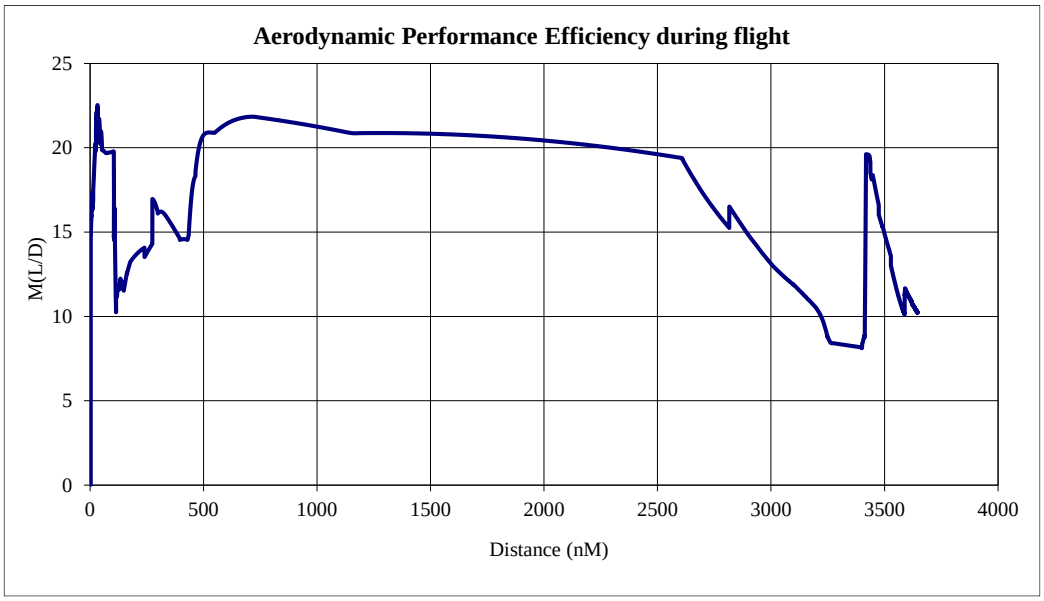

Figure 114 Variation of Aerodynamic Performance Efficiency of Aircraft with Respect to Distance Flown for Variable Sweep Aircraft with Maximum Weight of 635,000 lbm.

The flight performance results obtained for the B2707 flight analysis with variable sweep and the initial weight of 635,000 lbm are as mentioned in Table 10 below.

Flight Range	3,646 nM
Fuel Burned	270,456 lbm
Flight Time	3 hrs 24 min
Supersonic Cruise Altitude at Mach 2.7	70,000 ft
Subsonic Cruise Altitude at Mach 0.9	40,000 ft
Mean Thrust Specific Fuel Consumption	1.44 lb/lbf-hr
Mean Specific Range	0.0160 nM/lbm
Mean Subsonic Cruise Aerodynamic Efficiency	23.47

Mean Supersonic Cruise Aerodynamic Efficiency	7.60
Mean Subsonic Cruise Aerodynamic Performance Efficiency	21.15
Mean Supersonic Cruise Aerodynamic Performance Efficiency	20.54

Table 10 Flight Performance Results for Variable Sweep Operation for Maximum Analysis Weight of 635,000 lbm.

7.2. Constant Sweep Wing Mission

To study the impact of constant sweep wing during the flight on the key aerodynamics performance parameters, the mission input operation remains the same apart from a few altitude and power setting updates to make the aircraft capable of flight in such conditions. Hence, the flight range of every sweep aircraft must be within ~10 nM of each other and the variable sweep aircraft of same weight analysis.

The sweep angles selected for this case study are 35^{o}, 45^{o}, and 72^{o} which also is the full aft swept design condition for the aircraft. The weight used for predicting flight performance is 675,000 lbs, which is the maximum weight of the aircraft under any adverse or extreme condition.

A sample mission input file has been provided in Figure 115 representing each stage of the aircraft flight from takeoff to landing along with other key parameters regarding power setting changes, altitude changes, and Mach number transitions from subsonic to supersonic condition all on the same sweep angle of the aircraft.

```
W_START   675000
W_END     360000
NENG      4.75

* SET WING SWEEP BY PROVIDING AERODATABASE FOR SWEEP ANGLE
SET
AERO_FILE C:\Users\chaud\OneDrive\Desktop\MAE_564\PROJECT\Research_Papers\THESIS_FILES\b2707_72_database_rn.dat
DELTA_CD 0.0000

* TAKEOFF
GROUND_RUNUP
PLA 0.95
STOP TIME> 60.

MACH 0.25
ALTITUDE  400

* CLIMB W/O AFTERBURNER
CLIMB_CONST_KIAS
PLA 0.95
STOP ALT> 10000

* CLIMB W/O AFTERBURNER
ACCEL
PLA 0.95
STOP KIAS> 310.


* CLIMB W/O AFTERBURNER TO FL400 / M0.9
CLIMB_CONST_KIAS
PLA 0.95
STOP ALT> 25000 MACH> 0.9

CLIMB_CONST_MACH
PLA 0.95
STOP ALT> 40000

* LEVEL FLIGHT FOR FIRST 100 MILES
LEVEL
STOP DIST> 100

* ACCEL TO SUPERSONIC W/ AFTERBURNERS
ACCEL
PLA 0.97
STOP MACH> 1.3

CLIMB_CONST_KIAS
PLA 0.98
STOP MACH> 2.1 ALT> 60000

* MACH 2.7 CRUISE
ACCEL
PLA 0.98
STOP MACH> 2.7

CLIMB_CONST_MACH
PLA 0.98
STOP ALT> 70000

LEVEL
STOP DIST> 2600

CLIMB_CONST_KIAS
PLA 0.85
STOP ALT< 40000

* DESCENT
ACCEL
PLA 0.85
STOP MACH< 0.9
```

```
* SUBSONIC CRUISE
LEVEL
STOP RELATIVE_DIST> 150.

CLIMB_CONST_MACH
PLA 0.85
STOP KIAS< 310 ALT< 20000

CLIMB_CONST_KIAS
PLA 0.85
STOP ALT< 20000

* LANDING
ACCEL
PLA 0.85
STOP KIAS< 250

CLIMB_CONST_KIAS
PLA 0.85
STOP ALT< 400
```

Figure 115 Sample Flight Mission Input File for Fixed 72^{o} Sweep Geometry Operation of B2707 Over the Flight Span with Maximum Weight of 675,000 lbm.

Below are the flight performance at fixed sweep angles as described earlier using the flight mission as one displayed in Figure 114.

7.2.1. Sweep Angle = 35^{o}

The approach for generating mission for this flight remains same as the variable sweep geometry in order to compare and analyze data. The results obtained are as illustrated below from Figure 116 to Figure 120.

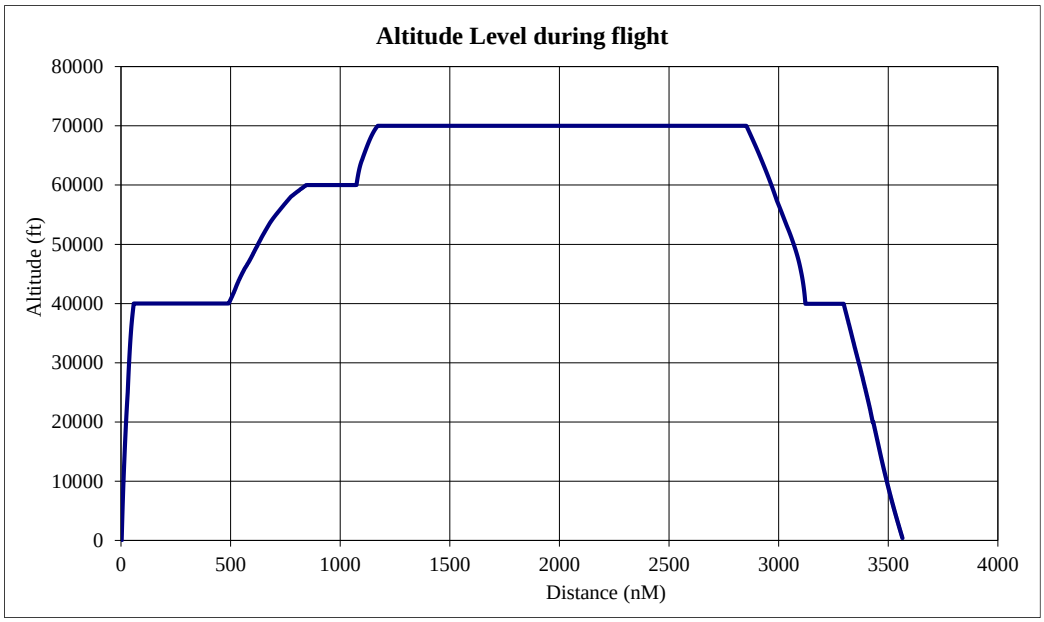

Figure 116 Line Plot of Altitude Variation with Respect to Distance Flown for Fixed 35º Sweep Aircraft with Maximum Weight of 675,000 lbm.

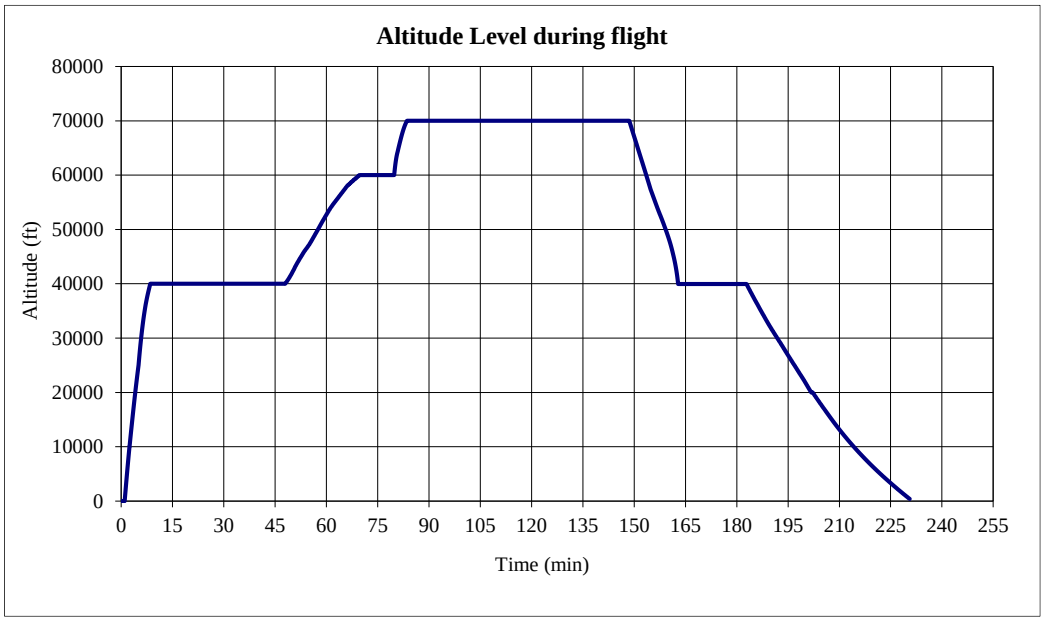

Figure 117 Line Plot of Altitude Level Variation with Respect to Time of Flight for Fixed 35º Sweep Aircraft with Maximum Weight of 675,000 lbm.

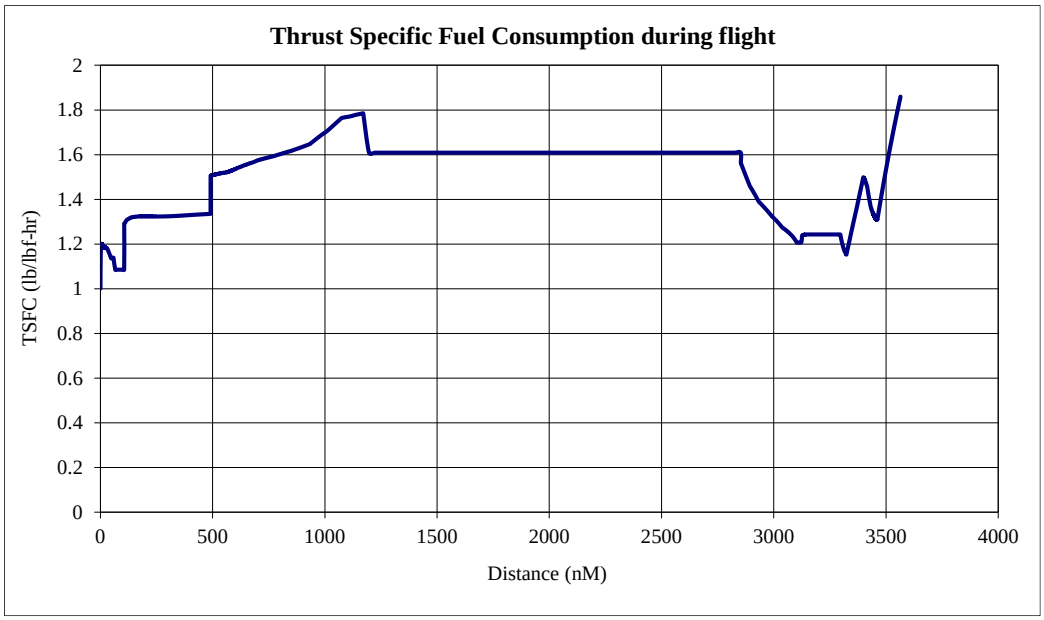

Figure 118 Line Plot of Variation of TSFC with Respect to Distance Covered on Flight for Fixed 35º Sweep Aircraft with Maximum Weight of 675,000 lbm.

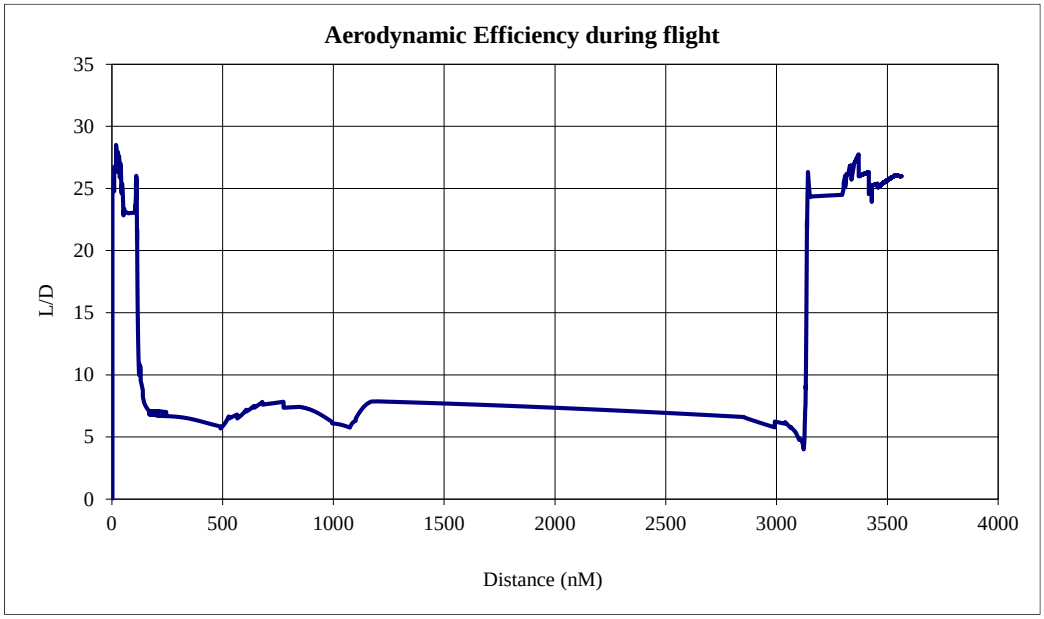

Figure 119 Variation of Aerodynamic Efficiency of the Aircraft with Respect to Distance Flown for Fixed 35º Sweep Aircraft with Maximum Weight of 675,000 lbm.

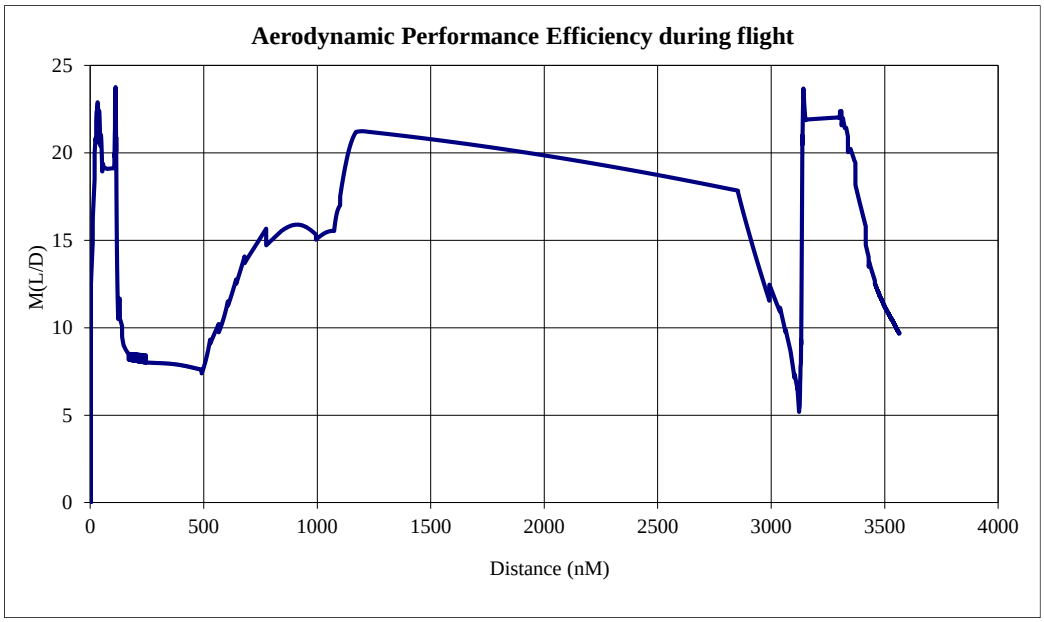

Figure 120 Variation of Aerodynamic Performance Efficiency of Aircraft with Respect to Distance Flown for Fixed 35^{o} Sweep Aircraft with Maximum Weight of 675,000 lbm.

The flight performance results obtained for the B2707 flight analysis with 35^{o} sweep and the initial weight of 675,000 lbm are as mentioned in Table 11 below.

Flight Range	3,565 nM
Fuel Burned	307,085 lbm
Flight Time	3 hrs 51 min
Supersonic Cruise Altitude at Mach 2.7	70,000 ft
Subsonic Cruise Altitude at Mach 0.9	40,000 ft
Mean Thrust Specific Fuel Consumption	1.43 lb/lbf-hr
Mean Specific Range	0.0156 nM/lbm

Mean Subsonic Cruise Aerodynamic Efficiency	21.69
Mean Supersonic Cruise Aerodynamic Efficiency	7.30
Mean Subsonic Cruise Aerodynamic Performance Efficiency	14.29
Mean Supersonic Cruise Aerodynamic Performance Efficiency	19.73

Table 11 Flight Performance Results of B2707 for Fixed Sweep Operation of 35^{o} for Maximum Analysis Weight of 675,000 lbm.

7.2.2. Sweep Angle = 45^{o}

Under the similar weight conditions as that of the first section of variable sweep flight mission, following results as displayed in Figure 121 through Figure 125 were obtained for constant sweep angle of 45^{o} of aircraft wing.

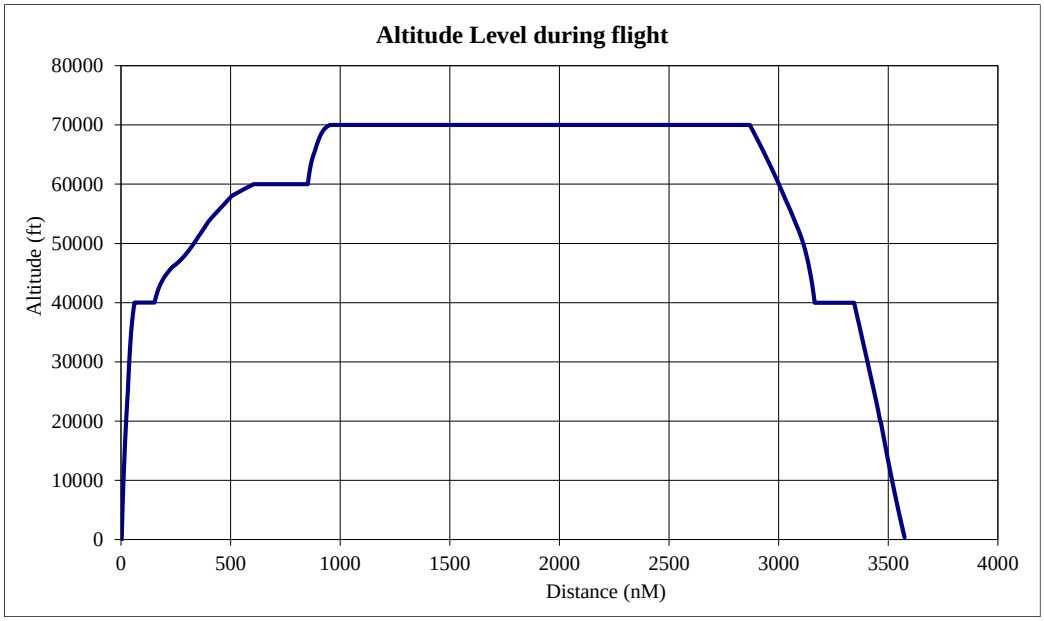

Figure 121 Line Plot of Altitude Variation with Respect to Distance Flown for Fixed 45^{o} Sweep Aircraft with Maximum Weight of 675,000 lbm.

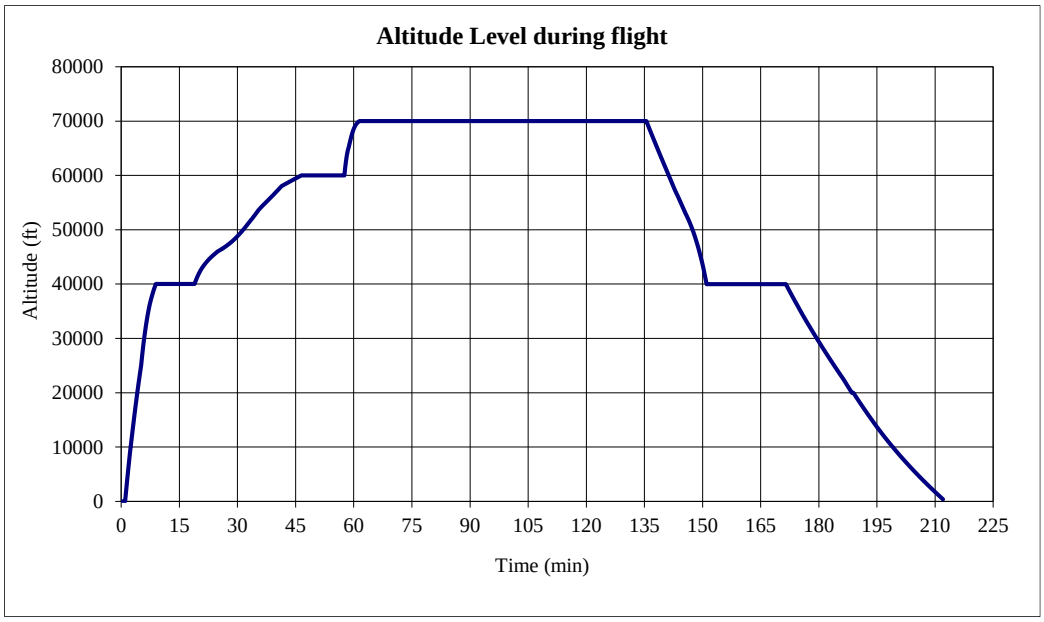

Figure 122 Line Plot of Altitude Level Variation with Respect to Time of Flight for Fixed 45º Sweep Aircraft with Maximum Weight of 675,000 lbm.

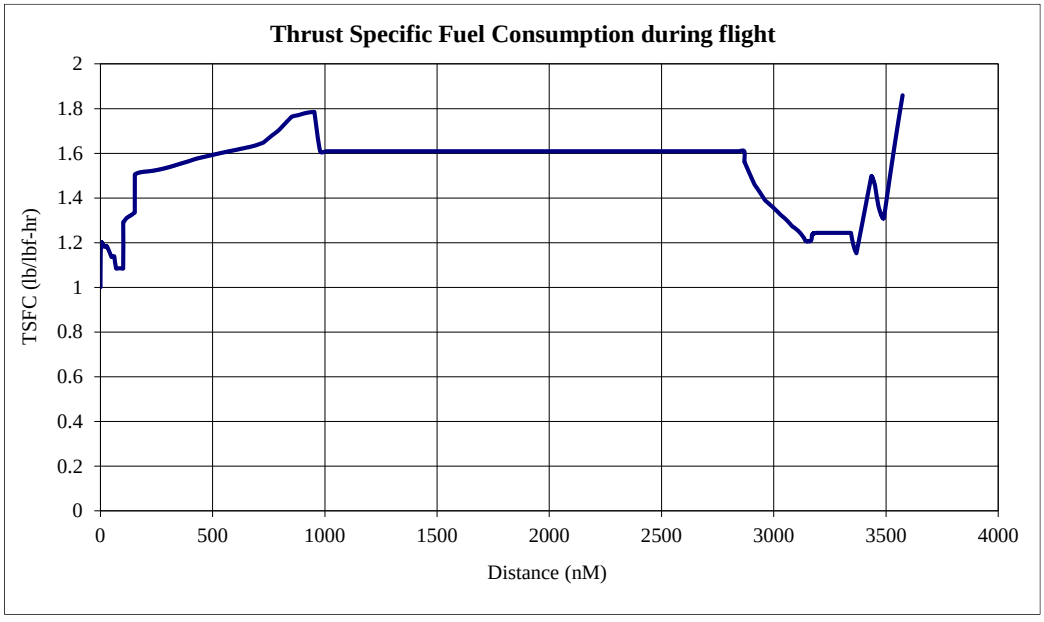

Figure 123 Line Plot of Variation of TSFC with Respect to Distance Covered on Flight for Fixed 45º Sweep Aircraft with Maximum Weight of 675,000 lbm.

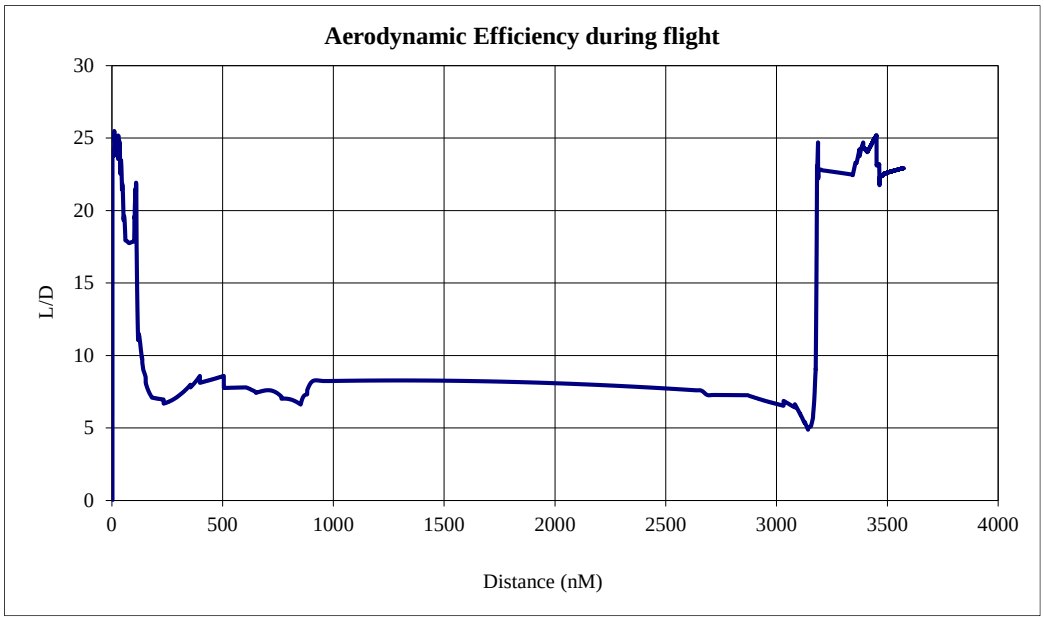

Figure 124 Variation of Aerodynamic Efficiency of the Aircraft with Respect to Distance Flown for Fixed 45º Sweep Aircraft with Maximum Weight of 675,000 lbm.

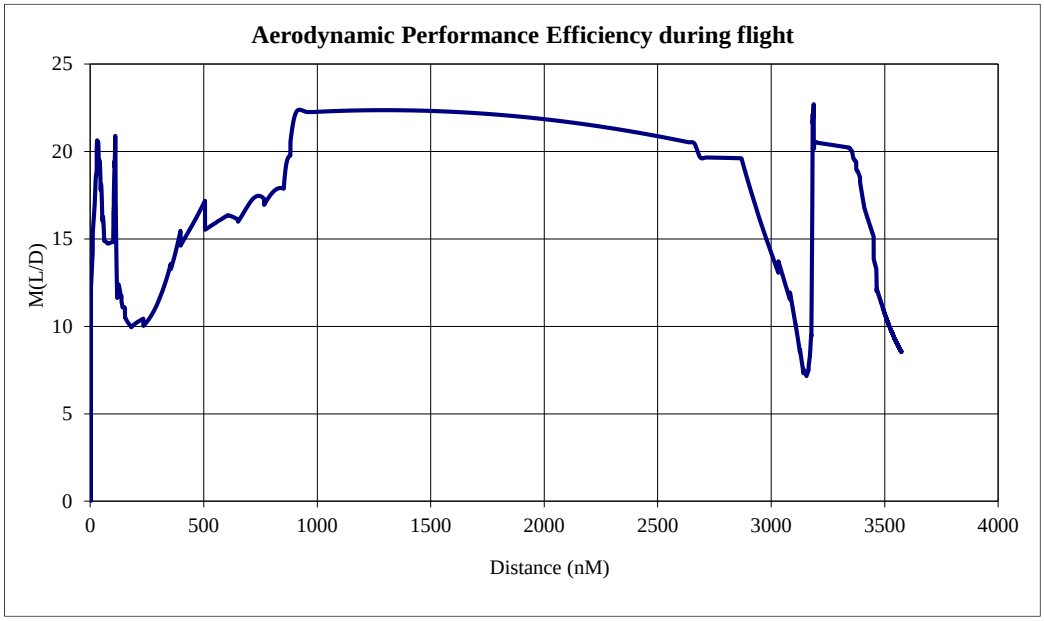

Figure 125 Variation of Aerodynamic Performance Efficiency of Aircraft with Respect to Distance Flown for Fixed 45º Sweep Aircraft with Maximum Weight of 675,000 lbm.

The flight performance results obtained for the B2707 flight analysis with 45^{o} sweep and initial weight of 675,000 lbm are summarized in Table 12 below.

Flight Range	3,567 nM
Fuel Burned	288,848 lbm
Flight Time	3 hrs 25 min
Supersonic Cruise Altitude at Mach 2.7	70,000 ft
Subsonic Cruise Altitude at Mach 0.9	40,000 ft
Mean Thrust Specific Fuel Consumption	1.47 lb/lbf-hr
Mean Specific Range	0.0155 nM/lbm
Mean Subsonic Cruise Aerodynamic Efficiency	13.64
Mean Supersonic Cruise Aerodynamic Efficiency	7.99
Mean Subsonic Cruise Aerodynamic Performance Efficiency	14.00
Mean Supersonic Cruise Aerodynamic Performance Efficiency	21.61

Table 12 Flight Performance Results of B2707 for Fixed Sweep Operation of 45^{o} for Maximum Analysis Weight of 675,000 lbm.

7.2.3. Sweep Angle = 72^{o}

The flight performance for 72^{o} sweep of the aircraft wing such that it resembles the shape of a traditional delta wing for the full aircraft weight i.e. 675,000 lbs. has been depicted below in Figure 126 through Figure 130.

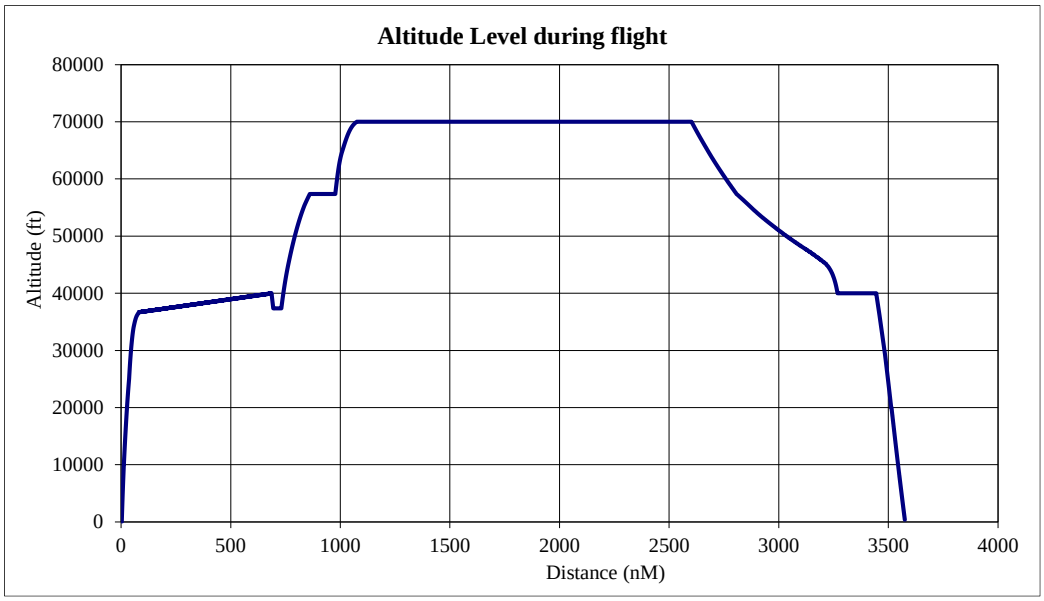

Figure 126 Line Plot of Altitude Variation with Respect to Distance Flown for Fixed 72^{o} Sweep Aircraft with Maximum Weight of 675,000 lbm.

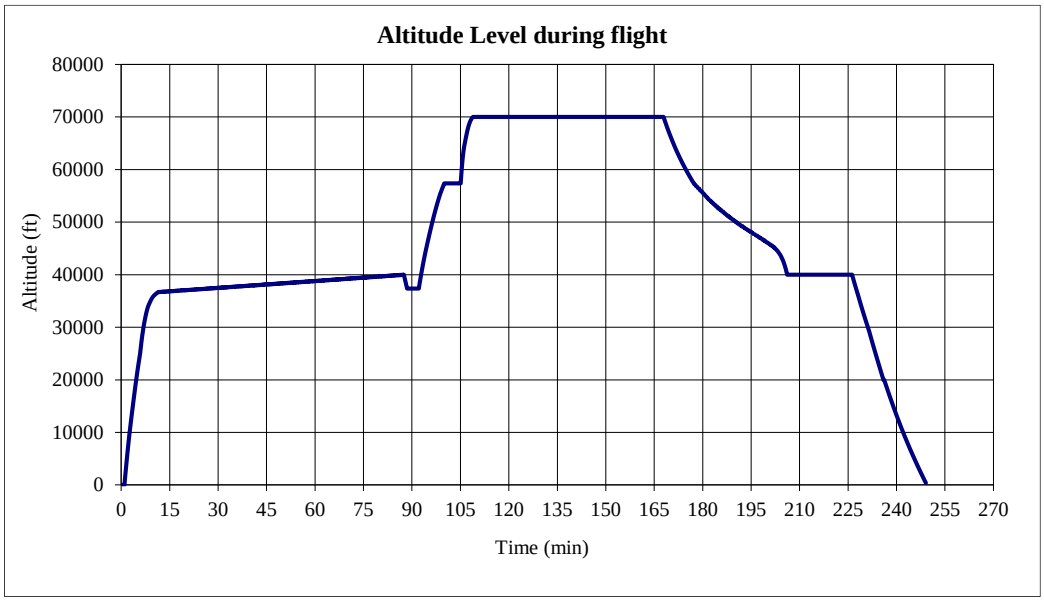

Figure 127 Line Plot of Altitude Level Variation with Respect to Time of Flight for Fixed 72^{o} Sweep Aircraft with Maximum Weight of 675,000 lbm.

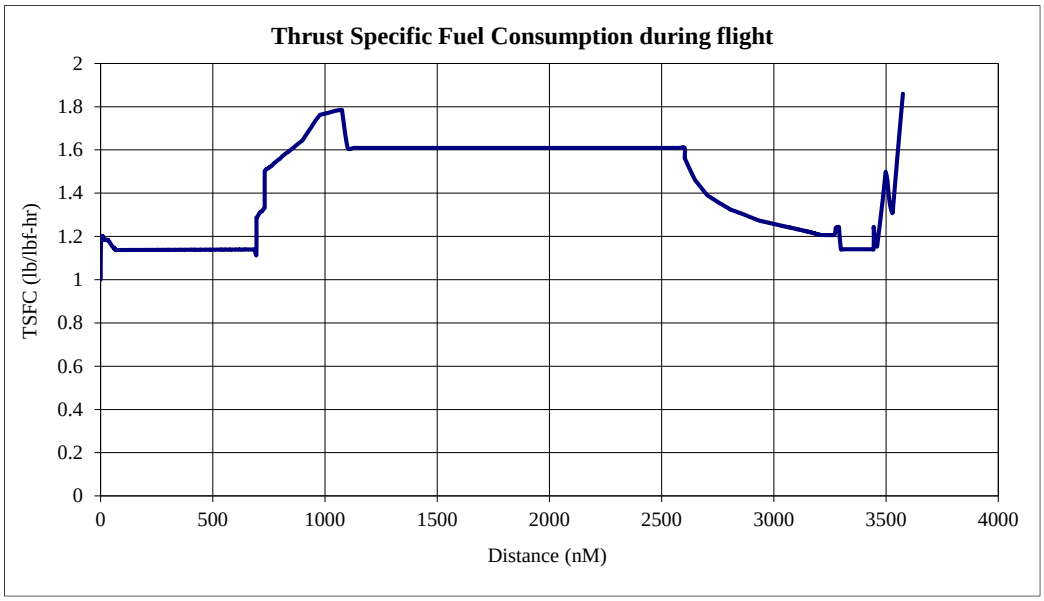

Figure 128 Line Plot of Variation of TSFC with Respect to Distance Covered on Flight for Fixed 72^{o} Sweep Aircraft with Maximum Weight of 675,000 lbm.

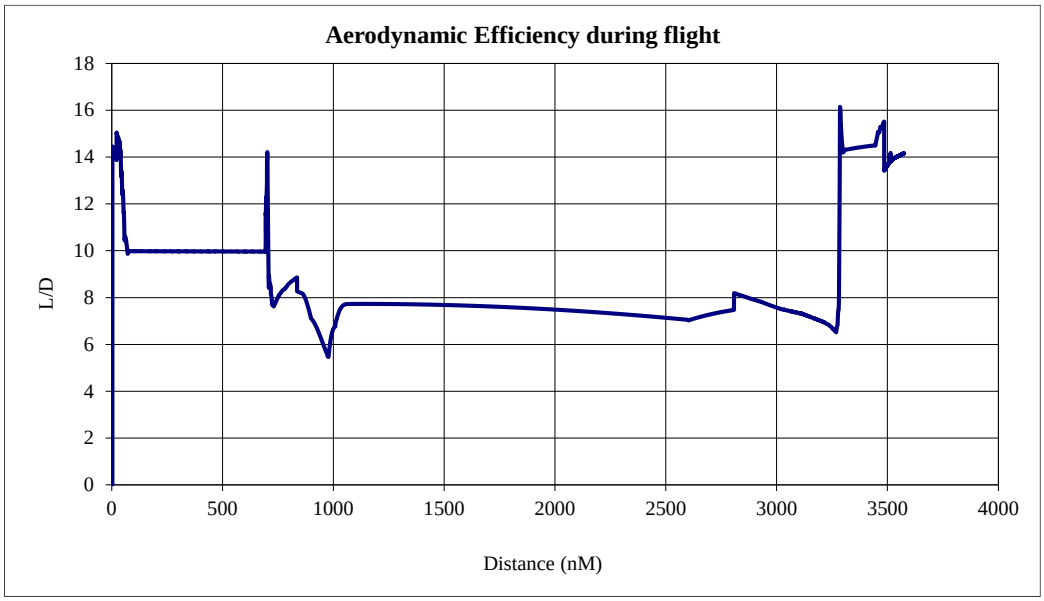

Figure 129 Variation of Aerodynamic Efficiency of the Aircraft with Respect to Distance Flown for Fixed 72^{o} Sweep Aircraft with Maximum Weight of 675,000 lbm.

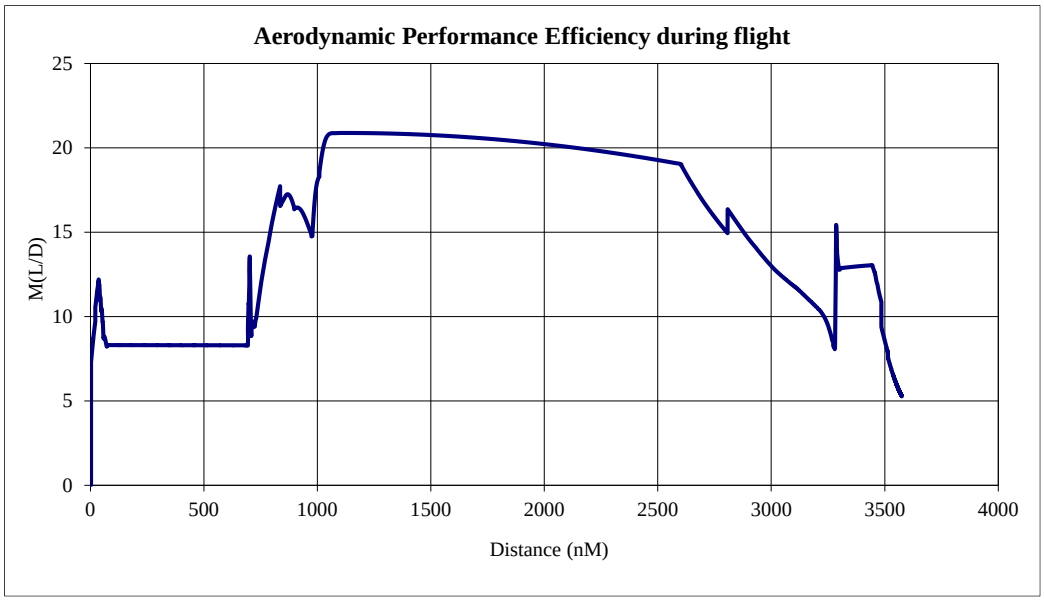

Figure 130 Variation of Aerodynamic Performance Efficiency of Aircraft with Respect to Distance Flown for Fixed 72^{o} Sweep Aircraft with Maximum Weight of 675,000 lbm.

The flight performance results obtained for the B2707 flight analysis with 72^{o} sweep and the initial weight of 675,000 lbm are summarized in Table 13 below.

Flight Range	3,575 nM
Fuel Burned	314,213 lbm
Flight Time	4 hrs 09 min
Supersonic Cruise Altitude at Mach 2.7	70,000 ft
Subsonic Cruise Altitude at Mach 0.9	40,000 ft
Mean Thrust Specific Fuel Consumption	1.27 lb/lbf-hr
Mean Specific Range	0.0152 nM/lbm
Mean Subsonic Cruise Aerodynamic Efficiency	10.06

Mean Supersonic Cruise Aerodynamic Efficiency	7.50
Mean Subsonic Cruise Aerodynamic Performance Efficiency	8.38
Mean Supersonic Cruise Aerodynamic Performance Efficiency	20.27

Table 13 Flight Performance Results of B2707 for Fixed Sweep Operation of 72^{o} for Maximum Analysis Weight of 675,000 lbm.

7.3. Flight Result Comparison

Table 14 below summarizes the results obtained from running the flight mission at different sweep settings at 675,000 lbm. of aircraft with similar flight range.

Flight Sweep Configuration	***Variable***	***Fixed - 35^o***	***Fixed - 45^o***	***Fixed - 72^o***
Flight Range (nM)	3,565	3,565	3,567	3,575
Fuel Burned (lbm)	280,506	307,085	288,848	314,213
Flight Time (hrs)	3:19	3:51	3:25	4:09
Supersonic Cruise Altitude at Mach 2.7 (ft)	70,000	70,000	70,000	70,000
Subsonic Cruise Altitude at Mach 0.9 (ft)	40,000	40,000	40,000	40,000
Average flight TSFC (lb/lbf-hr)	1.48	1.43	1.47	1.27
Mean Specific Range (nM/lbm)	0.0151	0.0156	0.0155	0.0152
Mean Subsonic Cruise L/D	21.98	21.69	13.64	10.06
Mean Supersonic Cruise L/D	7.76	7.30	7.99	7.50
Mean Subsonic Cruise M(L/D)	18.81	14.29	14.00	8.38
Mean Supersonic Cruise M(L/D)	20.95	19.73	21.61	20.27

Table 14 Comparison of Results for Same Flight Mission at Different Operation of Sweep of B2707 SST

On comparing the data at same weight and similar flight missions from Table 14, the variable sweep geometry does seem to be beneficial under both subsonic and supersonic speed regions when observed from *M(L/D)* perspective even though the *(L/D)* ratios might seem inferior in certain regions over the fixed sweep configurations. When using variable sweep configuration, the specific range observed for the aircraft is an added bonus to the considerably less fuel burnt to complete flight mission.

Moreover, the results obtained from three different weight analysis of the variable sweep B2707 SST operation as seen in Table 8, 9 and 10, seems to provide consistent results for flight performance. The flight range increases with reduction in weight. The thrust specific fuel consumption also reduces with weight reduction, and hence, the amount of fuel burnt to complete same distance also reduces. With this, the specific range of the aircraft also increases upon decreasing the initial weight of the aircraft at take-off.

All this can be linked with the improvements made in aerodynamic efficiency with weight reduction, since the coefficient of lift would also improve even when the drag component wouldn't alter significantly. When the results mentioned in Table 14 are observed, the better subsonic cruise aerodynamic efficiency and cruise aerodynamic performance efficiency, the variable sweep aircraft seems to have much better lift component or significantly less drag component over its counterparts (fixed sweep wing), as the results for variable sweep wing aircraft seems to be more than double that of fixed sweep wing aircraft.

8. CONCLUSION

Based on the results obtained using the flight envelope approach which utilized energy maneuverability theory and running the database gathered for individual sweep angles of the aircraft, it becomes evident that the variable sweep geometry could be economical and advantageous mode of supersonic civilian transport on large scale. The data obtained from flight envelope approach points out single points of usage during which the specific range could be the highest in the configurational setup, but on the other side, it might not readjust to utilize the best aerodynamic efficiency or aerodynamic performance efficiency.

The results from the point performance study carried out by using energy maneuverability theory leads to a conclusion that the specific range of the aircraft reduces non-linearly with the decrease in sweep angle. To get better results at higher sweep angles, the point performance charts suggest either to fly subsonic at very low altitude or fly very high, at around thrice the speed of sound to get the best possible specific range. For the first case, if the aircraft is to fly at low altitude with the speed of flight almost Mach 0.9, it might need a lot of power which would only be possible by using afterburners or any other augmented power source if the engines are not change. This would turn out to be uneconomical solution in long run. On the other hand, if the aircraft flies supersonic but at higher altitude, the effect on the environment could be reduced notably if not drastically, along with the power requirements, since at such high altitude the amount of thrust required would also fall off significantly as compared to low altitude, therefore eliminating need of augmented power during cruise condition. The *M(L/D)* and *(L/D)* charts provide the way

to successfully navigate through the flight speeds and altitude to increase the effectiveness of design of the aircraft. It should be clearer that an efficient and an economical flight could be achieved if the *M(L/D)* ratios are as high as possible. Moreover, the weight of the aircraft also impacts the specific range of the aircraft. From the research carried out earlier in the report, it is evident that the specific range of the aircraft is inversely proportional to the weight of the aircraft. Moreover, from observing the results of aerodynamic efficiency at different weights and sweep angles, allowed for interpretation of an important conclusion about aerodynamics efficiency. The maximum aerodynamic efficiency at a fixed sweep orientation of the aircraft irrespective of the analysis weight remained with certain limit of each other as can been seen in the Figure 131 below.

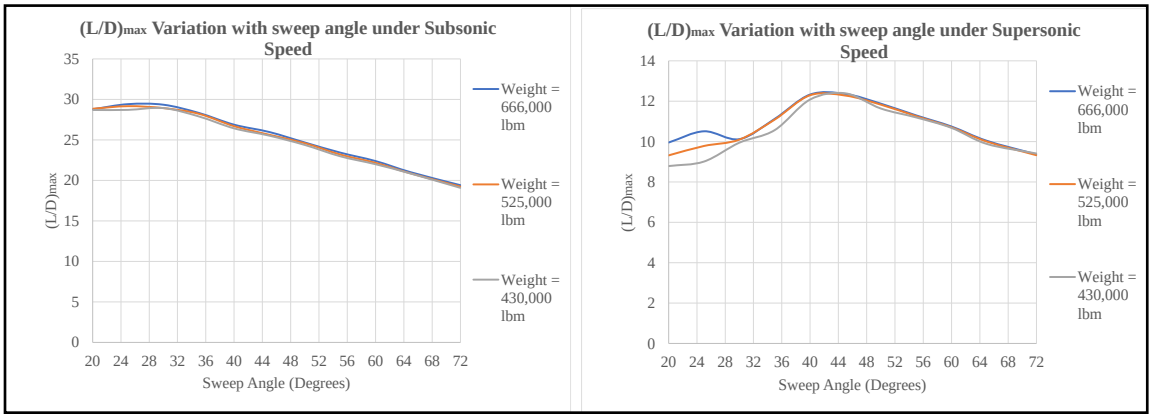

Figure 131 Maximum aerodynamic efficiency for different analysis weight and sweep angles of the tested aircraft

From what could be observed, the maximum aerodynamics efficiency associated with particular sweep orientation of the aircraft remains almost similar for different analysis weight, which goes on to prove the fact that aerodynamics efficiency is independent of the weight of the aircraft or wing loading. This is because, if the weight of the aircraft is

increased, only the point of maximum aerodynamic efficiency will be increased and not the aerodynamic efficiency.

The study on flight mission performance where similar inputs were provided to both the fixed sweep and variable sweep aircraft to understand performance under similar conditions, leads to much better results for swing wing aircraft compared to fixed sweep aircraft under both the subsonic and supersonic flight conditions. However, it cannot be underestimated that the fixed wing aircraft can have better performance at a particular altitude level or Mach number, but on a large scale the advantages observed under this condition does not provide enough evidence to not switch to different sweep during the flight since the performance in other sections of the flight might be abysmal. For instance, an aircraft with 65^{o} sweep angle might have a very good supersonic performance but it might suffer during the subsonic travel, which even though the designer might wish to avoid as much as possible but could not completely eliminate from the flight mission.

Based on the current readings from trade studies at different sweep angles and comparing that with the results obtained from variable sweep geometry, it seems like variable sweep geometry aircraft has a better aerodynamic efficiency when compared over the entire spectrum of the Mach number and altitude settings used over the fixed sweep aircraft. Moreover, the improved performance is also reflected in the aerodynamic performance efficiency plots which show that variable sweep aircraft have high *M(L/D)* ratios on either side of sonic speed. The specific range of variable sweep aircraft is better compared to fixed sweep angle aircrafts, which helps provide a strong case on merits of considering implementing variable sweep geometry for supersonic airliner development.

Moreover, the poor performance of the fixed sweep aircraft could also be justified by the higher amount of fuel burned for covering even lesser distance than the swing wing aircraft.

This results could be bettered even further upon using more sweep angles, altitude, and Mach numbers along with using higher fidelity drag and lift estimation methods to correctly estimate aerodynamic parameters value while assessing aerodynamics data. On the geometrical changes front, the results can be greatly improved by adding the thickness, camber, and twist effects of wing in VORLAX input file. All this changes can improve the coefficient of lift and drag estimation and can get close enough to replicating real-life simulation. Moreover, the results could be enhanced by performing instantaneous point performance estimation, which is a very computationally expensive method, but could be very useful to get exact insights.

REFERENCES

[1] S. Dowling, "The American Concordes that never flew," BBC, 2016. [Online]. Available: https://www.bbc.com/future/article/20160321-the-american-concordes-that-never-flew.

[2] R. M. Bush, "Boeing Model 2707 - Model Specification, Supersonic Transport Development Program, Phase III," The Boeing Company - Supersonic Transport Division, AD 827442, 1968.

[3] K. G. Brady, "Boeing Model 2707 - System Engineering Report, Supersonic Transport Development Program, Phase III Proposal," The Boeing Company, AD 804721, 1967.

[4] L. R. Miranda, R. D. Elliot and W. M. Baker, "A Generalized Vortex Lattice Method for Subsonic and Supersonic Flow Applications," Lockheed-California Company, Rept. LR-28112, 1977.

[5] E. C. Lan, "A Quasi-Vortex-Lattice Method in Thin Wing Theory," *Journal of Aircraft,* 1974.

[6] G. J. Hancock, "Comment on "Spanwise Distribution of Induced Drag in Subsonic Flow by the Vortex Lattice Method"," *Journal of Aircraft,* 1971.

[7] R. C. Feagin and W. D. Morrison, "Delta Method, An Empirical Drag Buildup Technique," Lockheed-California Company, Rept. LR-27975-VOL-1, 1978.

[8] R. V. J. Harris, "An Analysis and Correlation of Aircraft Wave Drag," NASA TM X-947, 1964.

[9] R. T. Whitcomb and J. R. Sevier, "A Supersonic Area Rule and an Application to the Design of a Wing - Body Combination With High Lift - Drag Ratios," NASA, 1960.

[10] T. T. Takahashi, "Aircraft Concept Design Performance Visualization Using an Energy-Maneuverability Presentation," AIAA, 2012.

[11] G. Gabrielli and Th. von Kármán, "What price speed? Specific power required for propulsion of vehicles," *Mechanical Engineering,* vol. 10, no. 72, pp. 775-781, 1950.

[12] "Engine Performance Report - GE4/J4C, Commercial Supersonic Transport Engine Proposal," General Electric - Flight Propulsion DIvision, Vol. E-IV GE4/J4C", DTIC AD 377961, 1964.

[13] "US Standard Atmosphere 1962," NASA, AD 659893, 1962.

[14] P. H. Wilkinson, Aircraft engines of the world, 1970.

[15] J. T. Anderson, *How Supersonic Inlets Work : Details of the Geometry and Operation of the SR-71 Mixed Compression Inlet*, Lockheed Martin Skunk Works, 2013.

[16] T. Benson, "Normal Shock Waves," NASA Glenn Research Center, 2014. [Online]. Available: https://www.grc.nasa.gov/www/BGH/normal.html.

[17] T. T. Takahashi and S. Cleary, "Inlet Diffusor Buoyancy – An Overlooked Term in the Thrust Equation," AIAA - 2020-2642, 2020.

[18] W. J. A. Dahm, *MAE 563 - Aircraft Propulsion*, Ira A. Fulton Schools of Engineering, Arizona State University, Fall 2019.